Journal of Medicinal Chemistry

Article

Novel 3-Aminothiazolquinolones: Design, Synthesis, Bioactive Evaluation, SARs and Preliminary Antibacterial Mechanism

Sheng-Feng Cui, Dinesh Addla, and Cheng-He Zhou

J. Med. Chem., **Just Accepted Manuscript** • DOI: 10.1021/acs.jmedchem.5b01678 • Publication Date (Web): 26 Apr 2016

Just Accepted

ACS Publications

Journal of Medicinal Chemistry is published by the American Chemical Society. 1155 Sixteenth Street N.W., Washington, DC 20036

Novel 3-Aminothiazolquinolones: Design, Synthesis, Bioactive Evaluation, SARs and Preliminary Antibacterial Mechanism

Sheng-Feng Cui[1,2], *Dinesh Addla*[1], *Cheng-He Zhou*[1,*]

[1] Institute of Bioorganic & Medicinal Chemistry, Key Laboratory of Applied Chemistry of Chongqing Municipality, School of Chemistry and Chemical Engineering, Southwest University, Chongqing 400715, China

[2] Department of Public Security Technology, Railway Police College, Zhengzhou 450053, China

KEYWORDS: Thiazole, Quinolone, Antibacterial, HSA, DNA

ABSTRACT: A series of novel 3-aminothiazolquinolones as analogs of quinolone antibacterial agents were designed and synthesized in an effort to circumvent quinolone resistance. Among these 3-aminothiazolquinolones, 3-(2-aminothiazol-4-yl)-7-chloro-6-(pyrrolidin-1-yl) quinolone **12b** exhibited potent antibacterial activity, low cytotoxicity to hepatocyte cells, strong inhibitory potency to DNA gyrase and a broad antimicrobial spectrum including against multidrug-resistant strains. This active molecule **12b** also induced bacterial resistance more slowly than Norfloxacin. Analysis of structure-activity relationships (SARs) disclosed that the 2-aminothiazole fragment at the 3-position of quinolone plays an important role in exerting antibacterial activity. Molecular

modeling and experimental investigation of aminothiazolquinolone **12b** with DNA from a sensitive methicillin-resistant *Staphylococcus aureus* (MRSA) strain revealed that the possible antibacterial mechanism might be related to the formation of a compound **12b**-Cu^{2+}-DNA ternary complex, in which the Cu^{2+} ion acts as a bridge between the backbone of 3-aminothiazolquinolone and the phosphate group of the nucleic acid.

1. INTRODUCTION

Quinolones with a 3-carboxyl benzopyridone skeleton are among the most important first-line antibacterial drugs because of their good treatment effectiveness, broad antibacterial spectra and suitable pharmacokinetics. Since this 3-carboxyl benzopyridone skeleton was discovered in the 1960s, structural modifications based on the skeleton have become an extremely attractive area of research, and many quinolones such as Levofloxacin, Sparfloxacin, Grepafloxacin, Trovafloxacin, Gatifloxacin and Moxifloxacin have been successfully and widely used in the clinic to treat genitourinary infections and common respiratory tract pathogens.[3] The structure-activity relationships (SARs) of quinolone antibacterial drugs have been clearly summarized and elucidated, disclosing that the special 3-carboxylic benzopyridone skeleton plays an important role in antimicrobial activity. Based on many valuable SAR studies, the 3-carboxyl and 4-carbonyl groups of quinolone can form stable complexes with DNA-gyrase or DNA-topoisomerase IV via a water-metal ion bridge to trigger irreparable DNA breakage, ultimately resulting in the death of the bacterial cell.[4] However, due to the wide use and even abuse of quinolone drugs in the clinic,[5] the chelating ability of the carbonyl and carboxyl moieties tends to damage the bacterial DNA and trigger an error-prone signal to the DNA repair system, which leads to specific mutations in gyrase and topoisomerase IV and an increase in quinolone-resistant bacterial strains.[6,7] Moreover, many of the severe side effects of quinolone drugs such as

gastroenteritis, vomiting and cartilage damage have been shown to be mainly induced by the carboxyl moieties.[8] Therefore, structural modification at the C-3 position should be a promising pathway to change the classic binding mode of quinolone to the enzyme-DNA complex and overcome the resistance, as well as the side effects caused by the carboxyl group.[9]

It is well known that 2-aminothiazole, as an quite important aromatic five-membered heterocycle, is present in a variety of clinical drugs, such as the antibacterial drugs cephalosporins Cefodizime, Cefoselis and Cefmenoxime, the anticancer drug Dasatinib and the anti-inflammatory drug Meloxicam.[11-12] The successful development of a variety of clinical 2-aminothiazole drugs has motivated extensive efforts to construct further bioactive molecules based on this fragment.[13] Structural modifications of clinical drugs by introducing a 2-aminothiazole group is one of the most convenient and rewarding methods to exploit new medicinal agents.[14] These 2-aminothiazole-modified drugs can generally overcome severe resistance and possess strong bioactivity, a high safety profile and good binding ability with their functional targets.[15] For example, the third-generation cephalosporin Cefdinir, the fourth-generation cephalosporin Cefepime and the fifth-generation cephalosporin Tigemonam all have good inhibitory potency against bacterial strains, including resistant ones, and have been widely used in the clinic to treat various types of infections (Figure 1). Furthermore, some 2-aminothiazole derivatives have been shown to be highly successful inhibitors of bacterial DNA gyrase, with the same targets as antibacterial quinolone drugs.[16] Therefore, the structural modification of quinolone by introducing a 2-aminothiazole fragment should be a highly attractive topic in the antibacterial field.

In our previous works, the introduction of azoles, such as triazoles, imidazoles, and nitroimidazoles, into the quinolone backbone was shown to not only improve antimicrobial potencies but also widen the antimicrobial spectrum, including against methicillin-resistant

Staphylococcus aureus (MRSA).[17-19] These hybrids of azoles and quinolones exhibit good antibacterial activity with low Minimum Inhibitory Concentration (MIC) values and strong binding ability to the DNA-topoisomerase IV complex. In view of the above considerations and as an extension of our previous work,[20-25] herein we for the first time replaced the carboxyl group of quinolone with a 2-aminothiazole fragment to produce a series of novel-structure 3-(2-aminothiazol-4-yl) quinolones. The 2-aminothiazole introduced at the 3-position of quinolone was expected to change the classic binding model of quinolone with enzyme-DNA complexes to overcome the resistance and side effects caused by the carboxyl group. Therefore, the antimicrobial activities *in vitro* for the target 3-aminothiazolquinolones and some intermediates were evaluated against eight bacterial strains including MRSA. The SARs, cytotoxicity, inhibitory activity of DNA gyrase and the development of resistance by MRSA and methicillin- and quinolone-resistant *Staphylococcus aureus* ATCC 700699 (MQRSA) to the highly active molecule were also evaluated. The binding behavior of the highly active molecule to human serum albumin (HSA) was investigated by fluorescence spectroscopy to preliminarily study its absorption, distribution, and metabolism. Moreover, the molecular modeling and experimental investigation of highly active 3-aminothiazolquinolone with genomic DNA isolated from a sensitive MRSA strain were further studied to explore the possible antibacterial mechanism of these new 3-aminothiazolquinolones.

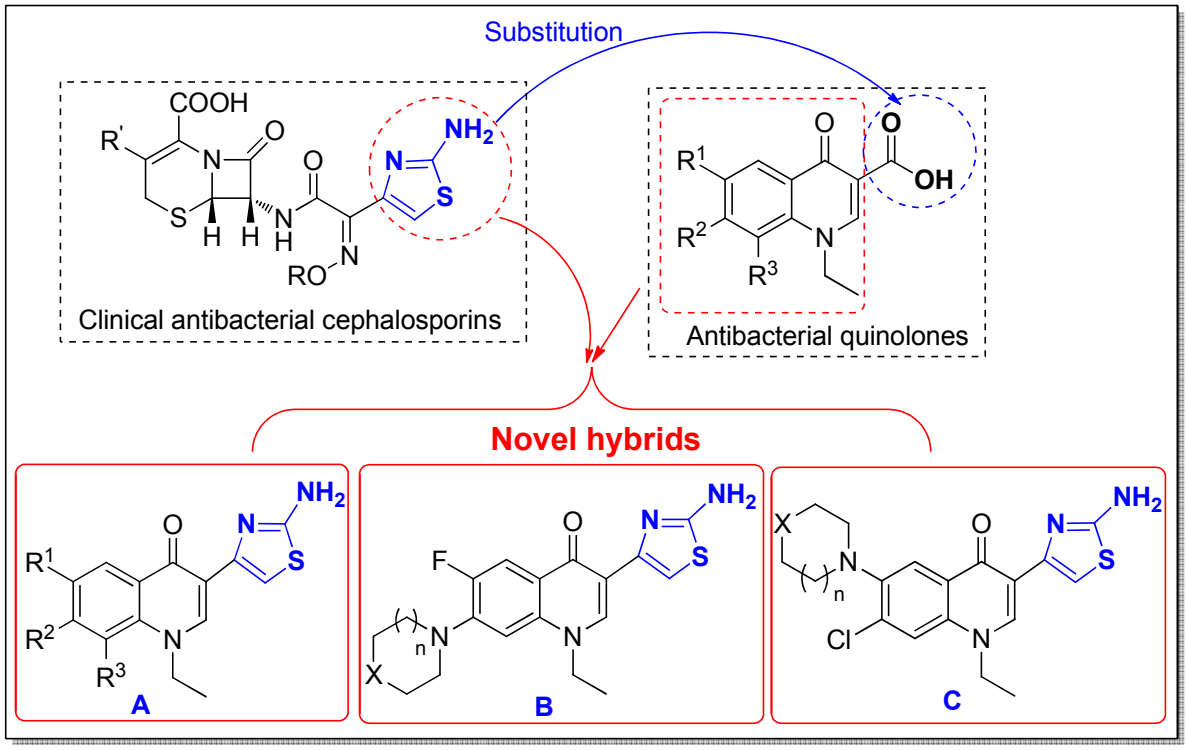

Figure 1. Design of novel 3-(2-aminothiazol-4-yl) quinolones.

2. CHEMISTRY

The synthetic routes of the target 3-(2-aminothiazol-4-yl) quinolones are outlined in Schemes 1–3. Ethyl 2-(ethoxymethylene)-3-oxobutanoate **1** was easily prepared by the reaction of commercial triethoxymethane, ethyl 3-oxobutanoate and propionic anhydride. The synthesized intermediate **1** was reacted with a series of substituted phenylamines in the absence of solvent to afford phenylamino butanoates **2a**–**i** in almost quantitative yields, and then the latter were further cyclized in phenoxybenzene under reflux conditions to produce the desired 3-acetyl quinolones **3a**–**i** in moderate yields ranging from 42.3% to 56.1%. Further *N*-alkylation of compounds **3a**–**i** by bromoethane gave 3-acetyl-1-ethyl derivatives **4a**–**i**. Further bromination of **4a**–**i** by bromine in acetic acid produced the corresponding 3-(2-bromoacetyl) quinolones **5a**–**i**. The cyclization of the bromoacetyl groups at the 3-positions of compounds **5a**–**i** with commercial thiourea in

ethanol at 60 °C readily yielded the target 3-(2-aminothiazol-4-yl) quinolones **6a**–**i** in high yields ranging from 76.2% to 86.5% (Scheme 1).

Scheme 1. Synthetic route of quinolone thiazoles **6a**−**i** [a]

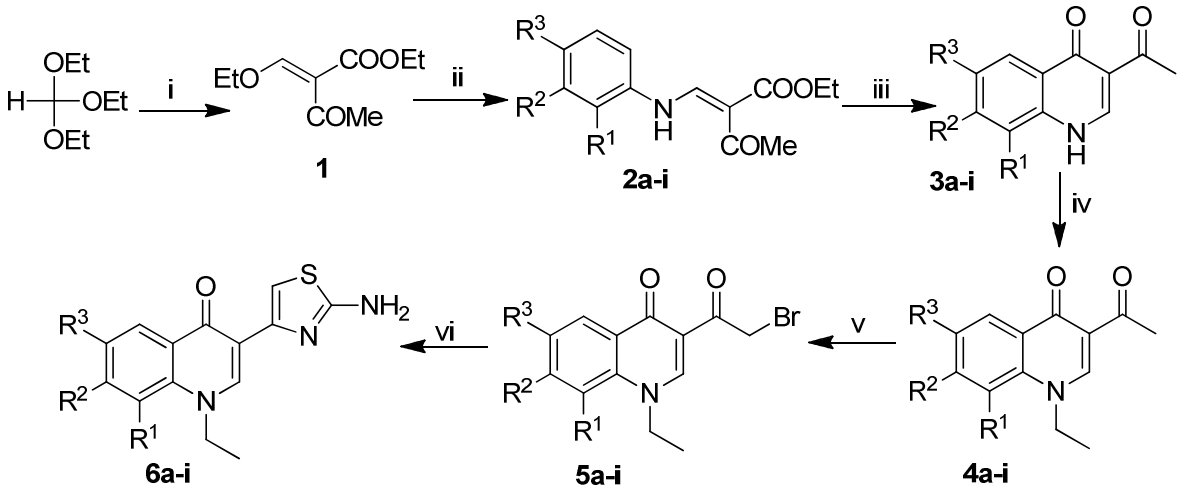

2-6: **a**, R^1 = F, R^2 = H, R^3 = F; **b**, R^1 = H, R^2 = F, R^3 = F; **c**, R^1 = F, R^2 = H, R^3 = H;
d, R^1 = H, R^2 = CF_3, R^3 = H; **e**, R^1 = H, R^2 = Cl, R^3 = F; **f**, R^1 = Cl, R^2 = H, R^3 = Cl;
g, R^1 = H, R^2 = H, R^3 = F; **h**, R^1 = H, R^2 = H, R^3 = OMe; **i**, R^1 = H, R^2 = H, R^3 = Me

[a] Reagents and conditions: (i) ethyl 3-oxobutanoate, propionic anhydride, reflux, 2 h; (ii) substituted aniline, 130 °C, 10 min; (iii) phenoxybenzene, reflux, 1.5 h; (iv) bromoethane, DMF, K_2CO_3, 100 °C, 12 h; (v) bromine, acetic acid, 0−40 °C, 6 h; (vi) thiourea, ethanol, 60 °C, 3 h.

As shown in Schemes 2 and 3, the target 3-aminothiazolquinolones **9a**–**e** and **12a**–**e** were prepared starting from the intermediate 7-chloro-6-fluoroquinolone **4e**. The substitution of compound **4e** with alicyclic amines in DMSO at 130 °C using triethylamine as a base afforded a mixture of 7-position substituted quinolones **7a**–**d** with relatively high yields of 40.5–49.1% and 6-position substituted quinolones **10a**–**d** in slightly lower yields of 31.6–35.4%. It was observed that 6-position substitution by pyrrolidine gave higher yields than piperidine and morpholine. The 7-alicyclic amino compounds **7a**–**d** and 6-alicyclic amino derivatives **10a**–**d** were reacted with bromine in acetic acid to produce the corresponding 3-(2-bromoacetyl) quinolones **8a**–**d** and **11a**–**d**, respectively, and then further cyclizations with thiourea in ethanol at 60 °C produced

target aminothiazolquinolones **9a**–**d** and **12a**–**d**, respectively. The deprotection of the Boc groups in compounds **9d** and **12d** in a solution of trifluoroacetic acid-CH_2Cl_2 produced the corresponding target compounds **9e** and **12e**, respectively. All the structures of the new compounds were confirmed by ^{1}H NMR, ^{13}C NMR, MS, HRMS and IR spectra. Furthermore, 1,3,5-trioxane was employed to check the purity of the target compounds using the quantitative nuclear magnetic resonance (QNMR) method. The results indicated that all the target compounds possess a purity of at least 95%, and their spectral data are provided in the experimental section.

Scheme 2. Synthetic route of quinolone thiazoles **9a**−**e** [a]

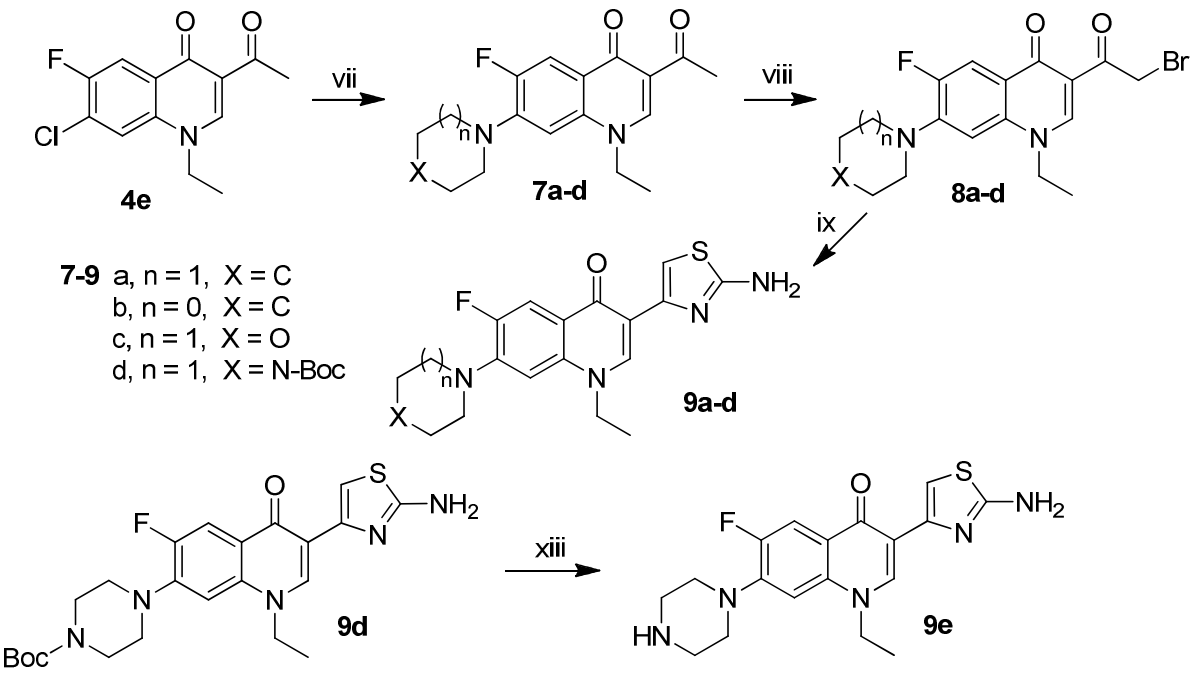

[a] Reagents and conditions: (vii) DMSO, triethylamine, alicyclic amines, 130 °C, 24 h; (viii) bromine, acetic acid, 0−40 °C, 4 h; (ix) thiourea, ethanol, reflux, 3 h; (xiii) CF_3COOH, CH_2Cl_2.

Scheme 3. Synthetic route of quinolone thiazoles **12a**−**e** [a]

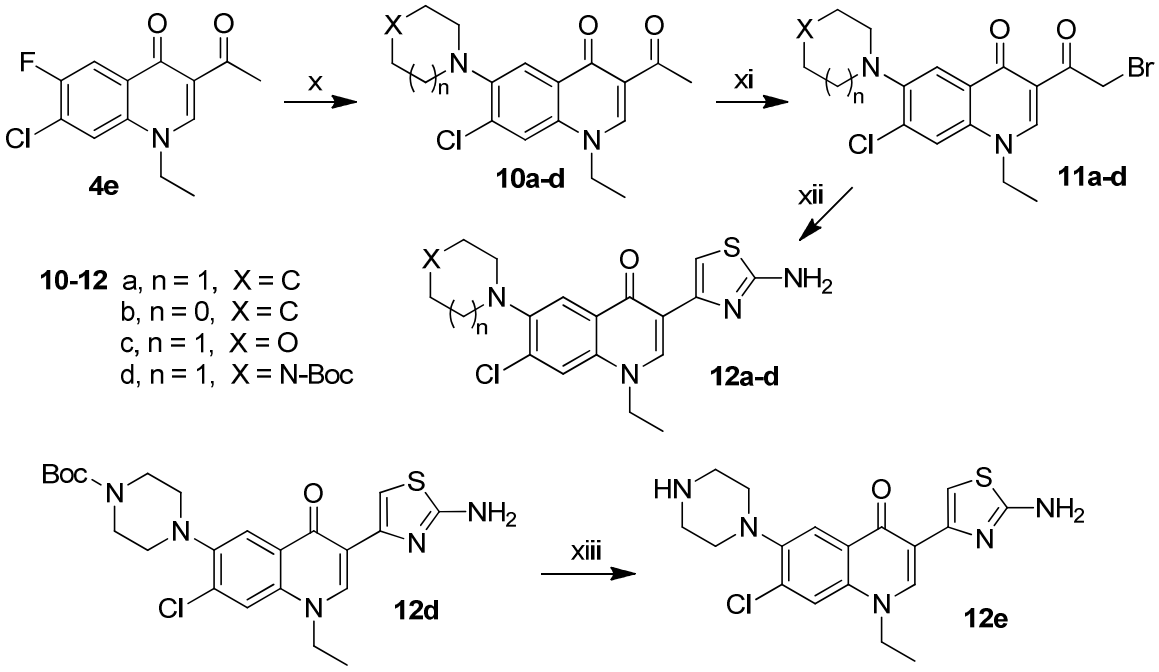

[a] Reagents and conditions: (x) DMSO, triethylamine, alicyclic amines, 130 °C, 24 h; (xi) bromine, acetic acid, 0−40 °C, 4 h; (xii) thiourea, ethanol, reflux, 3 h; (xiii) CF_3COOH, CH_2Cl_2.

3. BIOLOGICAL EVALUATION AND DISCUSSION

3.1. *In Vitro* Antibacterial Activity. The antibacterial results (Table 1) reveal that most of the intermediates and target compounds display biological activity *in vitro* against the eight tested bacterial strains. Most of the intermediates 3-acetyl-1-ethyl quinolones **4a**–**i**, **7a**–**d** and **10a**–**d**, a series of products substituted at the 6-, 7- and 8-positions of the 3-acetyl quinolone skeleton, showed weak activities against the eight bacteria. Nevertheless, 6-fluoro-7-morpholino quinolone **7c** exhibited much stronger antimicrobial efficacy against Gram-negative bacterial stains *B. proteus* and *E. typhosa*, with low MIC values of 2.7 and 2.3 μg/mL, than Norfloxacin (MIC = 13.3 and 5.3 μg/mL) and Chloromycin (MIC = 32.0 and 26.6 μg/mL). 6-Fluoro-7-(pyrrolidin-1-yl) quinolone **7b** also showed good anti-*S. aureus* activity, with an MIC value of 5.1 μg/mL.

The introduction of 2-aminothiazole at the 3-position of quinolone yielded compound series **6**. None of the tested strains were sensitive to 6,8-difluoro quinolone thiazole **6a** or 8-fluoro quinolone thiazole **6c**, which suggested that the fluorine modification at the 8-position of

quinolone is not beneficial for antibacterial activity. To further study the SARs of this new class of quinolone thiazoles, electron-withdrawing (CF_3, F, Cl) and electron-donating groups (methyl, methoxyl) were introduced at the 6- and 7-positions of this quinolone scaffold. These modifications produce a clear relationship between the antibacterial activity and the different substituents at the 6- and 7-positions of quinolone. The electron-withdrawing groups are effective at enhancing anti-Gram-negative bacterial activities. Specifically, 7-trifluoromethyl derivative **6d** showed good MIC values (1.7–13.3 μg/mL) against all tested Gram-negative strains, including *B. proteus*, *P. aeruginosa*, *E. typhosa*, and *E. coli* DH52, with much stronger antibacterial potency than reference drugs. Both 6,7-difluoro aminothiazolquinolone **6b** and 6-fluoro derivative **6g** exhibit superior or comparable inhibitory potency against the tested Gram-negative bacteria compared to Chloromycin and Norfloxacin. 6,7-Difluoro compound **6b** could not only efficiently inhibit the growth of *B. proteus* (MIC = 0.6 μg/mL) and *E. typhosa* (MIC = 1.2 μg/mL), with activities 22- and 4-fold greater in comparison to Norfloxacin, but it also displayed inhibitory potency against Gram-positive bacteria including *M. luteus* and *S. aureus* at low concentrations. On the other hand, 6-fluoro aminothiazolquinolone **6g** showed slightly weaker antibacterial activity against the tested strains than the 6,7-difluoro derivative **6b**, which suggests that the substituents at the 7-position of the quinolone ring should have an important effect on the antibacterial activity.

7-Chloro-6-fluoro quinolone thiazole **6e** not only exhibits effective inhibition toward the growth of Gram-negative bacteria but also enhances anti-Gram-positive bacterial potency. It exhibited good anti-MRSA activity (MIC = 8.0 μg/mL), which was more effective than clinical Norfloxacin and Chloromycin, with MIC values of 10.7 and 21.3 μg/mL, respectively.

Compared to electron-withdrawing groups, quinolone thiazoles **6h** and **6i** with electron-donating methyl and methoxyl groups showed better anti-Gram-positive bacterial potency,

especially against *S. aureus* strains. Generally, the target 3-(2-aminothiazol-4-yl) quinolones showed much higher inhibitory potency against all tested strains than most of their corresponding intermediates. This phenomenon suggests that the aminothiazolyl substituents at the 3-position of quinolones should play an important role in exerting antibacterial potency. On the other hand, the electron-donating groups at the 6- and 7-positions of quinolone were helpful for improving the anti-Gram-positive bacterial efficacy, whereas the electron-withdrawing groups were beneficial to the anti-Gram-negative bacterial potency.

Based on these obtained results, both electron-donating and electron-withdrawing groups were incorporated into the aminothiazolquinolone backbone, and the nucleophilic substitution at the 6- and 7-positions of the 7-chloro-6-fluoroquinolone nucleus **4e** provided some important results. By introducing piperidine, pyrrolidine, morpholine and piperazine into the 6- and 7-positions, the 7-position substituted series **7** and 6-position substituted series **10** were obtained, which showed weak inhibitory potency toward most of the evaluated bacteria. Nevertheless, intermediates **7a**−**d** and **10b** showed good inhibitory activity against S. *aureus* and MRSA strains. The active molecule **7a**, with a piperidine-1-yl group at the 7-position of quinolone, and 7-chloro-6-(pyrrolidin-1-yl) quinolone **10b** gave especially low inhibitory concentrations (MIC = 17.8 and 16.0 μg/mL) against the MRSA strain, with stronger activity than the antibacterial Chloromycin (MIC = 21.3 μg/mL) and slightly weaker than Norfloxacin (MIC = 10.7 μg/mL).

6-Fluoro-7-morpholino aminothiazolquinolone **9c** exhibited only good anti-*S. aureus* (MIC = 0.8 μg/mL) and anti-*B. proteus* (MIC = 1.7 μg/mL) potency. The desired targets 6-fluoro-7-Boc-piperazinyl aminothiazolquinolone **9d** and 6-fluoro-7-piperazinyl aminothiazolquinolone **9e** showed low MIC values against the tested Gram-negative bacteria but demonstrated moderate anti-Gram-positive activity. Meanwhile, 6-fluoro-7-(piperidin-1-yl) aminothiazolquinolone **9a** and 6-fluoro-7-(pyrrolidin-1-yl) compound **9b** also displayed disappointing results, with poor

antibacterial activity against the tested bacteria. Generally, compounds **9a**−**d** did not achieve the desired results. However, a turning point in our work was achieved by testing 7-chloro-6-(pyrrolidine-1-yl) aminothiazolquinolone **12b**, which was previously obtained as a byproduct and displayed a remarkable inhibitory potency against all tested strains. Notably, the tested Gram-negative bacteria including *E. Coli* DH52, *E. typhosa*, *P. aeruginosa* and *B. proteus* were quite sensitive to 7-chloro-6-(pyrrolidin-1-yl) aminothiazolquinolone **12b**, with low MIC values of 0.5–2.0 μg/mL, which was superior antibacterial activity to that of Chloromycin and Norfloxacin. The anti-Gram-positive bacterial activity against *M. luteus*, *S. aureus* and *B. subtilis* (MIC = 2.7, 0.6, and 1.3 μg/mL, respectively) was also comparable or even better in contrast to clinical Norfloxacin. Excitingly, the target compound **12b** exhibited remarkable biological activity toward MRSA at quite a low concentration (MIC = 0.8 μg/mL), being 13- and 27-fold more active than Norfloxacin and Chloromycin, respectively. Unfortunately, 7-chloro-6-(piperidin-1-yl) compound **12a**, 7-chloro-6-morpholin compound **12c**, 7-chloro-6-Boc-piperazinyl compound **12d** and 7-chloro-6-piperazinyl compound **12e** showed poor or even no activity against most of the tested bacterial strains, which suggested that the stereospecific blockade of the six-membered ring at the 6-position of quinolone should be negative with respect to the antibacterial potency.

Table 1. Antibacterial MIC values of compounds **6**, **7**, **9**, **10** and **12** (μg/mL) [a,b]

Compounds	Gram-positive bacterial strains				Gram-negative bacterial strains			
	M. luteus	*MRSA*	*S. aureus*	*B. subtilis*	*P. aeruginosa*	*E. coli*	*B. proteus*	*E. typhosa*

6a	256	NA	NA	NA	NA	64	NA	NA
6b	5.3	213.3	0.8	26.7	78.6	256	0.6	1.2
6c	2.7	NA	NA	13.3	24.0	9.3	256	NA
6d	NA	53.2	127.9	63.9	13.3	5.3	13.3	1.7
6e	26.6	8.0	NA	10.6	1.6	6.7	3.3	2.6
6f	16	NA	3.0	2.7	2.3	21.2	3.3	2.7
6g	18.7	NA	128.0	3.3	13.3	24.0	10.7	21.3
6h	42.7	256	18.8	10.7	21.3	13.3	2.7	8.0
6i	5.4	128.8	2.4	64.4	2.7	4.7	0.8	24.1
7a	10.1	17.8	8.9	12.7	22.8	40.6	20.3	121.2
7b	244.4	50.9	5.1	244.5	12.7	43.3	33.1	122.2
7c	128.0	256	53.3	NA	256	256	2.7	2.3
7d	NA	64.0	16.0	21.3	NA	128.0	16.0	42.7
9a	NA	53.3	64.0	42.7	42.7	128.0	37.3	74.7
9b	106.7	17.3	32.0	53.3	42.7	9.3	128.0	42.7
9c	13.3	32.0	0.8	18.7	10.7	6.0	1.7	14.7
9d	32.0	10.7	64.0	42.7	8.0	10.7	2.6	5.3
9e	64.2	32.1	16.0	10.7	4.0	16.0	2.0	10.7
10a	37.3	128.0	37.3	35.4	42.7	13.3	170.7	NA
10b	10.7	16.0	18.7	10.7	9.3	26.7	64.0	18.7
10c	53.3	128.0	NA	NA	42.7	NA	13.3	37.3
12a	49.0	24.6	61.2	19.6	34.4	117.8	34.4	17.2
12b	2.7	0.8	0.6	1.3	0.5	0.8	1.0	2.0
12c	127.7	255.3	0.8	255.3	170.2	127.7	NA	95.7
12d	53.2	32.0	127.7	21.3	8.0	10.7	32.0	NA
12e	32.0	NA	8.0	2.0	10.7	128.0	6.4	8.0
Chloromycin	13.3	21.3	16.0	26.6	32.0	13.8	32.0	26.6
Norfloxacin	2.7	10.7	0.8	1.3	1.7	4.3	13.3	5.3

[a] *Micrococcus luteus* ATCC 4698, *M. luteus*; *Methicillin-Resistant Staphylococcus aureus* N315, MRSA; *Staphylococcus aureus* ATCC 25923, *S. aureus*; *Bacillus subtilis* ATCC 6633, *B. subtilis*; *Pseudomonas aeruginosa* ATCC 9027, *P. aeruginosa*; *Escherichia coli* ATCC 25922, *E. Coli*; *Bacillus proteus* ATCC 13315, *B. proteus*; *Eberthella typhosa* ATCC 14028, *E. typhosa*. [b] NA, no activity.

3.2. Cell Toxicity and DNA Gyrase Inhibitory Activity. The highly bioactive 3-aminothiazolquinolone **12b** was further evaluated for its toxicity against PC 12 cancer and normal human hepatocyte LO2 cells using the colorimetric cell proliferation MTT assay. Norfloxacin was selected as a positive control to reduce the impact of substituents at the *N*-position of the quinolones. The cell viability against 3-aminothiazolquinlone **12b** of both PC 12 and human hepatocyte LO2 cells was more than 88%, which suggested that this molecule showed low toxicity to the cells at concentrations below 512 μg/mL (Figure 2). On the whole, the cell viability against 3-aminothiazolquinlone **12b** was higher than that against Norfloxacin at concentrations of 128, 256 and 512 μg/mL, which indicated that the new 3-aminothiazolquinlone showed lower cell toxicity than the positive control Norfloxacin.

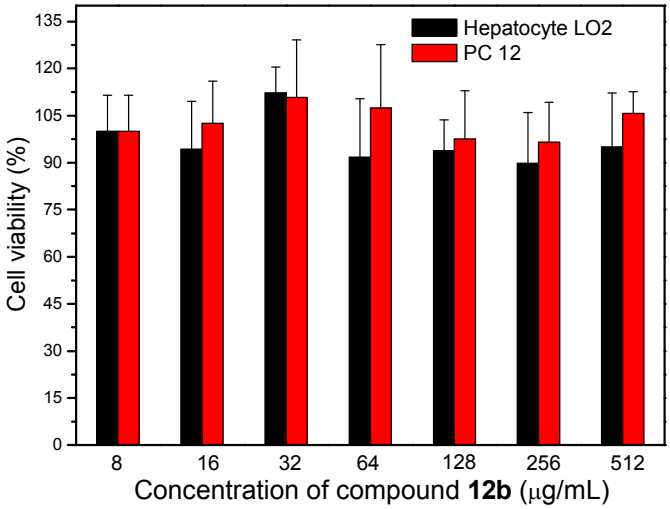

Figure 2. Cytotoxicity assay with 3-aminothiazolquinlone **12b** in the PC 12 and human hepatocyte LO2 cell lines tested by MTT methodology. Each data bar is an average of three replicates.

To investigate inhibitory activity against the target enzymes of quinolones at a molecular level, 3-aminothiazolquinlone **12b** and Norfloxacin were selected to test their DNA gyrase inhibitory activity. Table 2 shows that 3-aminothiazolquinlone **12b** could inhibit the supercoiling activity of

DNA gyrase with a low IC_{50} value of 11.5 μM, which is better inhibitory potency than the standard drug Norfloxacin (IC_{50} = 18.2 μM).

Table 2. Inhibition of DNA gyrase activity

Comps	DNA gyrase supercoiling (IC_{50}, μM)
12b	11.5
Norfloxacin	18.2

3.3 Development of Resistance to 3-Aminothiazolquinlone 12b. Resistance to quinolones among Gram-positive cocci has emerged in recent years.[26] The mutagenic properties of quinolones raises the possibility of the resistance even in smaller populations of bacteria exposed to low concentrations of quinolones, which may promote the ease of selection of low-level resistance mutations. Thus, the bacterial resistance against compound **12b** was also studied by investigating the resistance development rates of MRSA and MQRSA strains. Both strains were exposed to sub-MIC concentrations of 3-aminothiazolquinlone **12b** for sustained passages, and then the MIC values of compound **12b** were determined against each passage of the MQRSA and MRSA strains.[27] The freshly diluted MRSA and MQRSA strains (1.0×10^5 CFU) in the broth medium were cultured in 0.5 μg/mL (2/3 MIC) of compound **12b** at 37 °C for 12 h on a shaker bed at 90 rpm, and the sensitivity of each strain passage to compound **12b** was tested. After 12 passages of MQRSA and MRSA strains in the sub-MIC concentration of compound **12b**, bacterial resistance to the original MIC of compound **12b** (0.8 μg/mL) did not emerge, and the MIC values just changed between 0.5 μg/mL and 1.2 μg/mL (Figure 3). Meanwhile, after 7 passages, compound **12b** also showed good anti-MQRSA activity, with MIC values between 2 μg/mL and 8 μg/mL. On the other hand, to reduce the impact of substituents at the *N*-position of the quinolones, Norfloxacin, bearing the same ethyl group at the *N*-position as compound **12b**,

was chosen as a positive control. The MRSA and MQRSA strains quickly developed resistance to Norfloxacin (MIC = 266.7 μg/mL and 512 μg/mL) and showed strong resistance to the original MIC (10.7 μg/mL and 16 μg/mL) after just one passage. The Norfloxacin acquired 32-fold potency compared to the original MIC after six passages. This assay indicated that the MRSA and MQRSA strains did not develop significant resistance against 3-aminothiazolquinlone **12b** as easily as they did against the positive control Norfloxacin. Therefore, this result indicated that the 3-aminothiazolquinlone was helpful for overcoming the resistance to clinical quinolones.

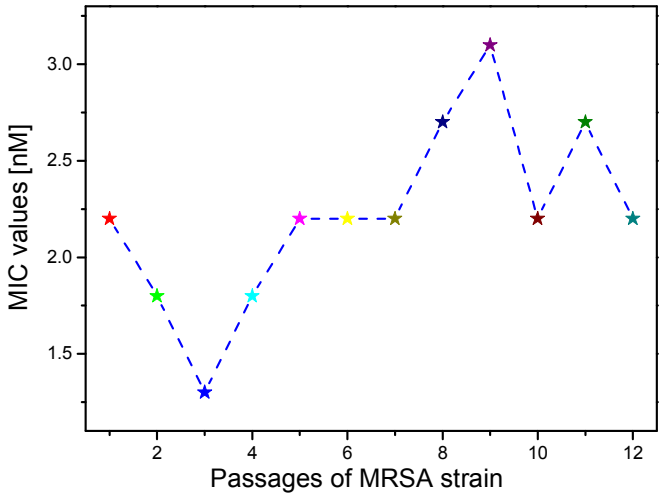

Figure 3. Development of MRSA resistance to compound **12b**, each MIC value of every passage was an average of three parallels.

3.4 Structure-Activity Relationship. Structural features play a remarkable role in the antibacterial potency of these aminothiazolquinolones, especially the substituents at the 3-, 6-, 7- and 8-positions of the quinolone skeleton. The following discussions encompass the correlation of each physical property discussed previously with the antibacterial activity.

3.4.1. Partition Coefficient and Molecular Shape Analysis. The physical characteristics of drugs govern many types of biological processes including absorption, distribution, and

secretion.[28] Therefore, it is quite necessary to acquire a good knowledge of these physical characteristics such as lipophilicity and hydrophilicity.[29] To achieve ideal pharmacokinetic and pharmacodynamic properties in a drug, the distribution coefficient should be intermediate between hydrophilic and hydrophobic. The partition coefficient is frequently used to define the lipophilic character of a drug. The theoretically calculated value of log P (ClogP) was calculated using the commercial ChemBioOffice 2010 (Cambridge Soft, Massachusettes, USA) and is presented in Table 3. In general, all the target compounds were lipophilic (ClogP = 2.88−4.58). The ClogP values of the quinolone thiazole derivatives **6a**−**i** were related to the number of fluorine and chlorine atoms in the benzene rings of the quinolones. The ClogP values followed the order of 7-trifluoromethyl quinolone (**6d**) > 6,8-difluoro derivative (**6a**) and 6,7-difluoro derivative (**6b**) > 6-fluoro derivative (**6g**) and 8-fluoro derivative (**6c**). In comparison to 6,7-difluoro quinolone thiazole **6b**, the 7-chloro-6-fluoro derivative **6e** showed greater lipophilicity, which suggests that the introduction of a chloro group into the quinolone backbone resulted in a stronger lipophilicity than that of a fluoro group. Therefore, 6,8-dichloro quinolone thiazole **6f** was the most lipophilic member of series **6**. It was also observed that compound **9e**, with a piperazin-1-yl group at the 7-position of quinolone, possessed the lowest calculated log P value (ClogP = 2.82) among all the target compounds. 7-Chloro-6-(pyrrolidin-1-yl) aminothiazolquinolone **12b** (ClogP = 4.16) showed stronger lipophilicity than aminothiazolquinolones **6a**−**h**. 7-Chloro-6-(piperidin-1-yl) aminothiazolquinolone **12a** provided the most hydrophobic surface and the highest value of ClogP (ClogP = 4.58) of all the target compounds..

Computational methods can be used to predict important pharmacokinetic properties of drug candidates such as the ability to permeate biological membranes and have been used to rationalize biological activity.[30] The molecular electrostatic potential (MEP) surface gives an

indication of the charged surface area and hydrophilicity of compounds. Therefore, MEP maps of the target compounds were generated to investigate key structural features such as steric and electrostatic interactions, hydrogen donor/acceptor properties and lipophilicity. Table 4 shows a comparison of the MEP surfaces that were generated for a selection of compounds at the neutral state *v*ia the DFT-B3LYP theoretical computation.

Table 3. ClogP values of compounds **6a**−**i**, **9a**−**e** and **12a**−**e**.

Compds.	ClogP	Compds.	ClogP	Compds.	ClogP
6a	3.32	**6h**	2.88	**12a**	4.58
6b	3.32	**6i**	3.49	**12b**	4.16
6c	3.16	**9a**	4.21	**12c**	3.45
6d	3.93	**9b**	3.76	**12d**	4.33
6e	3.72	**9c**	3.45	**12e**	3.22
6f	4.12	**9d**	3.93		
6g	3.16	**9e**	2.82		

In the comparison to the MEP maps of the two modes of quinolone derivatives, series **4** and series **6** were taken as examples. The most noticeable difference came from the 2-aminothiazole fragment at the 3-position of the quinolone backbone. In the optimized structures of series **6**, sulfur atoms with lone pairs were in similar positions to the carbonyl groups at the 3-position of the quinolone drugs and also had a weak ability to interact with the enzyme. On the other hand, the amino fragments at the 2-position of the thiazole rings were electronically available with their lone pairs, which were probably oriented toward the outer part of the molecules and therefore were accessible to interact with their surroundings. Because of the π-π conjugative effect and steric hindrance, the nitrogen lone pairs at the 3-position of the thiazole rings were buried in the structures and only partially available for interaction with solvents or other molecules. One

additional electronegative site could be observed at the 1-position of quinolone because of the ethyl group.

Table 4. Comparison of the MEP surfaces of some target 3-aminothiazolquinolones

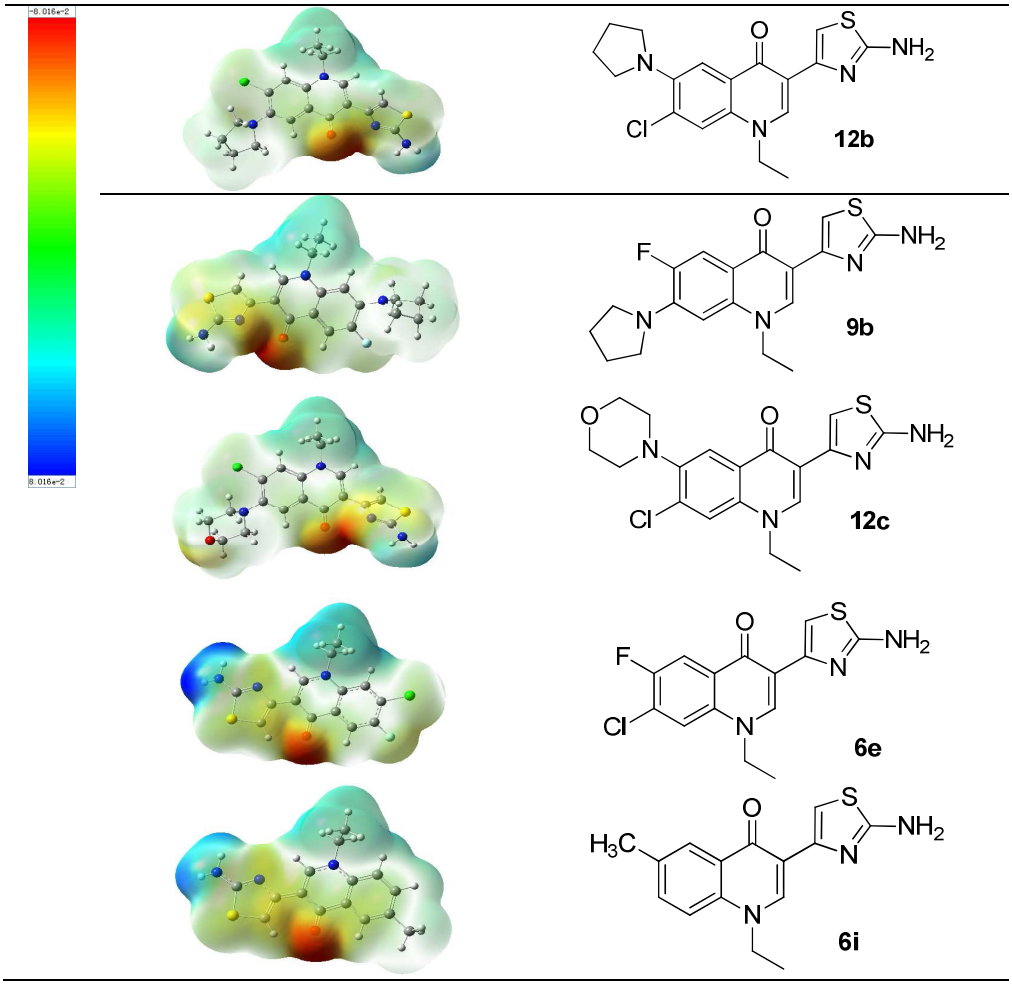

Compared to the MEP surfaces of target compounds **6a**−**i**, the electropositively charged zones of the carbonyl groups at the 4-position of quinolone thiazoles **9a**−**e** and **12a**−**e** are slightly decreased, as a result of the introduction of alicyclic amines at the 6- and 7-positions of the quinolone rings. The introduction of amines also led to the exchange of spatial positions between the 1-position sulfur atom and 3-position nitrogen atom in the thiazole ring, which resulted in positively charged surface areas for the nitrogen atoms of compounds **9a**−**e** and **12a**−**e**. The electron density associated with the amino group at the 2-position of the thiazole ring also

experienced a considerable decrease, which resulted from the inductive and electronic changes generated by the introduction of amines at the 6- and 7-positions of the quinolone rings. The different substitution positions of the alicyclic amino groups in quinolones **9a**−**e** and **12a**−**e** could affect their conformations and electrostatic distributions. The introduction of alicyclic amines at the 6-position of the quinolone backbones demonstrated a slightly smaller influence on the electron density of the carbonyl groups and thiazole rings than that at the 7-position.

3.4.2. Antibacterial Activity, **Substituents in 6-**, **7- and 8-Positions**. Based on the structural features and the antibacterial activity data, the SARs are summarized in Figure 4. Generally, the target 3-(2-aminothiazol-4-yl) quinolones showed much higher inhibitory potency against all the tested strains than most of the corresponding intermediates, especially against Gram-negative bacteria. It seems that the 2-aminothiazole fragments at the C-3 position of the quinolones are important for antibacterial potency and are feasible to replace the carboxyl groups of quinolone drugs. The poor antibacterial potency of 6,8-difluoroquinolone thiazole **6a**, 8-fluoroquinolone derivative **6c** and 6,8-dichloro derivative **6e** might suggest that modification at the 8-position is not favorable to improve antibacterial potency. Strong electron-withdrawing groups like the trifluoromethyl moiety at the 6- and 7-positions of quinolone could significantly increase the inhibitory potency against Gram-negative bacteria but reduce the anti-Gram-positive bacterial activity. It was beneficial to introduce some electron-donating substituents such as methyl, methoxyl or alicyclic amino groups, particularly for anti-Gram-positive bacteria activity. The stereospecific blockade of substituents at the 6-position of quinolone was found to be another influential factor. The pyrrolidin-1-yl group was more effective than the other fragments, including chloro, fluoro, piperidine-1-yl and morpholinyl moieties. To our surprise, 7-chloroquinolones showed better inhibitory potency than 7-fluoroquinolones.

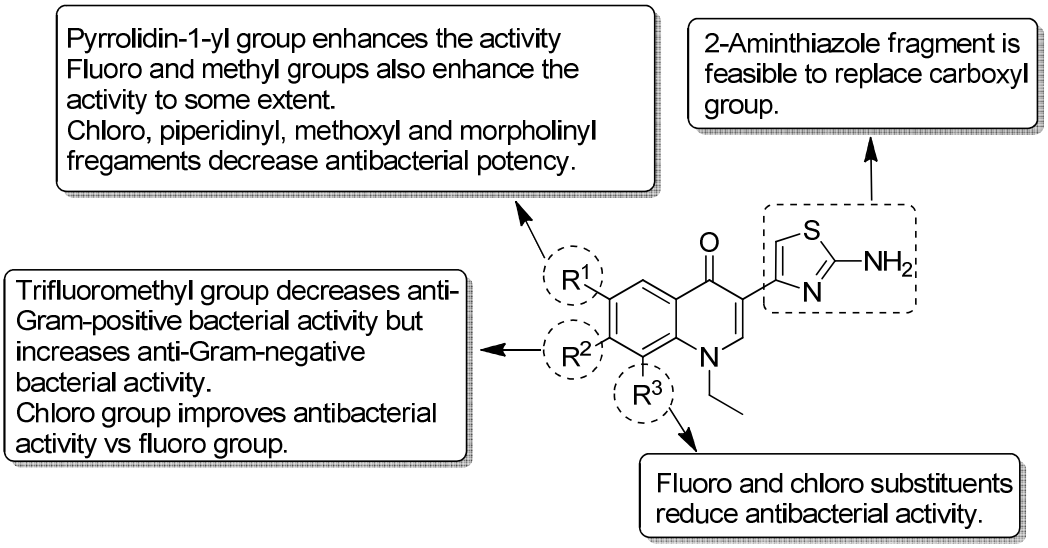

Figure 4. Primary summary of SAR of 3-(2-aminothiazol-4-yl) quinolones.

3.4.3. Antibacterial Activity, Lipophilicity and Hydrophilicity. The effect on the antibacterial activity of the overall balance between the lipophilicity and hydrophilicity of 3-(2-aminothiazol-4-yl) quinolones was investigated by examining the calculated lipophilicity. As shown in Figures 5−8, the compounds with low lipophilicity (ClogP < 3.3) exhibited high MIC values, which indicated that the introduction of hydrophilic groups like single fluorine, morpholinyl and methoxyl groups into the benzene rings of quinolone was detrimental to their antibacterial action. Nevertheless, in the case of high lipophilicity, the target compounds with high ClogP values (ClogP > 4.2) showed moderate to poor potency against *S. aureus*, *P. aeruginosa* and *E. typhosa* strains. These highly lipophilic substituents might result in significant decreases in antibacterial activity. Compared with other strains, the MRSA strain was more sensitive to the target compounds with high ClogP values (4.16, 4.21 and 4.58). The increase in lipophilicity might be beneficial for improving activity against this drug-resistant strain. Finally, it was very interesting that the ClogP values of the compounds with the best activity ranged from 3.3 to 4.2. The target aminothiazolquinolones with ClogP values in this range showed much better antibacterial activity in comparison with others.

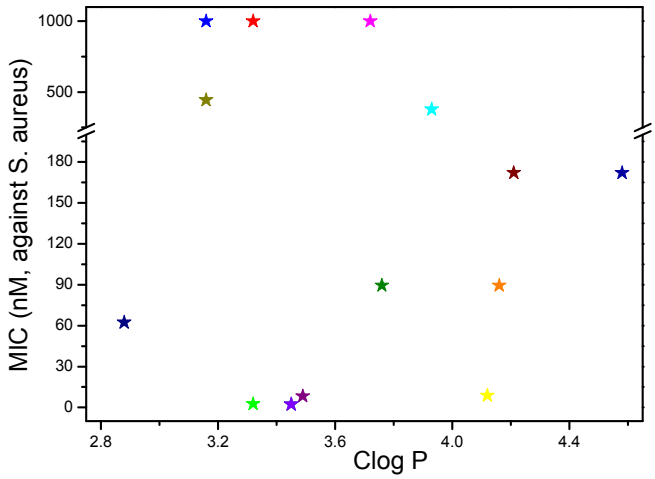

Figure 5. Calculated partition coefficients vs antibacterial activity against *S. aureus* strain. The most active compounds (low MIC) present partition coefficients in the range of ClogP from 3.3 to 3.6.

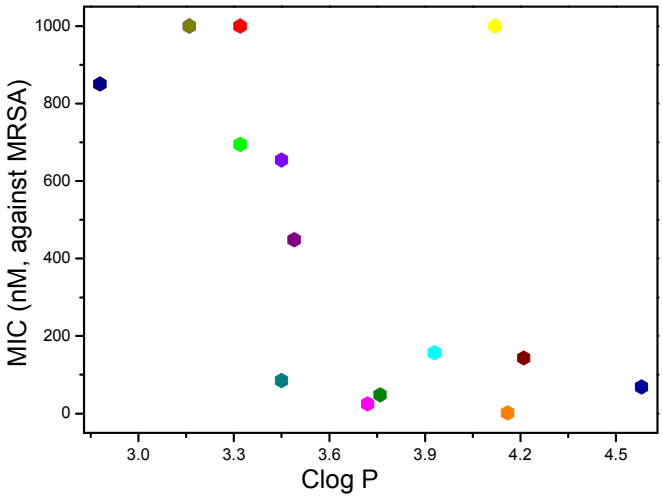

Figure 6. Calculated partition coefficients vs antibacterial activity against MRSA strain. The most active compounds (low MIC) present partition coefficients in the range of ClogP from 3.45 to 4.58.

The hydrophilicity of these compounds was studied via MEP surfaces. Among target compounds **6a**−**i**, those compounds with electron-withdrawing groups at the 6- and 7-positions of quinolone presented MEP surfaces with increased electronegatively charged areas, especially the

lone pair of the amino group, which was beneficial to anti-Gram-negative bacterial potency. However, those compounds with electron-donating groups demonstrated MEP surfaces with reduced electronegatively charged areas, which were helpful for anti-Gram-negative bacterial potency. For the compounds of series **9** and **12**, the introduction of alicyclic amines at the 6- and 7-positions of the quinolone rings resulted in changes to the thiazole rings' conformation, which decreased the positively charged surface areas at the 3- and 4-positions of the quinolones compared to series **6**. These introductions also affected the surfaces of the amino groups, which showed reduced electronegatively charged areas. The strong antibacterial potency and broad antibacterial spectrum, including against MRSA and MQRSA, may be explained by these differences between series **6** and compound **12b**.

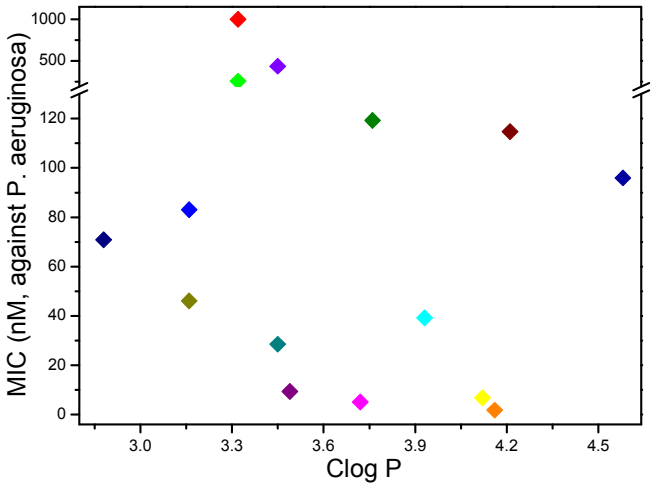

Figure 7. Calculated partition coefficients vs antibacterial activity against *P. aeruginosa* strain. The most active compounds (low MIC) present partition coefficients in the range of ClogP from 3.45 to 4.2.

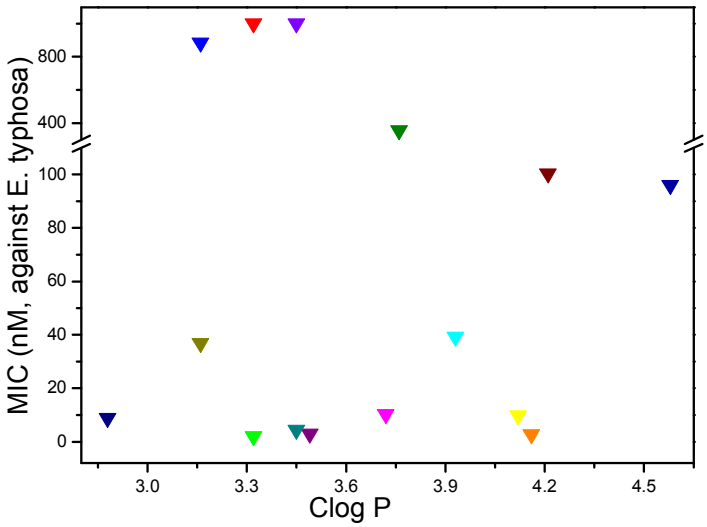

Figure 8. Calculated partition coefficients vs antibacterial activity against *E. typhosa* strain. The most active compounds (low MIC) present partition coefficients in the range of ClogP from 3.45 to 4.2.

3.5 Binding Behavior with HSA. It is well known that HSA is an important extracellular protein in the circulatory system and is closely related to drug absorption, distribution, and metabolism.[31] Drugs-albumin binding behaviors are important during drug discovery and lead optimization as strong or weak binding may reduce the bioavailability and/or increase the drug's *in vivo* half-life. Therefore, investigation of these binding behaviors is not only helpful for understanding the pharmacokinetic properties but also instructive of the design of drug molecules. Herein, highly active molecule **12b**-albumin binding was investigated by fluorescence spectroscopy on the molecular level to preliminarily study the absorption, distribution and metabolism.

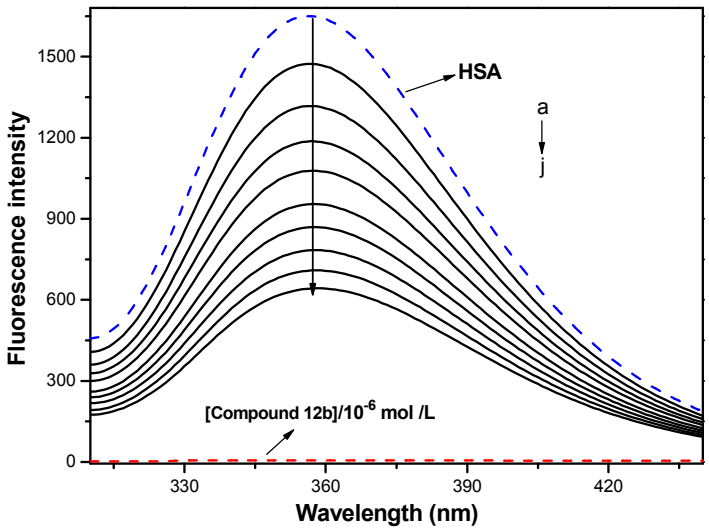

Figure 9. Emission spectra of HSA with different concentrations of compound **12b**. c(compound **12b**)/(10^{-6} M), a−j: from 0−8.56 at increments of 1.07; c(HSA) = 1.0×10^{-5} M; the red and blue dashed lines are the emission spectrum of compound **12b** only and HSA only, respectively; T = 298 K, λ_{ex} = 295 nm.

3.5.1. Fluorescence Quenching Mechanism. Two major methods (equilibrium dialysis and fluorescence competition experiments) are usually employed to study drug binding sites in albumin.[32,33] Fluorescence competition is generally accepted as a good approach to explore the binding behaviors between small molecules and HSA.[34] The tryptophan residue Trp 214 in HSA is a dominant fluorophore capable of fluorescence quenching that absorbs near 280 nm and emits near 340 nm. The emission of this fluorophore may be blue-shifted if the group is buried within a native protein, and its emission may shift to a longer wavelength (red-shift) when the protein is unfolded. Hence, changes in the fluorescence intensity can reflect the interaction of small molecules with Trp-214 in HSA.[35]

With a fixed amount of HSA, the fluorescence changes of HSA (T = 298 K, λ_{ex} = 295 nm) with increasing concentrations of compound **12b** were determined. The red dashed line in Figure 9 is

the only emission spectrum of the active molecule **12b**, which indicates that its fluorescence intensity is very weak and could be negligible in comparison with the fluorescence of HSA at the excitation wavelength. The maximum emission peak of HSA appeared at 356 nm in the fluorescence spectra, exhibiting a proportional decrease and slight red shift from 356 nm to 359 nm as the concentration of compound **12b** increased. According to the following well-known Stern-Volmer equation (1), the fluorescence quenching data of HSA could be analyzed:

$$\frac{F_0}{F} = 1 + K_{SV}[C] \qquad (1)$$

In this equation the F_0 is the steady-state fluorescence intensity of HSA alone, and F represents its fluorescence in the presence of compound **12b**. K_{SV} and [C] are the Stern-Volmer quenching constant and the concentration of compound **12b**, respectively. K_{SV} was obtained by performing a linear regression of a plot of F_0/F vs [C], and the results are shown in Table 5.

The values of the constant K_{SV} at three different temperatures (298, 303, and 310 K) were calculated from Stern-Volmer plots and are listed in Table 5. The quenching constant K_{SV} varies inversely with the temperature, which suggests that ground-state complex formation between compound **12b** and HSA (static quenching) governs the quenching mechanism of this complex.

Table 5. Stern-Volmer constants of interaction between HSA and compound **12b** at pH 7.4 [a]

Temperature (K)	K_{SV} (L/mol $\times 10^{-4}$)	R	SD
298	1.43	0.996	0.06
303	1.39	0.993	0.06
310	1.26	0.996	0.05

[a] R and SD are the correlation coefficient and standard deviation, respectively

3.5.2. Binding Sites and Constants. The static quenching data could be analyzed by the following modified Stern-Volmer formulas (2):

$$\frac{F_0}{\Delta F} = \frac{1}{f_a K_a}\frac{1}{[Q]} + \frac{1}{f_a} \qquad (2)$$

ΔF is the fluorescence difference of HSA in the presence and absence of compound **12b**, and f_a and K_a are the fraction of accessible fluorescence and the effective quenching constant for the accessible fluorophore, respectively. $F_0/\Delta F$ depends on the reciprocal value of the concentration $[Q]^{-1}$, which is linear with the slope on the basis of the $(f_a K_a)^{-1}$ value. Figure 10 shows modified Stern-Volmer plots, and the results are listed in Table 6.

The Scatchard equation (3) could be used to calculate the equilibrium binding constant (K_b) and the number of binding sites (n):

$$\frac{r}{D_f} = nK_b - rK_b \qquad (3)$$

D_f and r are the molar concentration of free small molecules and the moles of small molecules bound per mole of protein, respectively. K_b is the equilibrium binding constant, and n is the binding site multiplicity per class of binding sites. Figure 11 shows the Scatchard plots, and the K_b and n values are listed in Table 6.

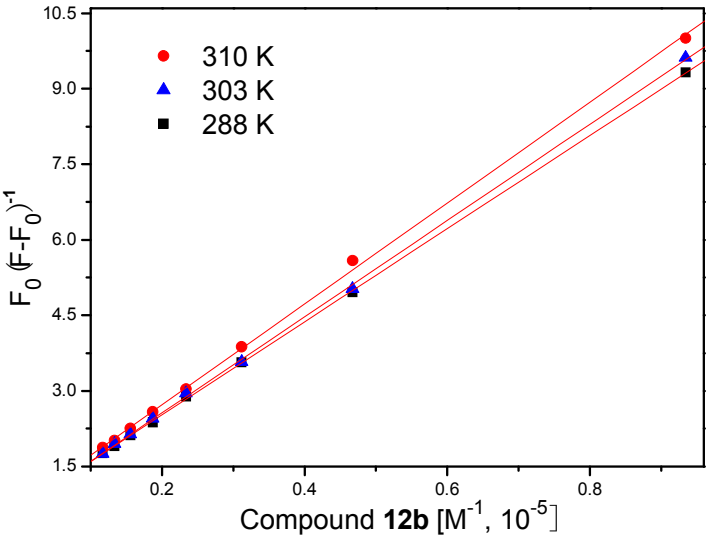

Figure 10. Modified Stern-Volmer plots for compound **12b**-HSA complex.

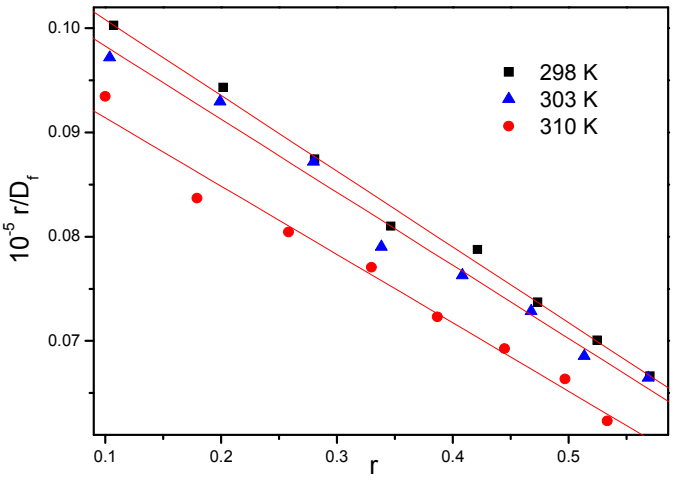

Figure 11. Scatchard plots of compound **12b**-HSA complex.

The binding constants and sites of the compound **12b**-HSA system at 288 K, 303 K, and 310K are listed in Table 6. The values of K_a and K_b decrease with increasing temperature, which is similar to the dependence of K_{SV} on the temperature. The binding site *n* was approximately equal to 1, which suggests that the compound **12b**-HSA complex should have one binding site. The binding constants of the compound **12b**-HSA complex were also suitable. Based on these results, compound **12b** could be transported by HSA.

Table 6. Binding sites and constants for compound **12b**-HSA complex in pH 7.4 solution

Temperature (K)	Modified Stern-Volmer formula method			Scatchard formula method			
	K_a (L/mol × 10^5)	R	SD	K_b (L/mol × 10^5)	R	SD	*n*
288	1.47	0.9999	0.03	0.726	0.997	0.002	1.4
303	1.39	0.9998	0.05	0.701	0.992	0.002	1.4
310	1.37	0.9996	0.08	0.656	0.991	0.001	1.4

3.6 Preliminary Antibacterial Mechanism of 3-Aminothiazolquinolones. Although a large amount of biological data has indicated that the functional targets of quinolones are topoisomerase IV and DNA gyrase, many studies of antibacterial mechanisms have dismissed

these two enzymes as targets and point to DNA as the direct binding species. Generally, this type of drug does not bind directly to DNA gyrase or DNA topoisomerase IV at their inhibitory concentration but rather specifically to a saturable site on the supercoiled DNA in a highly cooperative manner.[36] On the basis of previous observations and evidence, a model for the ternary complex has been proposed, in which magnesium or copper ions act as linkers between the groups at the 3- and 4- positions of quinolone and the DNA phosphate group.[37] Therefore, the *in vitro* enzyme inhibition assay against DNA gyrase or DNA topoisomerase IV is not enough to illustrate the antibacterial mechanism of quinolone drugs. Molecular modeling and the interaction between the active molecule and bacterial DNA is an important and helpful strategy for investigating preliminary antimicrobial mechanism. In our work, DNA was isolated from MRSA bacteria that were most sensitive to 3-aminothiazolquinolone **12b**, and the purity was checked by gel electrophoresis (Figure 12**)** and absorption spectroscopy. The concentration of MRSA DNA in stock solution was determined by UV absorption at 260 nm using a molar absorption coefficient ξ_{260} = 6600 L mol^{-1} cm^{-1} (expressed as molarity of phosphate groups) according to the Bouguer-Lambert-Beer law. The purity of MRSA DNA was checked by monitoring the ratio of the absorbance at 260 nm to that at 280 nm. The solution gave a ratio of > 1.8 at A260/A280, which indicated that the DNA was sufficiently free from protein.

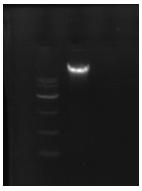

Figure 12. Purity of MRSA DNA checked by gel electrophoresis. The left is marker, and the right is the MRSA DNA

3.6.1. Molecular Docking Study. A docking investigation was undertaken to explore the possible mechanism of action of aminothiazolquinolones. Crystals of topoisomerase IV-DNA and gyrase-DNA complexes were selected as representative targets in the protein data bank.[38,39] The resolutions of the crystals were checked and determined to be not higher than 2 Å. Aminothiazolquinolone **12b** was used to dock with the gyrase-DNA and topoisomerase IV-DNA complexes.

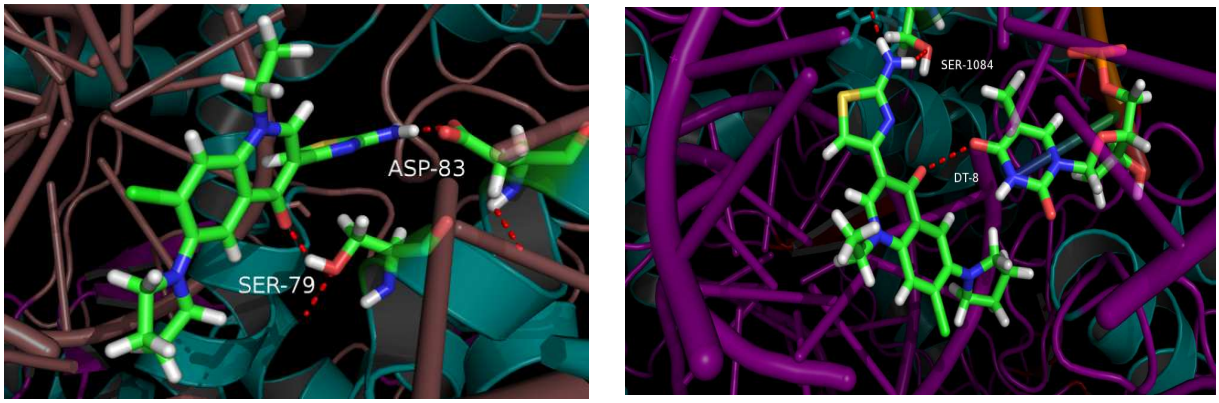

Figure 13. 3D conformations of 3-aminothiazolquinolone **12b** docked in the gyrase-DNA complex (left) and the topoisomerase IV-DNA complex (right).

The docking evaluation gave good total scores (5.68 and 6.46) for aminothiazolquinolone **12b** against topoisomerase IV-DNA and gyrase-DNA complexes, which might rationalize the antibacterial mechanism of aminothiazolquinolones. As shown in Figure 13, the carbonyl fragment of the aminothiazolquinolones **12b** was adjacent to the ASP-83 residue in the topoisomerase IV-DNA complex, forming a hydrogen bond with a distance of 2.9 Å. The amino group at the 2-position of the thiazole ring was close to conserve the ParC helix a4 residues Ser-79 (with the closest distances to the side chain atoms of 2.1 Å), whose mutation causes quinolone resistance in bacteria. Similar hydrogen bonds could also form between aminothiazolquinolone **12b** and the Ser-1084 and DT-8 base pairs of the gyrase-DNA complex. These hydrogen bonds

are stronger those between gyrase/topoisomerase IV and quinolone drugs reported in crystallographic studies. Nevertheless, their distances are not sufficiently close in space to mediate the drug binding directly to the amino acids and base pairs, which indicates that metal ions as bridges between the drug and amino acid/phosphate groups should play an important role in the antibacterial action.[40] Furthermore, as shown in Figure 14, aminothiazolquinolone **12b** was able to intercalate into DNA in the enzyme-DNA complex. The backbone of aminothiazolquinolone **12b** is prone to form stacking interactions with the bases in the negatively supercoiled region. This type of binding might be useful to the structural stability of the ternary complex, which is an important reason for the strong inhibitory efficacy of compound **12b** against strains of quinolone-resistant bacteria such as MRSA.

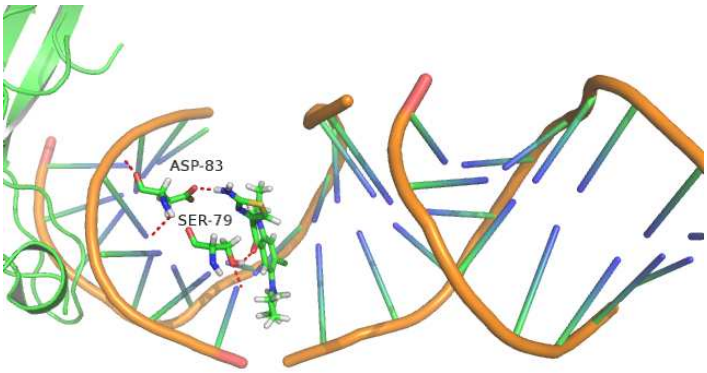

Figure 14. Three-dimensional conformation of compound **12b** with DNA in topoisomerase IV-DNA complex.

3.6.2. Absorption Spectroscopy Analysis. Hypochromism is a quite important feature in the structural changes of double-helical DNA.[41] The large hypochromism displayed in absorption spectroscopy is due to the strong interaction of electronic states between the intercalating chromophore and DNA base, which strongly suggests that the aromatic chromophore should be close to the DNA bases.[42] In our work, the concentration of MRSA DNA was fixed, and UV-vis absorption spectra were obtained with the increasing concentration of compound **12b**. In Figure

15, the maximum absorption peak of DNA shows a slight blue shift and proportional increase with increasing concentrations of compound **12b**. Moreover, a greater absorption sum value of free compound **12b** and free DNA was observed in the inset of Figure 15 in comparison with the measured complex value. This phenomenon suggests that a hypochromic effect (11.4%−22.7%) exists in the complex of DNA and compound **12b**. The obtained hypochromism in our study was similar to that in previous reports of quinolone drugs and stronger than that of Norfloxacin (16%−18%).[43] The intercalation of the chromophore fragment of aminothiazolquinolone **12b** into the DNA helix and its strong π-π* overlap of the aromatic skeleton with DNA bases supports the observed spectral changes in the spectrum of compound **12b** after mixing with DNA, which indicates that the active molecule directly (without Mg^{2+} or Cu^{2+} ion mediation) forms a complex with double-helical MRSA DNA. Based on these absorption spectra, the intrinsic binding constant (K) of compound **12b** and DNA could be calculated by the following equation (4).

$$\frac{A^0}{A - A^0} = \frac{\xi_C}{\xi_{D\text{-}C} - \xi_C} + \frac{\xi_C}{\xi_{D\text{-}C} - \xi_C} \cdot \frac{1}{K[Q]} \qquad (4)$$

A^0 is the maximum absorbance of DNA without aminothiazolquinolone **12b**, A is the maximum absorbance in the presence of aminothiazolquinolone **12b**, ξ_C and $\xi_{D\text{-}C}$ represent the absorption coefficients of aminothiazolquinolone **12b** and the complex, respectively, and Q is the tested concentration of aminothiazolquinolone **12b**. The absorption titration data and linear fitting were used to construct a plot of $A^0/(A\text{-}A^0)$ vs 1/[Q], thereby yielding the binding constant $K = 3.89 \times 10^3$ L/mol, the correlation coefficient R = 0.9997 and the standard deviation SD = 0.04. The obtained bonding constant ($K = 3.89 \times 10^3$ L/mol) was 1.5 times that of Norfloxacin ($K = 2.8 \times 10^3$ L/mol, at 25 °C), which indicates that aminothiazolquinolone **12b** shows a much stronger DNA-binding ability than Norfloxacin.

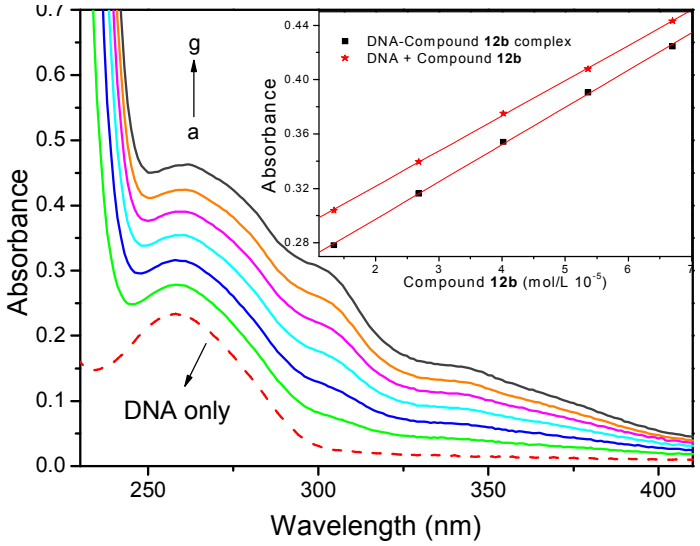

Figure 15. UV spectra of DNA with increasing concentrations of compound **12b**; Inset: the absorption of complex of DNA-compound **12b** and sum values of free compound **12b** and free DNA at 260 nm. Concentrations of compound **6b** are 0–6.70 × 10^{-5} M for curves a–g at increment of 0.67 × 10^{-5} respectively, and concentrations of DNA is 5.39 × 10^{-5} M; pH = 7.4, T = 294 K.

3.6.3. Steady-state Quenching Analysis by Potassium Iodide. Steady-state quenching is able to provide further beneficial information about the binding mode of a molecule with MRSA DNA. It is generally accepted that small molecules have three binding modes with DNA by non-covalent interactions, including intercalation with base pairs, groove binding, and electrostatic interaction with the anionic sugar phosphate backbone. The intercalative and groove binding modes are more effective to block DNA replication than that of electrostatic interaction.[44]

It has been revealed that when using an anionic quencher, the DNA base pairs around the intercalators hinder the accessibility of the fluorescent probe to the quencher. However, the use of electrostatic repulsion between the anionic quenchers and DNA phosphate backbones can be beneficial for the intercalated species. Thus, in the intercalation binding mode, the quenching of

the molecule by the anionic quenchers could be avoided. The K_{SV} value of the molecule bound to the DNA by groove binding should be higher than that bound by intercalation. In this work, KI quenching is introduced to investigate the binding mechanism. As shown in Figure 16, the K_{SV} value of compound **12b** (27.1 M^{-1}, R = 0.999, SD = 0.006) in the absence of MRSA DNA was lower than that (30.1 M^{-1}, R = 0.998, SD = 0.008) in the presence of MRSA DNA. Therefore, the binding mode of compound **12b** with DNA was of an electrostatic interaction nature, the same as in previous reports on the classic quinolone antibacterial drug Norfloxacin.

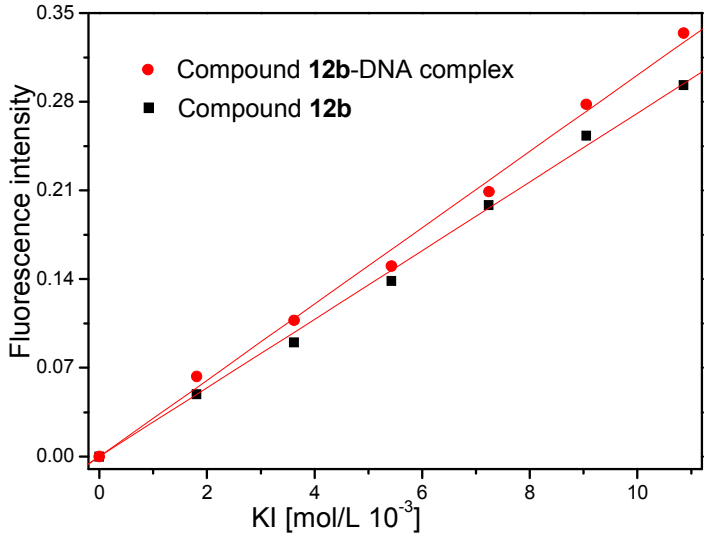

Figure 16. Fluorescence quenching plot of compound **12b** by I^- ions; c(compound **12b**) = 2.23 × 10^{-5} M, and c(DNA) = 4.05 × 10^{-5} M; pH = 7.4, T = 294 K.

3.6.4. Comparison of Interactions of Compound 12b with ssDNA and dsDNA. The interaction of compound **12b** with MRSA DNA was also directly determined by fluorescent spectra. A single-stranded DNA (ssDNA) solution was prepared by heating native double-stranded DNA (dsDNA) solution in a boiling water bath for 10 min and then cooling rapidly in an ice water bath.[45] As the concentration of dsDNA increased, the fluorescence intensity of compound **12b** remained nearly unaffected in the presence of excess double-stranded MRSA

DNA and an absence of Cu^{2+} ions. Little decrease in the fluorescence intensity of compound **12b** was shown, and the binding was poor for the linear double-helical sequence. However, as shown in Figure 17, the maximum fluorescence intensity of compound **12b** at 451 nm proportionally decreased with the increase in ssDNA, and the binding was good for the linear single-helical sequence. The difference in the fluorescence spectra of ssDNA and dsDNA indicates that the backbone of aminothiazolquinolone **12b** could form stacking interactions with the bases in a single-stranded region. Therefore, the preference of compound **12b** for ssDNA might play a role in the stabilization of the quinolone-DNA gyrase complex, as the gyrase catalyzes the conversion from the supercoiled form of relaxed DNA to a negatively supercoiled form. These results were consistent with those of molecular modeling.

.

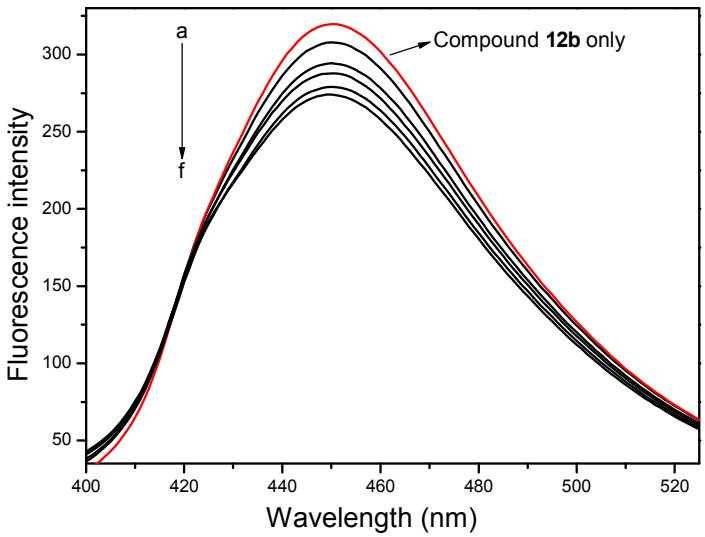

Figure 17. Emission spectra of compound **12b** in the absence of ssDNA, pH = 7.4, T = 294 K, λ_{ex} = 366 nm. c(compound **12b**) = 2.0 × 10^{-5} M, and c(DNA) *a*−f: from 0.0 to 5.4 × 10^{-4} at increments of 1.08; red line is the emission spectrum of compound **12b** only.

3.6.5. Compound 12b Binding to Copper(II) Ions. The hypochromism in the absorption spectrum and the results of the steady-state quenching analysis by KI indicate that compound **12b** could directly form a stable complex with MRSA dsDNA. The obtained binding constant (K = 3.89 × 10^3 M^{-1}) was 1.5 times that of Norfloxacin (K = 2.8 × 10^3 M^{-1}, at 25 °C), but was much lower than those of classical intercalative agents (K > 10^5 M^{-1}). Therefore, this binding was not strong enough to block DNA replication. Large amounts of biological data indicate that quinolones did not bind directly to DNA gyrase but interacted with the DNA itself in a cooperative manner.[46] A model for the ternary complex including metal ions has been proposed. Based on this, the highly active molecule **12b** and all the essential metals for the human body were chosen to investigate the interaction with MRSA DNA. As shown in Figure 18, the fluorescence emission of compound **12b** was remarkably decreased only by the addition of Cu^{2+} ions at pH = 7.4. The saturation occurred at the Cu^{2+} concentration of 4.69 × 10^{-5} M and was slightly influenced by the ionic strength at room temperature. This strong quenching suggests the formation of a compound **12b**-Cu^{2+} complex.

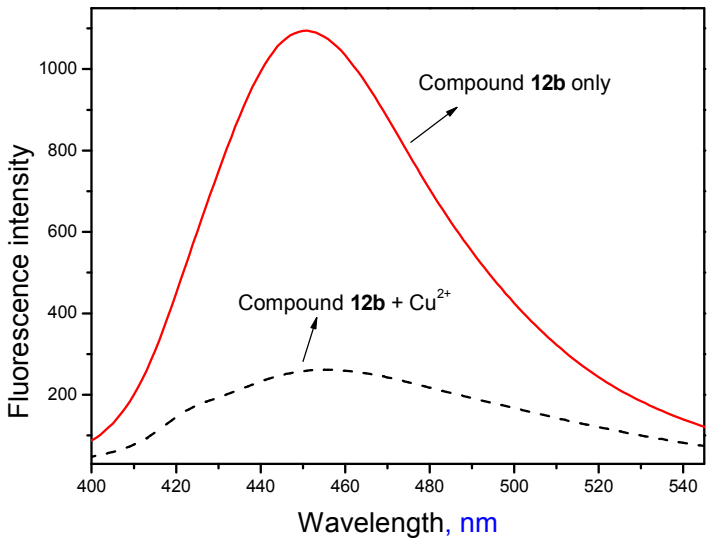

Figure 18. Emission spectra of compound **12b** at pH = 7.4, T = 294 K, λ_{ex} = 366 nm. c(compound **12b**) = 2.23 × 10^{-5} M, and c(Cu^{2+}) = 4.69 × 10^{-5} M; solid line is the spectrum of compound **12b** only; dash line is the spectrum of compound **12b**-Cu^{2+} complex.

Equations (5) and (6) can be used to deduce the composition of the binary complex.

$$M + nL = MLn \qquad (5)$$

$$\log[\frac{F_0 - F}{F}] = \log K_a + n\log[M] \qquad (6)$$

L is the pharmaceutical molecule of the fluorophore, *M* is the tested quencher, *MLn* is the formed complex, and K_a is the resultant constant. F_0 is the fluorescence of the overall amount of pharmaceutical molecule (bound and unbound), and *F* is the fluorescence of the unbound pharmaceutical molecule. A straight line with a slope of *n* and a *y*-axis intercept log K_a will be obtained from the plot of log[(F_0−*F*)/*F*] vs log[*M*].

Figure 19 was obtained by keeping the compound **12b** concentration (2.23 × 10^{-5} M) constant and gradually increasing the concentration of Cu^{2+} ions. The data were well fitted to Eq. (5) and (6), and the slope was 0.949. The result indicates that aminothiazolquinolone **12b** could interact with Cu^{2+} ions to form a stable 1:1 complex.

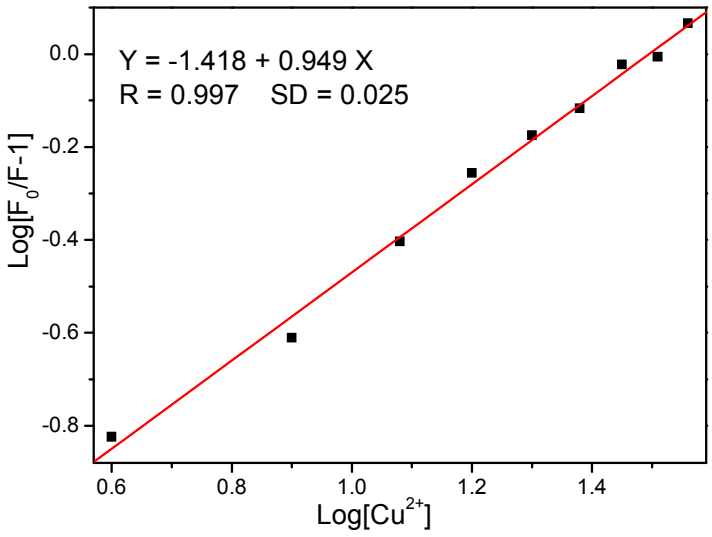

Figure 19. Estimation of composition of the compound **12b**-Cu^{2+} complex. c(compound **12b**) = 2.23×10^{-5} M, and c(Cu^{2+}) = 0–6.03×10^{-5} M at increment 0.67×10^{-5}; pH = 7.4, T = 294 K, λ_{ex} = 366 nm.

3.6.6. Binding to MRSA DNA Mediated by Copper Ions. The above results from the interaction of compound **12b** with dsDNA show that the fluorescence of compound **12b** remained practically unaffected in the absence of Cu^{2+} ions and the presence of excess MRSA DNA. However, at a Cu^{2+} concentration in the millimolar range, which is similar to the intracellular concentrations of Cu^{2+} ions in bacteria, a fluorescence quenching took place in the MRSA DNA-compound **12b** system. The fluorescence spectra of compound **12b** in the presence and absence of MRSA DNA were recorded along with the increase in Cu^{2+} ions. In Figure 20, the apparent difference indicates that a compound **12b**-MRSA DNA complex was formed in the presence of Cu^{2+} ions. The minimum value of the fluorescence intensity appeared at a concentration of Cu^{2+} ions of 20×10^{-5} M. With fixed concentrations of compound **12b** (2.23×10^{-5} M) and Cu^{2+} ions (0.4×10^{-6} M), the fluorescence intensity of compound **12b** could also be decreased by MRSA DNA (Figure 21), which was very different from the process in the absence of Cu^{2+} ions. The data were well fitted to Eq. (5) and (6), with a good linear fit. These results indicate that there was not only competition between the Cu^{2+} ions and MRSA DNA in the system of metal ions-DNA-compound **12b** but also formation of a ternary compound **12b**-Cu^{2+}-DNA complex, in which compound **12b** with DNA could produce a stable 1:1 complex in the presence of Cu^{2+} ions.

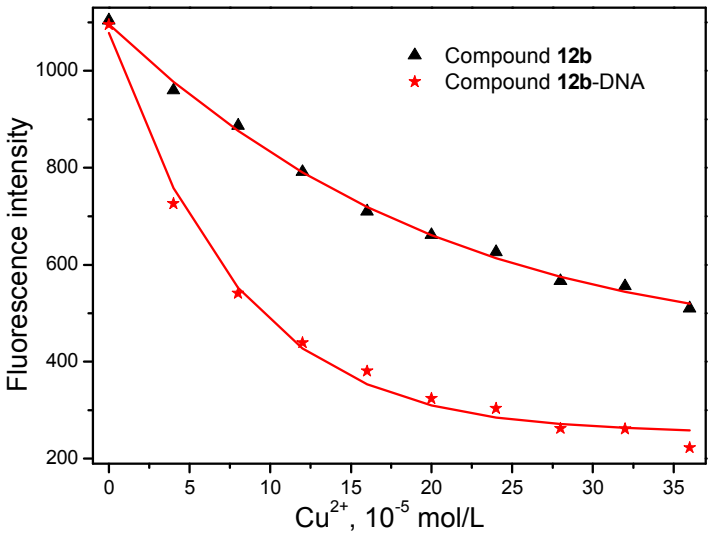

Figure 20. Effects of Cu^{2+} ions and MRSA DNA in Tris-HCl on the fluorescence response (451 nm) of 2.23×10^{-6} M compound **12b**, pH = 7.4, 25°C. Triangles, fluorescence emission readings in the absence of the MRSA DNA; Stars, fluorescence emission readings in the presence of MRSA DNA (0.78×10^{-3} M, calculated on a phosphate basis).

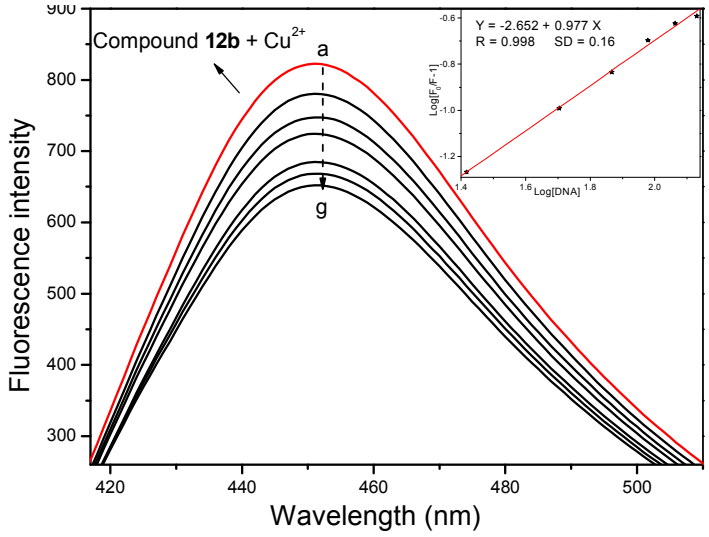

Figure 21. Composition of the compound **12b**-Cu^{2+} complex. *c*(compound **12b**) = 2.23×10^{-5} M, *c*(Cu^{2+})/(4.0×10^{-5} M), *c*(DNA) *a*−g: from 0.0 to 3.24×10^{-4} at increments of 0.54, λ_{ex} = 366 nm; red line is the spectrum of compound **12b** in the presence of Cu^{2+} ion only. Inset: the composition of Cu^{2+}-DNA-compound **12b** complex.

In these experiments, as deduced from the fluorescence spectra, a groundstate ternary complex could be formed among compound **12b**, a Cu^{2+} ion and MRSA DNA. The extent of the binding ability of compound **12b** to MRSA DNA was modulated by the concentration of Cu^{2+} ions. The modulation was not simply the result of competition between the metal ion and DNA for binding to compound **12b**, as the linear quenching by the dsDNA was poor in the fluorescence spectra, and the quenching extent of the drug-DNA complex exhibited a minimum as a function of the Cu^{2+} ion content. The Cu^{2+} ion was able to bind to compound **12b** with a stable constant in a model of 1:1. The carbonyl and 2-aminothiazolyl moieties in the quinolone ring probably played an important role in chelating the metal ions. Therefore, the binding model might be the formation of a ternary complex, in which the Cu^{2+} ion might form a bridge between the quinolone moiety and the nucleic acid. In addition, the fact that the binding was poor for a linear double-helical sequence compared to a single-stranded sequence suggested that the bases not involved in pairing could stabilize the drug-Cu^{2+} complex by forming stacking interactions with the bases in a single-stranded region in the DNA of MRSA.

4. CONCLUSIONS

In this work, starting from commercial materials, a series of novel aminothiazolquinolones were for the first time designed and synthesized via a convenient procedure. All the structures of the new compounds were characterized by MS, HRMS, NMR and IR spectra. The *in vitro* biological evaluation revealed that some of the new compounds showed good antibacterial activity. 3-(2-Aminothiazol-4-yl)-7-chloro-6-(pyrrolidin-1-yl) quinolone **12b** exhibited particularly strong antibacterial activity against all eight tested bacterial strains with low MICs ranging from 0.5 to 2.7 μg/mL, a broad antibacterial spectrum, low cytotoxicity to human hepatocyte cells and strong inhibitory activity to DNA gyrase in comparison with Norfloxacin. Notably, the MRSA strain was very sensitive to aminothiazolquinolone **12b** (MIC = 0.8 μg/mL).

Further research suggested that compound **12b** induced MRSA and MQRSA resistance more slowly than Norfloxacin. SARs suggested that the 2-aminothiazole fragment was feasible to replace the 3-carboxyl group in the classical quinolone agent and that the substituents in the benzene ring of quinolone could also influence the antibacterial potency. It was found that ClogP values ranging from 3.3 to 4.2 gave the best balance. The binding investigation of compound **12b** with HSA revealed that this molecule could be effectively transported by HSA. Molecular modeling showed that the hydrogen bonds at the resistance mutation region and the interaction in the negatively supercoiled region might be the important reason for the compound's strong inhibitory efficacy against strains of quinolone-resistant bacteria. The binding mode of compound **12b** to MRSA DNA was the formation of a ternary complex mediated by Cu^{2+} ions, in which the copper ion acts as a bridge between the DNA phosphate groups and aminothiazole and carbonyl moieties of 3-aminothiazolquinolone **12b**. The optimal concentration of Cu^{2+} ion for ternary complex formation was in the range of intracellular Cu^{2+} ion concentrations in bacteria, so this binding mode might be biologically relevant. In addition, the preference exhibited by aminothiazolquinolone **12b** for ssDNA indicates that additional stabilization might arise from stacking interactions between the backbone of aminothiazolquinolone **12b** and DNA bases. Further studies, including the *in vivo* bioactive evaluation and the testing of other groups at the *N*-1, 6-, and 7-positions of quinolone, are now in progress.

5. EXPERIMENTAL SECTION

Melting points were recorded on X-6 melting point apparatus and uncorrected. TLC analysis was done using pre-coated silica gel plates. FT-IR spectra were carried out on Bruker RFS100/S spectrophotometer (Bio-Rad, Cambridge, MA, USA) using KBr pellets in the 400–4000 cm^{-1} range. NMR spectra were recorded on a Bruker AV 300/600 spectrometer using TMS as an internal standard. The chemical shifts were reported in parts per million (ppm), the coupling

constants (J) were expressed in hertz (Hz) and signals were described as singlet (s), doublet (d), triplet (t), as well as multiplet (m). The mass spectra were recorded on LCMS-2010A and the high-resolution mass spectra (HRMS) were recorded on an IonSpec FT-ICR mass spectrometer with ESI resource. All fluorescence spectra were recorded on F-7000 Spectrofluorimeter (Hitachi, Tokyo, Japan) equipped with 1.0 cm quartz cells. The UV spectrum was recorded at room temperature on a TU-2450 spectrophotometer (Puxi Analytic Instrument Ltd. of Beijing, China) equipped with 1.0 cm quartz cells. HSA, lysozyme, lysostaphin and 1,3,5-trioxane (> 99.5 %) were obtained from Sigma-Aldrich (St. Louis, MO, USA). Tris, NaCl, HCl and EDTA were analytical purity. Sample masses were weighed on a microbalance with a resolution of 0.1 mg. All other chemicals and solvents were commercially available, and were used without further purification.

5.1. Cytotoxicity Assay. The stock solutions of compound **12b** and Norfloxacin (1024 μg/mL, in DMSO) were prepared in medium and serially diluted. PC 12 cells and human hepatocyte LO2 cells were grown as monolayer in medium (90% DMEM medium, 10% fetal bovine serum, 1% penicillin/streptomycin; 90% RPMI-1640 medium, 10% fetal bovine serum, 1% penicillin/streptomycin) and maintained at 37 °C in a humidified atmosphere containing 5% CO_2, respectively. Cells were detached from culture flasks with 0.25% trypsin and 0.03% EDTA and resuspended in fresh culture medium at a density of 3.0×10^5 cells/mL (PC 12 cells) and 1.5×10^5 cells/mL (human hepatocyte LO2 cells). By use of a Falcon 96-well, flat-bottom plate, 100 μL of the cell suspension was added to each of the wells, and the cells were incubated for 24 h. The cells were treated with compound **12b** in triplicate at concentrations of 8, 16, 32, 64, 128, 256 and 512 μg/mL. After incubation with compound **12b** for 72 h, 50 μL of a 2.5 mg/mL solution of MTT in PBS was added to each well and further incubated for 3−4 h. The supernatant

was removed, and the cells were dissolved in 150 μL of DMSO. Absorbance values were measured at 490 nm by microplate reader.

5.2. DNA Gyrase Supercoiling Inhibition Assay. DNA supercoiling assay was performed in 96-well PCR plates in 30 μL volume. The reaction mixture contained 12.5 nM *Escherichia coli* DNA gyrase holoenzyme, 30 ng pBR322 DNA (Sigmae-Aldrich, St. Louis, MO, USA), 1.4 mM ATP, 1.8 mM spermidine, 5 mM Dithiothreitol, 0.14 mM Na_2EDTA, 6.5% glycerol, 24 mM KCl, 4 mM $MgCl_2$, 0.36 mg/mL bovine serum albumin (Sigmae-Aldrich, St. Louis, MO, USA), and 35 mM Tris-HCl (pH = 7.5), different concentrations drug (2.73, 1.37, 0.68, 0.34, 0.17, 0.085, 0.043, 0.021 μM). Each reaction mixture was incubated for 1.5 h at 37 °C, and reactions were stopped by the addition 3 μL of 2% Sodium dodecyl sulfate and 5.35% glycerol containing 0.013% bromophenol blue. The reaction mixture was loaded onto 1% TAE agarose gel, and the supercoiled and relaxed forms of DNA were separated by gel electrophoresis for 9 h at 1 V/cm. The gels were stained for 12 min with ethidium bromide (0.6 μg/mL) and destained in water for 30 min. The percent supercoiling DNA was determined by the densitometric tracing of supercoiling versus relaxed DNA.

5.3. Antibacterial Assay. MICs were determined as described by the NCCLS (see National Committee for Clinical Laboratory Standards. Performance Standards for Antimicrobial Susceptibility Testing: 11th Informational Supplement; National Committee for Clinical Laboratory Standards: Wayne, PA, 2001; Vol. 21, No. 1, M100-S11). The MIC was defined as the lowest concentration of each compound resulting in inhibition of visible growth of bacteria after incubation at 37 °C for 18−24 h. The bacterial suspension was adjusted with sterile saline to a concentration of 1×10^5 CFU. Initially the compounds were dissolved in DMSO to prepare the stock solutions, then the tested compounds and reference drugs were prepared in Muellere-Hinton broth (Guangdong huaikai microbial sci. & tech co., Ltd, Guangzhou, Guangdong, China)

to obtain the required concentrations of 512, 256, 128, 64, 32, 16, 8, 4, 2, 1, 0.5 μg/mL. These dilutions were inoculated and incubated at 37 °C for 24 h.

5.4. Compound 12b-HSA Complex Assay. All fluorescence spectra were recorded on F-7000 Spectrofluorimeter (Hitachi, Tokyo, Japan) equipped with 1.0 cm quartz cells, the widths of both the excitation and emission slit were set as 2.5 nm, and the excitation wavelength was 295 nm. Fluorescence spectra were recorded at 298 K in the range of 300–450 nm. HSA was obtained from Sigmae-Aldrich (St. Louis, MO, USA). HSA was dissolved in Tris-HCl buffer solution (0.05 M Tris, 0.15 M NaCl, pH = 7.4). Sample masses were weighed on a microbalance with a resolution of 0.1 mg. All other chemicals and solvents were commercially available, and were used without further purification. Graphs were produced using the OriginPro 7.5 software.

5.5 Compound 12b-DNA-Cu^{2+} Complex Assay. All fluorescence spectra were recorded on F-7000 Spectrofluorimeter (Hitachi, Tokyo, Japan) equipped with 1.0 cm quartz cells, the widths of both the excitation and emission slit were set as 5.0 nm, and the excitation wavelength was 366 nm. Fluorescence spectra were recorded at 298 K in the range of 386–550 nm. DNA was isolated from MRSA strain by column bacterial DNAOUT (from Sigmae-Aldrich, St. Louis, MO, USA). The purity and concentration of DNA was checked gel electrophoresis and UV spectrum. All other chemicals and solvents were commercially available, and were used without further purification. Graphs were produced using the OriginPro 7.5 software.

5.6 Purities of target compounds. The Purities of target aminothiazolquinolones were established by quantitative NMR. 1,3,5-Trioxane (>99.5%, 6.0 mg) and target aminothiazolquinolone (8.0 mg) were dissolved in DMSO-d_6. The ^{1}H NMR spectrum of this mixture was recorded on a Bruker AV 600 spectrometer using TMS as an internal standard. According the ^{1}H NMR spectrum, the absolute weight of aminothiazolquinolone can be deduced from the following equation:

$$W_X = W_S \times \frac{A_X}{A_S} \times \frac{M_X}{M_S} \times \frac{N_S}{N_X}$$

W_x and W_s represent the absolute weight of aminothiazolquinolone and 1,3,5-trioxane. A_x and A_s are the integral area of protons of methyl group in *N*-1 position of aminothiazolquinolone and protons of 1,3,5-trioxane. M_x and M_s are the molar mass of aminothiazolquinolone and 1,3,5-trioxane. N_x and N_s are the numbers of protons of methyl group in *N*-1 position of aminothiazolquinolone and protons of 1,3,5-trioxane.

General procedures for the preparation of intermediates (***1 and 2a–h***). Compounds **1** and **2a**–**h** were prepared according to the literature procedures.[47,48]

Ethyl 2-(((2,4-difluorophenyl)amino)methylene)-3-oxobutanoate (2a). Compound **1** (1.86 g, 0.01 mol) was stirred at 130 °C for 0.5 h, and then 2,4-difluoroaniline (1.29 g, 0.01 mol) was poured into the mixture. After the reaction was completed (monitored by TLC, eluent, petroleum/ethyl acetate 20/3, V/V), the mixture was cooled to room temperature, and then the generated ethanol was evaporated under reduced pressure. The residue was purified via silica gel column chromatography (eluent, petroleum/ethyl acetate 20/3, V/V) to give compound **2a** (2.46 g) as light yellow solid (Yield 91.5%, mp 78−80 °C). IR (KBr, cm^{-1}) ν: 3431 (*N*-H), 3100 (Ar-H), 3016 (=C-H), 2988, 2902 (CH_2, CH_3), 1715, 1745 (C=O); ^{1}H NMR (300 MHz, $CDCl_3$, ppm) δ 12.81 (d, *J* = 12.1 Hz, N-*H*, 1H), 8.41 (d, *J* = 12.9 Hz, C=C*H*, 1H), 7.31 (dd, *J* = 8.7, 5.5 Hz, 2,4-2F-Ph-3-*H*, 1H), 6.96 (ddd, *J* = 10.3, 6.8, 2.4 Hz, 2,4-2F-Ph-5,6-*H*, 2H), 4.27 (q, *J* = 7.1 Hz, COOC*H*$_2$CH$_3$, 2H), 2.56 (s, COC*H*$_3$, 3H), 1.35 (t, *J* = 7.1 Hz, COOCH$_2$C*H*$_3$, 3H); ^{13}C NMR (150 MHz, $CDCl_3$, ppm): δ 196.6, 166.7, 158.6, 153.4, 150.3, 123.3, 120.7, 111.3, 105.5, 103.8, 62.6, 29.5, 14.5; MS (ESI): m/z 270 $[M+H]^+$; HRMS (ESI) calcd. for $C_{13}H_{13}F_2NO_3$ $[M+H]^+$, 270.0942; found, 270.0941.

Ethyl 2-(((3,4-difluorophenyl)amino)methylene)-3-oxobutanoate (2b). Compound **2b** was prepared according to the procedure depicted for compound **2a**, starting from compound **1** (1.86 g, 0.01 mol) and 3,4-difluoroaniline (1.29 g, 0.01 mol). The desired product **2b** (2.41 g) was obtained as yellow solid (Yield 89.5%, mp 83−84 °C). IR (KBr, cm^{-1}) ν: 3430 (*N*-H), 3100 (Ar-H), 3015 (=C-H), 2985, 2932 (CH_2, CH_3), 1715, 1743 (C=O); ^{1}H NMR (300 MHz, $CDCl_3$, ppm): δ 12.75 (d, *J* = 12.2 Hz, N-*H*, 1H), 8.36 (d, *J* = 12.9 Hz, C=C*H*, 1H), 7.25–7.13 (m, 3,4-2F-Ph-2-*H*, 1H), 7.09–6.98 (m, 3,4-2F-Ph-6-*H*, 1H), 6.95–6.85 (m, 3,4-2F-Ph-5-*H*, 1H), 4.27 (q, *J* = 7.1 Hz, COOCH_2CH$_3$, 2H), 2.55 (s, COCH_3, 3H), 1.35 (t, *J* = 7.1 Hz, COOCH$_2$CH_3, 3H); ^{13}C NMR (150 MHz, $CDCl_3$, ppm): δ 195.6, 165.7, 149.5, 147.3, 141.3, 139.6, 116.3, 115.5, 106.8, 103.8, 62.6, 29.5, 14.5; MS (ESI): m/z 270 $[M+H]^+$; HRMS (ESI) calcd. for $C_{13}H_{13}F_2NO_3$ $[M+H]^+$, 270.0942; found, 270.0941.

Ethyl 2-(((4-fluorophenyl)amino)methylene)-3-oxobutanoate (2c). Compound **2c** was prepared according to the procedure depicted for compound **2a**, starting from compound **1** (1.86 g, 0.01 mol) and 2-fluoroaniline (1.11 g, 0.01 mol). The desired product **2c** (2.78 g) was obtained as yellow solid (Yield 90.1%, mp 68−69 °C). IR (KBr, cm^{-1}) ν: 3432 (*N*-H), 3105 (Ar-H), 3013 (=C-H), 2988, 2931 (CH_2, CH_3), 1715, 1745 (C=O); ^{1}H NMR (400 MHz, $CDCl_3$, ppm): δ 12.79 (s, N-*H*, 1H), 8.42 (d, *J* = 7.3 Hz, C=C*H*, 1H), 7.18 (d, *J* = 11.4 Hz, 2-F-Ph-4,6-*H*, 2H), 7.14−7.06 (m, 2-F-Ph-3,5-*H*, 2H), 4.27 (q, *J* = 7.1 Hz, COOCH_2CH$_3$, 2H), 2.56 (s, COCH_3, 3H), 1.36 (t, *J* = 7.1 Hz, COOCH$_2$CH_3, 3H); ^{13}C NMR (150 MHz, $CDCl_3$, ppm): δ 194.5, 165.0, 153.3, 149.8, 130.5, 127.6, 122.8, 117.6, 116.4, 103.8, 62.6, 29.5, 14.5; MS (ESI): m/z 252 $[M+H]^+$; HRMS (ESI) calcd. for $C_{13}H_{14}FNO_3$ $[M+H]^+$, 252.1036; found, 252.1037.

Ethyl 3-oxo-2-(((3-(trifluoromethyl)phenyl)amino)methylene)butanoate (2d). Compound **2d** was prepared according to the procedure depicted for compound **2a**, starting from compound **1** (1.86 g, 0.1 mol) and 3-(trifluoromethyl) aniline (1.61 g, 0.01 mol). Product **2d** (2.86 g) was

obtained as yellow solid (Yield 95.1%, mp 97−98 °C). IR (KBr, cm^{-1}) ν: 3432 (*N*-H), 3100 (Ar-H), 3013 (=C-H), 2988, 2931 (CH_2, CH_3), 1715, 1745 (C=O); ^{1}H NMR (300 MHz, $CDCl_3$, ppm): δ 12.84 (d, *J* = 12.2 Hz, N-*H*, 1H), 8.49 (d, *J* = 12.9 Hz, C=C*H*, 1H), 7.53 (t, *J* = 7.8 Hz, 3-CF_3-Ph-2-*H*, 1H), 7.40 (dd, *J* = 22.4, 9.2 Hz, 3-CF_3-Ph-4,5,6-*H*, 3H), 4.29 (q, *J* = 7.1 Hz, COOC*H*$_2$CH$_3$, 2H), 2.57 (s, COC*H*$_3$, 3H), 1.36 (t, *J* = 7.1 Hz, COOCH$_2$C*H*$_3$, 3H); ^{13}C NMR (150 MHz, $CDCl_3$): δ 194.6, 165.0, 149.5, 144.5, 131.8, 129.8, 124.1, 120.4, 119.5, 115.2, 103.7, 62.6, 29.5, 14.5; MS (ESI): m/z 302 $[M+H]^+$; HRMS (ESI) calcd. for $C_{14}H_{14}F_3NO_3$ $[M+H]^+$, 302.1004; found, 302.1003.

Ethyl 2-(((3-chloro-4-fluorophenyl)amino)methylene)-3-oxobutanoate (2e). Compound **2e** was prepared according to the procedure depicted for compound **2a**, starting from compound **1** (1.86 g, 0.01 mol) and 3-chloro-4-fluoroaniline (1.45 g, 0.01 mol). Product **2e** (2.62 g) was obtained as yellow solid (Yield 92.0%, mp 74−76 °C). IR (KBr, cm^{-1}) ν: 3432 (*N*-H), 3100 (Ar-H), 3013 (=C-H), 2988, 2931 (CH_2, CH_3), 1715, 1745 (C=O); ^{1}H NMR (300 MHz, $CDCl_3$, ppm): δ 12.75 (d, *J* = 12.3 Hz, N-*H*, 1H), 8.36 (d, *J* = 12.9 Hz, C=C*H*, 1H), 7.26–7.22 (m, 3-Cl-4-F-Ph-2-*H*, 1H), 7.17 (dd, *J* = 11.2, 5.9 Hz, 3-Cl-4-F-Ph-6-*H*, 1H), 7.09–7.01 (m, 3-Cl-4-F-Ph-5-*H*, 1H), 4.27 (q, *J* = 7.1 Hz, COOC*H*$_2$CH$_3$, 2H), 2.55 (s, COC*H*$_3$, 3H), 1.36 (t, *J* = 7.1 Hz, COOCH$_2$C*H*$_3$, 3H); ^{13}C NMR (150 MHz, $CDCl_3$, ppm): δ 194.6, 165.0, 149.5, 148.6, 141.4, 121.5, 118.3, 117.5, 114.2, 103.7, 62.6, 29.5, 14.5; MS (ESI): m/z 286 $[M+H]^+$; HRMS (ESI) calcd. for $C_{13}H_{13}FClNO_3$ $[M+H]^+$, 286.0646; found, 286.0644.

Ethyl 2-(((2,4-dichlorophenyl)amino)methylene)-3-oxobutanoate (2f). Compound **2f** was prepared according to the procedure depicted for compound **2a**, starting from compound **1** (1.86 g, 0.01 mol) and 2,4-dichloroaniline (1.61 g, 0.01 mol). Product **2f** (2.70 g) was obtained as yellow solid (Yield 90.0%, mp 63−65 °C). IR (KBr, cm^{-1}) ν: 3432 (*N*-H), 3100 (Ar-H), 3013 (=C-H), 2988, 2931 (CH_2, CH_3), 1715, 1745 (C=O); ^{1}H NMR (300 MHz, $CDCl_3$, ppm): δ 12.79

(s, N-*H*, 1H), 8.37 (s, C=C*H*, 1H), 7.36 (d. *J* = 7.2 Hz, 2,4-2Cl-Ph-6-*H*, 1H), 7.18−7.04 (m, 2,4-2Cl-Ph-3,5-*H*, 2H), 4.27 (q, *J* = 7.1 Hz, COOC*H*$_2$CH$_3$, 2H), 2.56 (s, COCH$_3$, 3H), 1.36 (t, *J* = 7.1 Hz, COOCH$_2$C*H*$_3$, 3H); ^{13}C NMR (150 MHz, CDCl$_3$, ppm): δ 194.5, 165.0, 149.8, 141.6, 131.2, 125.7, 123.6, 122.6, 121.6, 103.8, 62.6, 29.5, 14.5; MS (ESI): m/z 302 $[M+H]^+$; HRMS (ESI) calcd. for $C_{13}H_{13}Cl_2NO_3$ $[M+H]^+$, 302.0351; found, 302.0352.

Ethyl 2-(((4-fluorophenyl)amino)methylene)-3-oxobutanoate (2g). Compound **2g** was prepared according to the procedure depicted for compound **2a**, starting from compound **1** (1.86 g, 0.01 mol) and 4-dichloroaniline (1.11 g, 0.01 mol). Product **2g** (2.23 g) was obtained as yellow solid (Yield 89.1%, mp 71−73 °C). IR (KBr, cm^{-1}) ν: 3432 (*N*-H), 3100 (Ar-H), 3013 (=C-H), 2988, 2931 (CH$_2$, CH$_3$), 1715, 1745 (C=O); ^{1}H NMR (400 MHz, CDCl$_3$, ppm): δ 12.79 (s, N-*H*, 1H), 8.42 (d, *J* = 7.3 Hz, C=C*H*, 1H), 7.18 (d, *J* = 11.4 Hz, 4-F-Ph-2,6-*H*, 2H), 7.14−7.06 (m, 4-F-Ph-3,5-*H,* 2H), 4.27 (q, *J* = 7.1 Hz, COOC*H*$_2$CH$_3$, 2H), 2.56 (s, COC*H*$_3$, 3H), 1.36 (t, *J* = 7.1 Hz, COOCH$_2$C*H*$_3$, 3H); ^{13}C NMR (150 MHz, CDCl$_3$, ppm): δ 194.5, 165.0, 157.3, 149.8, 135.4, 120.8, 116.4, 103.8, 62.6, 29.5, 14.5; MS (ESI): m/z 252 $[M+H]^+$; HRMS (ESI) calcd. for $C_{13}H_{14}FNO_3$ $[M+H]^+$, 252.1036; found, 352.1034.

Ethyl 2-(((4-methoxyphenyl)amino)methylene)-3-oxobutanoate (2h). Compound **2h** was prepared according to the procedure depicted for compound **2a**, starting from compound **1** (1.86 g, 0.01 mol) and 4-methoxyaniline (1.23 g, 0.01 mol). Product **2h** (2.45 g) was obtained as yellow solid (Yield 93.1%, mp 56−58 °C). IR (KBr, cm^{-1}) ν: 3432 (*N*-H), 3100 (Ar-H), 3013 (=C-H), 2988, 2931 (CH$_2$, CH$_3$), 1715, 1745 (C=O); ^{1}H NMR (300 MHz, CDCl$_3$, ppm): δ 12.71 (s, N-*H*, 1H), 8.40 (d, *J* = 7.3 Hz, C=C*H*, 1H), 7.16 (d, *J* = 11.4 Hz, 4-CH$_3$O-Ph-2,6-*H*, 2H), 7.08 (d, *J* = 11.3 Hz, 4-CH$_3$O-Ph-3,5-*H,* 2H), 4.27 (q, *J* = 7.1 Hz, COOC*H*$_2$CH$_3$, 2H), 2.56 (s, COC*H*$_3$, 3H), 1.35 (t, *J* = 7.1 Hz, COOCH$_2$C*H*$_3$, 3H); ^{13}C NMR (150 MHz, CDCl$_3$, ppm): δ 194.5, 165.0,

157.4, 149.8, 136.2, 117.6, 115.3, 103.8, 62.6, 52.6, 29.5, 14.5; MS (ESI): m/z 264 $[M+H]^+$; HRMS (ESI) calcd. for $C_{13}H_{17}NO_4$ $[M+H]^+$, 264.1236; found, 264.1235.

Ethyl 3-oxo-2-((p-tolylamino)methylene)butanoate (2i). Compound **2i** was prepared according to the procedure depicted for compound **2a**, starting from compound **1** (1.86 g, 0.01 mol) and 4-methoxyaniline (1.07 g, 0.01 mol). Product **2i** (2.17 g) was obtained as yellow solid (Yield 88.0%, mp 53−55 °C). IR (KBr, cm^{-1}) ν: 3432 (*N*-H), 3100 (Ar-H), 3013 (=C-H), 2988, 2931 (CH_2, CH_3), 1715, 1745 (C=O); ^{1}H NMR (300 MHz, $CDCl_3$, ppm): δ 12.76 (d, *J* = 12.7 Hz, N-*H*, 1H), 8.47 (d, *J* = 13.2 Hz, C=C*H*, 1H), 7.18 (d, *J* = 7.8 Hz, 4-CH_3-Ph-2,6-*H*, 2H), 7.07 (d, *J* = 8.1 Hz, 4-CH_3-Ph-3,5-*H*, 2H), 4.25 (q, *J* = 7.0 Hz, COOC*H*$_2$$CH_3$, 2H), 2.55 (s, COC*H*$_3$, 3H), 2.34 (s, $COOCH_2CH_3$, 3H), 1.34 (t, *J* = 7.1 Hz, $COOCH_2CH_3$, 3H); ^{13}C NMR (150 MHz, $CDCl_3$, ppm): δ 199.9, 167.0, 152.0, 136.6, 135.4, 130.3, 117.7, 117.3, 102.1, 77.5, 59.8, 31.1, 20.9, 14.5; MS (ESI): m/z 248 $[M+H]^+$; HRMS (ESI) calcd. for $C_{14}H_{17}NO_3$ $[M+H]^+$, 248.1287; found, 248.1285

3-Acetyl-6,8-difluoroquinolin-4(1H)-one (3a). Compound **2a (**2.69 g, 0.01 mol) was added portion wise to of boiling diphenyl ether (50 mL) previously heated at 250 ^{o}C. The solution was kept under reflux for 1.5 h. When the reaction was completed (monitored by TLC, eluent, chloroform/methanol 70/1, V/V), the mixture was cooled to room temperature, the formed precipitate was collected. The crude product was purified by chromatography on silica gel column (eluent, chloroform/methanol 70/1, V/V) to provide pure compound **2a** (1.15 g) as brown solid (Yield 51.3%, mp >250 °C). IR (KBr, cm^{-1}) ν: 3475 (*N*-H), 3027 (=C-H), 2950 (CH_3), 1740, 1711 (C=O); ^{1}H NMR (600 MHz, $CDCl_3$, ppm) δ 12.72 (s, N-*H*, 1H), 8.32 (s, quinolone-2-*H*, 1H), 7.87 (m, quinolone-5-*H*, 1H), 6.97 (m, quinolone-5-*H*, 1H), 2.69 (s, COC*H*$_3$, 3H); ^{13}C NMR (150 MHz, $CDCl_3$, ppm): δ 197.0, 173.1, 157.1, 149.8, 133.7, 129.5, 123.1, 118.7, 117.5,

108.9, 31.4; MS (ESI): m/z 224 $[M+H]^+$; HRMS (ESI) calcd. for $C_{11}H_7F_2NO_2$ $[M+H]^+$, 224.0523; found, 224.0524.

3-Acetyl-6,7-difluoroquinolin-4(1H)-one (3b). Compound **3b** was prepared according to the procedure depicted for compound **3a**, starting from compound **2b** (2.69 g, 0.01 mol). Product **3b** (1.17 g) was obtained as yellow solid (Yield 56.1%, mp >250 °C). IR (KBr, cm^{-1}) ν: 3475 (*N*-H), 3027 (=C-H), 2950 (CH_3), 1741, 1711 (C=O); ^{1}H NMR (600 MHz, $CDCl_3$, ppm) δ 12.71 (s, N-*H*, 1H), 8.51 (s, quinolone-5-*H*, 1H), 8.27 (s, quinolone-5-*H*, 1H), 7.21 (s, quinolone-8-*H*, 1H), 2.79 (s, COCH_3, 3H); ^{13}C NMR (150 MHz, $CDCl_3$, ppm): δ 197.5, 176.3, 152.8, 148.4, 147.6, 135.1, 128.7, 118.2, 117.5, 110.1, 31.4; MS (ESI): m/z 224 $[M+H]^+$; HRMS (ESI) calcd. for $C_{11}H_7F_2NO_2$ $[M+H]^+$, 224.0523; found, 224.0522.

3-Acetyl-8-fluoroquinolin-4(1H)-one (3c). Compound **3c** was prepared according to the procedure depicted for compound **3a**, starting from compound **2c** (2.51 g, 0.01 mol). Product **3c** (0.92 g) was obtained as yellow solid (Yield 46.0%, mp >250 °C). IR (KBr, cm^{-1}) ν: 3475 (*N*-H), 3027 (=C-H), 2950 (CH_3), 1737, 1710 (C=O); ^{1}H NMR (300 MHz, $CDCl_3$, ppm) δ 12.71 (s, N-*H*, 1H), 8.52 (s, quinolone-2-*H*, 1H), 7.52 (d, *J* = 2.8 Hz, quinolone-5-*H*, 1H), 7.24 (d, *J* = 2.1 Hz, quinolone-7-*H*, 1H), 6.92 (m, quinolone-6-*H*, 1H), 2.62 (s, COCH_3, 3H); ^{13}C NMR (150 MHz, $CDCl_3$, ppm): δ 197.5, 175.5, 154.6, 151.1, 131.3, 130.7, 125.5, 123.6, 123.1, 115.1, 32.3; MS (ESI): m/z 206 $[M+H]^+$; HRMS (ESI) calcd. for $C_{11}H_8FNO_2$ $[M+H]^+$, 206.0617; found, 206.0618.

3-Acetyl-7-(trifluoromethyl)quinolin-4(1H)-one (3d). Compound **3d** was prepared according to the procedure depicted for compound **3a**, starting from compound **2d** (3.01 g, 0.01 mol). Product **3d** (1.40 g) was obtained as yellow solid (Yield 55.2%, mp >250 °C). IR (KBr, cm^{-1}) ν: 3475 (*N*-H), 3027 (=C-H), 2950 (CH_3), 1742, 1716 (C=O); ^{1}H NMR (300 MHz, $CDCl_3$, ppm) δ 12.81 (s, N-*H*, 1H), 8.71 (s, quinolone-2-*H*, 1H), 7.57 (d, *J* = 3.1 Hz, quinolone-5-*H*, 1H),

7.32 (d, *J* = 3.4 Hz, quinolone-6-*H*, 1H), 7.12 (s, quinolone-8-*H*, 1H), 2.61 (s, COCH_3, 3H); ^{13}C NMR (150 MHz, $CDCl_3$, ppm): δ 197.4, 174.4, 152.8, 137.2, 135.8, 131.62, 126.2, 123.7, 113.6, 113.1, 112.0, 32.4; MS (ESI): m/z 256 $[M+H]^+$; HRMS (ESI) calcd. for $C_{12}H_8F_3NO_2$ $[M+H]^+$, 256.0585; found, 256.0583.

3-Acetyl-7-chloro-6-fluoroquinolin-4(1H)-one (3e). Compound **3e** was prepared according to the procedure depicted for compound **3a**, starting from compound **2e** (2.85 g, 0.01 mol). Product **3e** (1.22 g) was obtained as yellow solid (Yield 51.2%, mp >250 °C). IR (KBr, cm^{-1}) ν: 3475 (*N*-H), 3027 (=C-H), 2950 (CH_3), 1740, 1711 (C=O); ^{1}H NMR (300 MHz, $CDCl_3$) δ 12.71 (s, N-*H*, 1H), 8.62 (s, quinolone-2-*H*, 1H), 8.21 (d, *J* = 6.1 Hz, quinolone-5-*H*, 1H), 8.05 (d, *J* = 9.4 Hz, quinolone-8-*H*, 1H), 2.62 (s, COCH_3, 2H); ^{13}C NMR (150 MHz, $CDCl_3$, ppm): δ 197.5, 176.0, 156.9, 151.3, 142.4, 134.7, 127.6, 126.2, 118.2, 115.1, 32.3; MS (ESI): m/z 240 $[M+H]^+$; HRMS (ESI) calcd. for $C_{11}H_7ClFNO_2$ $[M+H]^+$, 240.0228; found, 240.0230.

3-Acetyl-6,8-dichloroquinolin-4(1H)-one (3f). Compound **3f** was prepared according to the procedure depicted for compound **3a**, starting from compound **2f** (3.01 g, 0.01 mol). Product **3f** (1.07 g) was obtained as yellow solid (Yield 42.3%, mp >250 °C). IR (KBr, cm^{-1}) ν: 3475 (*N*-H), 3027 (=C-H), 2950 (CH_3), 1741, 1710 (C=O); ^{1}H NMR (300 MHz, $CDCl_3$, ppm) δ 12.73 (s, N-*H*, 1H), 8.62 (s, quinolone-2-*H*, 1H), 8.09 (s, quinolone-5-*H*, 1H), 7.28 (s, quinolone-7-*H*, 1H), 2.61 (s, COCH_3, 3H); ^{13}C NMR (150 MHz, $CDCl_3$, ppm): δ 197.5, 172.5, 152.4, 142.1, 136.4, 134.7, 134.1, 121.3, 120.1, 112.1, 32.5; MS (ESI): m/z 255 $[M+H]^+$; HRMS (ESI) calcd. for $C_{11}H_7Cl_2NO_2$ $[M+H]^+$, 255.9932; found, 255.9931.

3-Acetyl-6-fluoroquinolin-4(1H)-one (3g). Compound **3g** was prepared according to the procedure depicted for compound **3a**, starting from compound **2g** (2.51 g, 0.01 mol). Product **3g** (1.02 g) was obtained as yellow solid (Yield 49.7%, mp >250 °C). IR (KBr, cm^{-1}) ν: 3475 (*N*-H), 3027 (=C-H), 2950 (CH_3), 1735, 1707 (C=O); ^{1}H NMR (400 MHz, DMSO-d_6, ppm) δ 12.70 (s,

N-*H*, 1H), 8.56 (s, quinolone-2-*H*, 1H), 7.88 (dd, *J* = 9.3, 2.8 Hz, quinolone-5-*H*, 1H), 7.73 (dd, *J* = 9.0, 4.7 Hz, quinolone-7-*H*, 1H), 7.65 (m, quinolone-8-*H*, 1H), 2.62 (s, COCH_3, 3H); ^{13}C NMR (150 MHz, DMSO-d_6, ppm): δ 197.5, 174.7, 157.5, 151.1, 135.5, 130.4, 123.9, 113.6, 113.0, 115.0, 32.3; MS (ESI): m/z 206 $[M+H]^+$; HRMS (ESI) calcd. for $C_{11}H_8FNO_2$ $[M+H]^+$, 206.0617; found, 206.0616.

3-Acetyl-6-methoxyquinolin-4(1H)-one (3h). Compound **3h** was prepared according to the procedure depicted for compound **3a**, starting from compound **2h** (2.63 g, 0.01 mol). Product **3h** (1.02 g) was obtained as yellow solid (Yield 49.7%, mp >250 °C). IR (KBr, cm^{-1}) ν: 3475 (*N*-H), 3027 (=C-H), 2950 (CH_3), 1732, 1701 (C=O); ^{1}H NMR (300 MHz, $CDCl_3$, ppm) δ 12.72 (s, N-*H*, 1H), 8.71 (s, quinolone-2-*H*, 1H), 7.46 (s, quinolone-5-*H*, 1H), 7.12 (d, *J* = 3.4 Hz, quinolone-7-*H*, 1H), 7.02 (d, *J* = 2.1 Hz, quinolone-8-*H*, 1H), 3.81 (s, quinolone-6-OCH_3, 3H), 2.63 (s, quinolone-3-COCH_3, 3H); ^{13}C NMR (150 MHz, $CDCl_3$, ppm): δ 197.4, 173.8, 152.7, 151.7, 132.7, 132.1, 121.7, 115.6, 112.8, 112.2, 51.8, 32.3; MS (ESI): m/z 218 $[M+H]^+$; HRMS (ESI) calcd. for $C_{12}H_{11}NO_3$ $[M+H]^+$, 218.0817; found, 218.0815.

3-Acetyl-6-methylquinolin-4(1H)-one (3i). Compound **3i** was prepared according to the procedure depicted for compound **3a**, starting from compound **2i** (2.47 g, 0.01 mol). Product **3i** (1.07 g) was obtained as yellow solid (Yield 53.1%, mp >250 °C). IR (KBr, cm^{-1}) ν: 3475 (*N*-H), 3027 (=C-H), 2950 (CH_3), 1727, 1710 (C=O); ^{1}H NMR (300 MHz, $CDCl_3$, ppm): δ 12.71 (s, N-*H*, 1H), 8.56 (s, quinolone-2-*H*, 1H), 7.25 (s, quinolone-5-*H*, 1H), 7.08 (d, *J* = 2.1 Hz, quinolone-7-*H*, 1H), 6.71 (d, *J* = 2.3 Hz, quinolone-8-*H*, 1H), 2.54 (s, COCH_3, 3H), 2.31 (s, quinolone-6-CH_3, 3H); ^{13}C NMR (150 MHz, $CDCl_3$, ppm): δ 197.3, 171.4, 151.9, 134.1, 132.6, 131.7, 131.1, 127.7, 113.5, 111.1, 32.3, 21.2; MS (ESI): m/z 202 $[M+H]^+$; HRMS (ESI) calcd. for $C_{12}H_{11}NO_2$ $[M+H]^+$, 202.6808; found, 202.6809.

3-Acetyl-1-ethyl-6,8-difluoroquinolin-4(1H)-one (4a). To a stirred suspension of potassium carbonate (1.51 g, 0.01 mol) in *N*,*N*-dimethylformamide (25 mL) was added intermediate **3a** (2.23 g, 0.01 mol). The mixture was stirred at 60 °C for 1.5 h, and then was cooled to room temperature. Bromoethane (5.35 g, 0.05 mol) was added, and the mixture was stirred at 130 ^{o}C for 12 h. After the reaction came to end (monitored by TLC, eluent, chloroform), the solvent was evaporated under reduced pressure and the residue was treated with water and extract with chloroform (3 × 20 mL). The combined organic extracts was dried over anhydrous sodium sulfate and concentrated. The crude product was purified via silica gel column chromatography (eluent, chloroform) to yield compound **4a** (1.53 g) as yellow solid (Yield: 61.2%, mp >250 °C). IR (KBr, cm^{-1}) ν: 3100 (Ar-H), 3051 (=C-H), 2989, 2946 (CH_2, CH_3), 1735, 1716 (C=O); ^{1}H NMR (600 MHz, $CDCl_3$, ppm): δ 8.35 (s, quinolone-2-*H*, 1H), 7.98 (s, quinolone-5-*H*, 1H), 6.97 (d, *J* = 50.0 Hz, quinolone-7-*H*, 1H), 4.33 (q, *J* = 7.3 Hz, C*H*$_2$CH$_3$, 2H), 2.69 (s, COC*H*$_3$, 3H), 1.45 (s, CH$_2$C*H*$_3$, 3H); ^{13}C NMR (150 MHz, $CDCl_3$, ppm): δ 197.0, 173.4, 157.2, 149.8, 133.8, 129.7, 123.2, 118.9, 117.8, 109.4, 53.7, 31.4, 16.1; MS (ESI): m/z 252 $[M+H]^+$; HRMS (ESI) calcd. for $C_{13}H_{11}F_2NO_2$ $[M+H]^+$, 252.0836; found, 252.0835.

3-Acetyl-1-ethyl-6,7-difluoroquinolin-4(1H)-one (4b). Compound **4b** was prepared according to the procedure depicted for compound **4a**, starting from compound **3b** (2.23 g, 0.01 mol), potassium carbonate (1.51 g, 0.01 mol) and bromoethane (5.35 g, 0.05 mol). Product **4b** (1.63 g) was obtained as yellow solid (Yield 64.8%, mp >250 °C). IR (KBr, cm^{-1}) ν: 3085 (Ar-H), 3047 (=C-H), 2989, 2942 (CH_2, CH_3), 1735, 1716 (C=O); ^{1}H NMR (600 MHz, $CDCl_3$, ppm): δ 8.53 (s, quinolone-2-*H*, 1H), 8.34 (s, quinolone-5-*H*, 1H), 7.31 (s, quinolone-8-*H*, 1H), 4.25 (q, *J* = 7.3 Hz, C*H*$_2$CH$_3$, 2H), 2.79 (s, COC*H*$_3$, 3H), 1.65 (s, CH$_2$C*H*$_3$, 3H); ^{13}C NMR (150 MHz, $CDCl_3$, ppm): δ 197.5, 177.5, 153.1, 148.4, 147. 7, 135.1, 129.7, 118.4, 117.6, 110.1, 53.6, 31.4,

16.1; MS (ESI): m/z 252 $[M+H]^+$; HRMS (ESI) calcd. for $C_{13}H_{11}F_2NO_2$ $[M+H]^+$, 252.0836; found, 252.0835.

3-Acetyl-1-ethyl-8-fluoroquinolin-4(1H)-one (4c). Compound **4c** was prepared according to the procedure depicted for compound **4a**, starting from compound **3c** (2.05 g, 0.01 mol), potassium carbonate (1.51 g, 0.01 mol) and bromoethane (5.35 g, 0.05 mol). The desired product **4c** (1.72 g) was obtained as yellow solid (Yield 74.2%, mp >250 °C). IR (KBr, cm^{-1}) ν: 3090 (Ar-H), 3050 (=C-H), 2989, 2943 (CH_2, CH_3), 1735, 1716 (C=O); ^1H NMR (400 MHz, $CDCl_3$, ppm): δ 8.58 (s, quinolone-2-*H*, 1H), 7.54 (d, *J* = 7.1, quinolone-5-*H*, 1H), 7.45 (m, quinolone-7-*H*, 1H), 7.16 (m, quinolone-6-*H*, 1H), 4.28 (q, *J* = 7.1 Hz, C*H*$_2$CH$_3$, 2H), 2.62 (s, COC*H*$_3$, 3H), 1.54 (t, *J* = 7.2 Hz, CH$_2$C*H*$_3$, 3H); ^{13}C NMR (150 MHz, $CDCl_3$, ppm): δ 197.1, 173.2, 151.6, 142.9, 131.4, 128.5, 125.4, 121.1, 119.2, 105.6, 53.6, 31.4, 16.1; MS (ESI): m/z 234 $[M+H]^+$; HRMS (ESI) calcd. for $C_{13}H_{12}FNO_2$ $[M+H]^+$, 234.0930; found, 234.0931.

3-Acetyl-1-ethyl-7-(trifluoromethyl)quinolin-4(1H)-one (4d). Compound **4d** was prepared according to the procedure depicted for compound **4a**, starting from compound **3d** (2.55 g, 0.01 mol), potassium carbonate (1.51 g, 0.01 mol) and bromoethane (5.35 g, 0.05 mol). Product **4d** (2.01 g) was obtained as yellow solid (Yield 70.6%, mp >250 °C). IR (KBr, cm^{-1}) ν: 3110 (Ar-H), 3050 (=C-H), 2989, 2945 (CH_2, CH_3), 1735, 1716 (C=O); ^1H NMR (300 MHz, $CDCl_3$, ppm): δ 8.68 (d, *J* = 8.3 Hz, quinolone-2-*H*, 1H), 8.60 (s, quinolone-5-*H*, 1H), 7.78–7.65 (m, quinolone-6,8-*H*, 2H), 4.34 (q, *J* = 7.3 Hz, C*H*$_2$CH$_3$, 2H), 2.80 (s, COC*H*$_3$, 3H), 1.59 (t, *J* = 7.2 Hz, CH$_2$C*H*$_3$, 3H); ^{13}C NMR (150 MHz, $CDCl_3$, ppm): δ 197.1, 177.4, 143.9, 140.1, 137.3, 128.2, 126.1, 124.1, 114.3, 112.2, 109.8, 53.6, 31.4, 16.1; MS (ESI): m/z 306 $[M+Na]^+$; HRMS (ESI) calcd. for $C_{14}H_{12}F_3NO_2$ $[M+Na]^+$, 306.0718; found, 306.0716.

3-Acetyl-7-chloro-1-ethyl-6-fluoroquinolin-4(1H)-one (4e). Compound **4e** was prepared according to the procedure depicted for compound **4a**, starting from compound **3e** (2.39 g, 0.01

mol), potassium carbonate (1.51 g, 0.01 mol) and bromoethane (5.35 g, 0.05 mol). Product **4e** (1.83 g) was obtained as yellow solid (Yield 68.8%, mp >250 °C). IR (KBr, cm^{-1}) ν: 3090 (Ar-H), 3050 (=C-H), 2989, 2955 (CH_2, CH_3), 1735, 1716 (C=O); ^{1}H NMR (300 MHz, DMSO-d_6, ppm): δ 8.67 (s, quinolone-2-*H*, 1H), 8.22 (d, *J* = 6.0 Hz, quinolone-5-*H*, 1H), 8.10 (d, *J* = 9.4 Hz, quinolone-8-*H*, 1H), 4.46 (q, *J* = 7.0 Hz, C*H*$_2$CH$_3$, 2H), 2.61 (s, COCH$_3$, 2H), 1.35 (t, *J* = 7.0 Hz, CH$_2$C*H*$_3$, 3H); ^{13}C NMR (150 MHz, DMSO-d_6, ppm): δ 197.5, 177.5, 157.6, 154.3, 142.8, 134.3, 128.9, 127.2, 118.2, 115.1, 51.6, 32.3, 14.3; MS (ESI): m/z 290 $[M+Na]^+$; HRMS (ESI) calcd. for $C_{13}H_{11}ClFNO_2$ $[M+Na]^+$, 290.0360; found, 290.0361.

3-Acetyl-6,8-dichloro-1-ethylquinolin-4(1H)-one (4f). Compound **4f** was prepared according to the procedure depicted for compound **4a**, starting from compound **3f** (2.54 g, 0.01 mol), potassium carbonate (1.51 g, 0.01 mol) and bromoethane (5.35 g, 0.05 mol). Product **4f** (1.85 g) was obtained as yellow solid (Yield 65.2%, mp >250 °C). IR (KBr, cm^{-1}) ν: 3102 (Ar-H), 3050 (=C-H), 2989, 2935 (CH_2, CH_3), 1735, 1716 (C=O); ^{1}H NMR (300 MHz, $CDCl_3$, ppm) δ 8.65 (s, quinolone-2-*H*, 1H), 8.01 (s, quinolone-5-*H*, 1H), 7.15 (s, quinolone-7-*H*, 1H), 4.28 (q, *J* = 7.1 Hz, C*H*$_2$CH$_3$, 2H), 2.61 (s, COC*H*$_3$, 3H), 1.54 (t, *J* = 7.2 Hz, CH$_2$C*H*$_3$, 3H); ^{13}C NMR (150 MHz, $CDCl_3$, ppm): δ 196.5, 172.4, 151.2, 140.0, 135.3, 133.71, 134.1, 121.3, 120.1, 112.1, 53.6, 32.6, 14.3; MS (ESI): m/z 255 $[M+H]^+$; HRMS (ESI) calcd. for $C_{13}H_{11}Cl_2NO_2$ $[M+H]^+$, 284.0245; found, 284.0243.

3-Acetyl-1-ethyl-6-fluoroquinolin-4(1H)-one (4g). Compound **4g** was prepared according to the procedure depicted for compound **4a**, starting from compound **3g** (2.05 g, 0.01 mol), potassium carbonate (1.51 g, 0.01 mol) and bromoethane (5.35 g, 0.05 mol). Product **4g** (1.40 g) was obtained as yellow solid (Yield 60.0%, mp >250 °C). IR (KBr, cm^{-1}) ν: 3070 (Ar-H), 3048 (=C-H), 2989, 2935 (CH_2, CH_3), 1735, 1716 (C=O); ^{1}H NMR (400 MHz, DMSO-d_6, ppm) δ 8.56 (s, quinolone-2-*H*, 1H), 7.68 (m, quinolone-5-*H*, 1H), 7.65 (m, quinolone-7-*H*, 1H), 7.55 (m,

quinolone-8-*H*, 1H), 4.28 (d, *J* = 14.3, 7.1 Hz, C*H*$_2$CH$_3$, 2H), 2.62 (s, 3H), 1.54 (t, *J* = 7.2 Hz, COC*H*$_3$,3 CH$_2$C*H*$_3$, H); ^{13}C NMR (150 MHz, DMSO-d$_6$, ppm): δ 197.0, 173.2, 157.6, 142.9, 134.5, 130.5, 121.4, 117.1, 113.3, 105.6, 53.6, 31.4, 16.1; MS (ESI): m/z 234 $[M+H]^+$; HRMS (ESI) calcd. for $C_{13}H_{12}FNO_2$ $[M+H]^+$, 234.0930; found, 234.0931.

3-Acetyl-1-ethyl-6-methoxyquinolin-4(1H)-one (4h). Compound **4h** was prepared according to the procedure depicted for compound **4a**, starting from compound **3h** (2.17 g, 0.01 mol), potassium carbonate (1.51 g, 0.01 mol) and bromoethane (5.35 g, 0.05 mol). Product **4h** (1.45 g) was obtained as yellow solid (Yield 58.9%, mp >250 °C). IR (KBr, cm^{-1}) ν: 3090 (Ar-H), 3050 (=C-H), 2989, 2935 (CH$_2$, CH$_3$), 1735, 1716 (C=O); ^{1}H NMR (300 MHz, CDCl$_3$, ppm) δ 8.53 (s, quinolone-2-*H*, 1H), 8.45 (s, quinolone-5-*H*, 1H), 7.53 (d, *J* = 8.4 Hz, quinolone-7-*H*, 1H), 7.46 (d, *J* = 8.5 Hz, quinolone-8-*H*, 1H), 4.28 (d, *J* = 14.3, 7.1 Hz, C*H*$_2$CH$_3$, 2H), 3.81 (s, quinolone-6-OC*H*$_3$, 3H), 2.50 (s, COCH$_3$, 3H), 1.54 (t, *J* = 7.2 Hz, CH$_2$C*H*$_3$, 3H); ^{13}C NMR (150 MHz, CDCl$_3$, ppm): δ 197.0, 173.2, 153.7, 142.5, 131.2, 130.3, 120.4, 112.2, 111.3, 105.6, 53.6, 31.4, 20.3, 16.1; MS (ESI): m/z 246 $[M+H]^+$; HRMS (ESI) calcd. for $C_{14}H_{15}NO_2$ $[M+H]^+$, 246.1130; found, 246.1128.

3-Acetyl-1-ethyl-6-methylquinolin-4(1H)-one (4i). Compound **4i** was prepared according to the procedure depicted for compound **4a**, starting from compound **3i** (2.01 g, 0.01 mol), potassium carbonate (1.51 g, 0.01 mol) and bromoethane (5.35 g, 0.05 mol). Product **4g** (1.41 g) was obtained as yellow solid (Yield 65.0%, mp >250 °C). IR (KBr, cm^{-1}) ν: 3085 (Ar-H), 3035 (=C-H), 2989, 2935 (CH$_2$, CH$_3$), 1735, 1716 (C=O); ^{1}H NMR (300 MHz, CDCl$_3$, ppm) δ 8.23 (s, quinolone-2-*H*, 1H), 8.35 (s, quinolone-5-*H*, 1H), 7.54 (d, *J* = 8.5 Hz, quinolone-7-*H*, 1H), 7.40 (d, *J* = 8.6 Hz, quinolone-8-*H*, 1H), 4.28 (dd, *J* = 14.3, 7.1 Hz, C*H*$_2$CH$_3$, 2H), 2.81 (s, COC*H*$_3$, 3H), 2.50 (s, CH$_2$C*H*$_3$, 3H), 1.54 (t, *J* = 7.2 Hz, CH$_2$C*H*$_3$, 3H); ^{13}C NMR (150 MHz, CDCl$_3$, ppm): δ 197.0, 173.2, 142.5, 135.7, 130.7, 126.4, 124.3, 121.3, 112.2, 109.8, 53.6, 31.4, 20.3,

16.1; MS (ESI): m/z 230 $[M+H]^+$; HRMS (ESI) calcd. for $C_{14}H_{15}NO_2$ $[M+H]^+$, 230.1181; found, 230.1180.

3-(2-Aminothiazol-4-yl)-1-ethyl-6,8-difluoroquinolin-4(1H)-one (6a). A mixture of compound **5a** (0.33 g, 1 mmol) and thiourea (0.076 g, 1 mmol) was stirred at 60 ^oC in ethanol (30 mL) for 3 h. When the reaction was completed (monitored by TLC, eluent, chloroform/methanol 50/1, V/V), the mixture was cooled to room temperature, and then the solvent was evaporated under reduced pressure. After ethyl acetate was added, the resulting mixture was washed with saturated sodium bicarbonate solution (3 × 20 mL). The organic phase was dried over anhydrous sodium sulfate and concentrated under reduced pressure. The residue was purified via silica gel column chromatography (eluent, chloroform/ methanol 50/1, V/V) to give compound **6a** (0.246 g) as light yellow solid (Yield 80.0%, mp 240−242 °C). IR (KBr, cm^{-1}) ν: 3463, 3432 (*N*-H), 3170 (Ar-H), 3036 (=C-H), 2995, 2945 (CH_2, CH_3), 1756 (C=O); ^1H NMR (600 MHz, $CDCl_3$, ppm) δ 8.59 (s, quinolone-2-*H*, 1H), 8.09 (d, *J* = 7.5 Hz, quinolone-5-*H*, 1H), 7.94 (s, thiazole-5-*H*, 1H), 7.18 (ddd, *J* = 14.1, 7.5, 2.7 Hz, quinolone-7-*H*, 1H), 4.98 (s, thiazole-2-NH_2, 2H), 4.43 (tt, *J* = 6.9, 3.5 Hz, CH_2CH$_3$, 2H), 1.52 (t, *J* = 7.1 Hz, CH$_2$CH_3, 3H); ^{13}C NMR (150 MHz, $CDCl_3$): δ 172.8, 165.8, 158.8, 144.6, 144.0, 130.8, 125.0, 115.3, 108.3, 108.1, 107.9, 107,7, 51.0, 16.2; MS (ESI): m/z 308 $[M+H]^+$; HRMS (ESI) calcd. for $C_{14}H_{11}F_2N_3OS$ $[M+H]^+$, 308.0669; found, 308.0670.

3-(2-Aminothiazol-4-yl)-1-ethyl-6,7-difluoroquinolin-4(1H)-one (6b). Compound **6b** was prepared according to the procedure depicted for compound **6a**, starting from compound **5b** (0.33 g, 1 mmol) and thiourea (0.076 g, 1 mmol). Product **6b** (0.261 g) was obtained as yellow solid (Yield 85.1%, mp 238−240 °C). IR (KBr, cm^{-1}) ν: 3463, 3432 (*N*-H), 3170 (Ar-H), 3036 (=C-H), 2995, 2945 (CH_2, CH_3), 1756 (C=O); ^1H NMR (600 MHz, $CDCl_3$, ppm): δ 8.64 (s, quinolone-2-*H*, 1H), 8.35 (dd, *J* = 10.7, 9.0 Hz, quinolone-5-*H*, 1H), 7.95 (s, thiazole-5-*H*, 1H), 7.31–7.27 (m,

quinolone-8-*H*, 1H), 4.85 (s, thiazole-2-NH_2, 2H), 4.23 (q, *J* = 7.3 Hz, CH_2CH$_3$, 2H), 1.55 (t, *J* = 7.2 Hz, CH$_2$CH_3, 3H); ^{13}C NMR (150 MHz, CDCl$_3$, ppm): δ 179.3, 165.5, 154.6, 150.9, 142.3, 133.9, 130.7, 124.5, 118.7, 115.0, 107.5, 103.7, 48.8, 14.6; MS (ESI): m/z 308 $[M+H]^+$; HRMS (ESI) calcd. for $C_{14}H_{11}F_2N_3OS$ $[M+H]^+$, 308.0669; found, 308.0667.

3-(2-Aminothiazol-4-yl)-1-ethyl-8-fluoroquinolin-4(1H)-one (6c). Compound **6c** was prepared according to the procedure depicted for compound **6a**, starting from compound **5c** (0.31 g, 1 mmol) and thiourea (0.076 g, 1 mmol). Product **6c** (0.231 g) was obtained as yellow solid (Yield 82.5%, mp 236−237 °C). IR (KBr, cm^{-1}) ν: 3463, 3432 (*N*-H), 3170 (Ar-H), 3036 (=C-H), 2995, 2945 (CH$_2$, CH$_3$), 1756 (C=O); ^{1}H NMR (300 MHz, CDCl$_3$, ppm): δ 8.57 (s, quinolone-2-*H*, 1H), 8.04 (s, thiazole-5-*H*, 1H), 7.98 (d, *J* = 2.4 Hz, quinolone-5-*H*, 1H), 7.58–7.28 (m, quinolone-6,7-*H*, 2H), 4.84 (s, thiazole-2-NH_2, 2H), 4.32 (q, *J* = 7.1 Hz, CH_2CH$_3$, 2H), 1.37 (t, *J* = 7.2 Hz, CH$_2$CH_3, 3H); ^{13}C NMR (150 MHz, CDCl$_3$, ppm): δ 175.5, 167.3, 153.6, 144.5, 142.1, 128.5, 126.8, 123.5, 119.6, 113.8, 112.2, 112.9, 48.8, 14.8; MS (ESI): m/z 290 $[M+H]^+$; HRMS (ESI) calcd. for $C_{14}H_{12}FN_3OS$ $[M+H]^+$, 290.0763; found, 290.0762.

3-(2-Aminothiazol-4-yl)-1-ethyl-7-(trifluoromethyl)quinolin-4(1H)-one (6d). Compound **6d** was prepared according to the procedure depicted for compound **6a**, starting from compound **5d** (0.36 g, 1 mmol) and thiourea (0.076 g, 1 mmol). Product **6d** (0.291 g) was obtained as yellow solid (Yield 85.5%, mp 240−242 °C). IR (KBr, cm^{-1}) ν: 3463, 3432 (*N*-H), 3170 (Ar-H), 3036 (=C-H), 2995, 2945 (CH$_2$, CH$_3$), 1756 (C=O); ^{1}H NMR (300 MHz, CDCl$_3$, ppm): δ 8.62 (d, *J* = 8.7 Hz, quinolone-2,5-*H*, 2H), 7.90 (s, thiazole-5-*H*, 1H), 7.65 (s, quinolone-6-*H*, 1H), 7.54 (d, *J* = 8.3 Hz, quinolone-8-*H*, 1H), 5.02 (s, thiazole-2-NH_2, 2H), 4.26 (q, *J* = 7.0 Hz, CH_2CH$_3$, 2H), 1.49 (t, *J* = 7.0 Hz, CH$_2$CH_3, 3H); ^{13}C NMR (150 MHz, CDCl$_3$, ppm): δ 172.4, 168.5, 144.1, 135.5, 128.1, 127.8, 124.0, 120.2, 116.1, 115.3, 114.3, 112.6, 112.2, 48.8, 14.7; MS (ESI): m/z 340 $[M+H]^+$; HRMS (ESI) calcd. for $C_{15}H_{12}F_3N_3OS$ $[M+H]^+$, 340.0731; found, 340.0733.

3-(2-Aminothiazol-4-yl)-7-chloro-1-ethyl-6-fluoroquinolin-4(1H)-one (6e). Compound **6e** was prepared according to the procedure depicted for compound **6a**, starting from compound **5e** (0.35 g, 1 mmol) and thiourea (0.076 g, 1 mmol). Product **6e** (0.278 g) was obtained as yellow solid (Yield 86.5%, mp 232−234 °C). IR (KBr, cm^{-1}) ν: 3463, 3432 (*N*-H), 3170 (Ar-H), 3036 (=C-H), 2995, 2945 (CH_2, CH_3), 1756 (C=O); ^{1}H NMR (300 MHz, DMSO-d_6, ppm): δ 8.86 (s, quinolone-2-*H*, 1H), 8.27 (d, *J* = 6.0 Hz, quinolone-5-*H*, 1H), 8.13 (s, thiazole-5-*H*, 1H), 7.49 (s, quinolone-8-*H*, 1H), 4.46 (d, *J* = 7.0 Hz, C*H*$_2$CH$_3$, 2H), 1.39 (t, *J* = 6.9 Hz, CH$_2$C*H*$_3$, 3H); ^{13}C NMR (150 MHz, DMSO-d_6, ppm): δ 172.4, 168.4, 152.7, 147.7, 144.2, 135.6, 123.9, 120.2, 112.6, 112.2, 108.9, 102.9, 48.9, 15.0; MS (ESI): m/z 324 $[M+H]^+$; HRMS (ESI) calcd. for $C_{14}H_{11}ClFN_3OS$ $[M+H]^+$, 324.0374; found, 324.0335.

3-(2-Aminothiazol-4-yl)-6,8-dichloro-1-ethylquinolin-4(1H)-one (6f). Compound **6f** was prepared according to the procedure depicted for compound **6a**, starting from compound **5f** (0.36 g, 1 mmol) and thiourea (0.076 g, 1 mmol). Product **6f** (0.268 g) was obtained as yellow solid (Yield 78.5%, mp 230−231 °C). IR (KBr, cm^{-1}) ν: 3463, 3432 (*N*-H), 3170 (Ar-H), 3036 (=C-H), 2995, 2945 (CH_2, CH_3), 1756 (C=O); ^{1}H NMR (600 MHz, $CDCl_3$, ppm): δ 8.59 (s, quinolone-2-*H*, 1H), 8.09 (d, *J* = 7.5 Hz, quinolone-5-*H*, 1H), 7.96 (s, thiazole-5-*H*, 1H), 7.15 (m, quinolone-7-*H*, 1H), 4.76 (s, thiazole-5-N*H*$_2$, 2H), 4.43 (q, *J* =7.0 Hz, C*H*$_2$CH$_3$, 2H), 1.52 (t, *J* = 7.1 Hz, CH$_2$C*H*$_3$, 3H); ^{13}C NMR (150 MHz, $CDCl_3$, ppm): δ 172.8, 165.8, 144.6, 141.8, 132.6, 130.8, 125.0, 115.2, 108.4, 108.1, 107.9, 107,7, 51.0, 16.3; MS (ESI): m/z 340 $[M+H]^+$; HRMS (ESI) calcd. for $C_{14}H_{11}Cl_2N_3OS$ $[M+H]^+$, 340.0078; found, 340.0080.

3-(2-Aminothiazol-4-yl)-1-ethyl-6-fluoroquinolin-4(1H)-one (6g). Compound **6g** was prepared according to the procedure depicted for compound **6a**, starting from compound **5g** (0.31 g, 1 mmol) and thiourea (0.076 g, 1 mmol). Product **6g** (0.238 g) was obtained as yellow solid (Yield 82.2%, mp 236−238 °C). IR (KBr, cm^{-1}) ν: 3463, 3432 (*N*-H), 3170 (Ar-H), 3036 (=C-H),

2995, 2945 (CH_2, CH_3), 1756 (C=O); ^{1}H NMR (300 MHz, $CDCl_3$, ppm): δ 8.57 (s, quinolone-2-*H*, 1H), 8.09 (s, quinolone-5-*H*, 1H), 7.98 (s, thiazole-5-*H*, 1H), 7.56–7.47 (m, quinolone-7-*H*, 1H), 7.08 (d, *J* = 8.4 Hz, quinolone-8-*H*, 1H), 4.81 (s, thiazole-5-NH_2, 2H), 4.46 (q, *J* = 7.0 Hz, CH_2CH$_3$, 2H), 1.39 (t, *J* = 7.2 Hz, CH$_2$CH_3, 3H); ^{13}C NMR (150 MHz, $CDCl_3$): δ 175.4, 168.4, 156.6, 146.5, 143.7, 135.6, 122.8, 120.2, 116.6, 113.9, 112.2, 112.9, 48.9, 14.9; MS (ESI): m/z 290 $[M+H]^+$; HRMS (ESI) calcd. for $C_{14}H_{12}FN_3OS$ $[M+H]^+$, 290.0763; found, 290.0761.

3-(2-Aminothiazol-4-yl)-1-ethyl-6-methoxyquinolin-4(1H)-one (6h). Compound **6h** was prepared according to the procedure depicted for compound **6a**, starting from compound **5h** (0.32 g, 1 mmol) and thiourea (0.076 g, 1 mmol). Product **6h** (0.240 g) was obtained as yellow solid (Yield 79.7%, mp 230−231 °C). IR (KBr, cm^{-1}) ν: 3463, 3432 (*N*-H), 3170 (Ar-H), 3036 (=C-H), 2995, 2945 (CH_2, CH_3), 1756 (C=O); ^{1}H NMR (300 MHz, $CDCl_3$, ppm): δ 8.58 (s, quinolone-2-*H*, 1H), 8.35 (s, quinolone-5-*H*, 1H), 8.01 (s, thiazole-5-*H*, 1H), 7.63–7.54 (m, quinolone-7-*H*, 1H), 7.12 (d, *J* = 8.4 Hz, quinolone-8-*H*, 1H), 4.92 (s, thiazole-5-NH_2, 2H), 4.33 (q, *J* = 6.9 Hz, CH_2CH$_3$, 2H), 3.86 (s, quinolone-6-OCH_3, 3H), 1.51 (t, *J* = 7.2 Hz, CH$_2$CH_3, 3H); ^{13}C NMR (150 MHz, $CDCl_3$, ppm): δ 172.8, 165.8, 153.7, 143.6, 142.8, 130.8, 128.9, 115.2, 108.3, 108.2, 107.9, 107,7, 58.7, 48.8, 16.2; MS (ESI): m/z 302 $[M+H]^+$; HRMS (ESI) calcd. for $C_{15}H_{15}N_3O_2S$ $[M+H]^+$, 302.0963; found, 302.0961.

3-(2-Aminothiazol-4-yl)-1-ethyl-6-methylquinolin-4(1H)-one (6i). Compound **6i** was prepared according to the procedure depicted for compound **6a**, starting from compound **5i** (0.31 g, 1 mmol) and thiourea (0.076 g, 1 mmol). Product **6i** (0.217 g) was obtained as yellow solid (Yield 76.2%, mp 235−237 °C). IR (KBr, cm^{-1}) ν: 3463, 3432 (*N*-H), 3170 (Ar-H), 3036 (=C-H), 2995, 2945 (CH_2, CH_3), 1756 (C=O); ^{1}H NMR (300 MHz, $CDCl_3$, ppm): δ 8.58 (s, quinolone-2-*H*, 1H), 8.36 (s, quinolone-5-*H*, 1H), 7.93 (s, thiazole-5-*H*, 1H), 7.53–7.44 (m, quinolone-7-*H*, 1H), 7.01 (d, *J* = 8.5 Hz, quinolone-8-*H*, 1H), 5.30 (s, thiazole-5-NH_2, 2H), 4.33–4.21 (m,

C*H*$_2$CH$_3$, 2H), 2.48 (s, quinolone-6-C*H*$_3$, 3H), 1.51 (t, *J* = 7.2 Hz, CH$_2$C*H*$_3$, 3H); ^{13}C NMR (150 MHz, CDCl$_3$): δ 172.8, 165.8, 158.8, 144.6, 144.0, 130.8, 125.0, 115.3, 108.3, 108.1, 107.9, 107,7, 51.0, 48.8, 16.2; MS (ESI): m/z 286 [M+H]$^+$; HRMS (ESI) calcd. for $C_{15}H_{15}N_3OS$ [M+H]$^+$, 286.1014; found, 286.1015.

3-Acetyl-1-ethyl-6-fluoro-7-(piperidin-1-yl)quinolin-4(1H)-one (7a). A mixture of compound **4e** (0.267 g, 1 mmol), triethylamine (0.505g, 5 mmol) and piperidine (0.255 g, 3 mmol) was stirred at 120 ^{o}C in DMSO (20 mL) for 24 h. When the reaction was completed (monitored by TLC, eluent, chloroform), the mixture was cooled to room temperature, and then the solvent was evaporated under reduced pressure. After ethyl acetate was added, the resulting mixture was washed with saturated sodium chloride (3 × 20 mL). The organic phase was dried over anhydrous sodium sulfate and concentrated under reduced pressure. The residue was purified via silica gel column chromatography (eluent, chloroform) to give compound **7a** (0.134 g) as yellow solid (Yield 42.5%, mp >250 °C). IR (KBr, cm^{-1}) ν: 3121 (Ar-H), 3045 (=C-H), 2985, 2835 (CH$_2$, CH$_3$), 1735, 1716 (C=O); ^{1}H NMR (300 MHz, CDCl$_3$, ppm): δ 8.40 (s, quinolone-2-*H*, 1H), 8.06 (s, quinolone-5-*H*, 1H), 7.45 (s, quinolone-8-*H*, 1H), 4.16 (d, *J* = 7.3 Hz, C*H*$_2$CH$_3$, 2H), 3.05–2.92 (m, piperidine-2,6-C*H*$_2$, 4H), 2.72 (s, COC*H*$_3$, 3H), 1.69 (dd, *J* = 10.1, 5.2 Hz, piperidine-3,5-C*H*$_2$, 4H), 1.55 (d, *J* = 5.0 Hz, piperidine-4-C*H*$_2$, 2H), 1.47 (t, *J* = 7.2 Hz, CH$_2$C*H*$_3$, 3H); ^{13}C NMR (150 MHz, CDCl$_3$, ppm): δ 197.6, 175.1, 148.4, 146.9, 135.0, 134.2, 129.1, 118.1, 118.0, 117.7, 53.0, 48.9, 31.5, 26.0, 24.0, 14.5; MS (ESI): m/z 317 [M+H]$^+$; HRMS (ESI) calcd. for $C_{18}H_{21}FN_2O_2$ [M+H]$^+$, 317.1665; found, 317.1663.

3-Acetyl-1-ethyl-6-fluoro-7-(pyrrolidin-1-yl)quinolin-4(1H)-one (7b). Compound **7b** was prepared according to the procedure depicted for compound **7a**, starting from compound **4e** (0.267 g, 1 mmol), triethylamine (0.505g, 5 mmol) and piperidine (0.255 g, 3 mmol). Product **7b** (0.122 g) was obtained as yellow solid (Yield 40.5%, mp >250 °C). IR (KBr, cm^{-1}) ν: 3121 (Ar-

H), 3055 (=C-H), 2985, 2935 (CH_2, CH_3), 1735, 1716 (C=O); ^{1}H NMR (300 MHz, $CDCl_3$, ppm): δ 8.44 (s, quinolone-2-*H*, 1H), 7.89 (s, quinolone-5-*H*, 1H), 7.46 (s, quinolone-8-*H*, 1H), 4.21 (q, *J* = 7.2 Hz, CH_2CH_3, 2H), 3.50 (t, *J* = 6.4 Hz, pyrrolidine-2,5-CH_2, 4H), 2.79 (s, $COCH_3$, 3H), 1.99 (t, *J* = 6.5 Hz, pyrrolidine-3,4-CH_2, 4H), 1.54 (t, *J* = 7.2 Hz, CH_2CH_3, 3H); ^{13}C NMR (150 MHz, $CDCl_3$, ppm): δ 197.8, 175.1, 146.3, 145.0, 131.8, 129.2, 129.0, 118.5, 117.5, 113.2, 51.2, 48.9, 31.6, 25.4, 14.6; MS (ESI): m/z 303 $[M+H]^+$; HRMS (ESI) calcd. for $C_{17}H_{19}FN_2O_2$ $[M+H]^+$, 303.1509; found, 303.1510.

3-Acetyl-1-ethyl-6-fluoro-7-morpholinoquinolin-4(1H)-one (7c). Compound **7c** was prepared according to the procedure depicted for compound **7a**, starting from compound **4e** (0.267 g, 1 mmol), triethylamine (0.505g, 5 mmol) and piperidine (0.255 g, 3 mmol). Product **7c** (0.139 g) was obtained as yellow solid (Yield 43.8%, mp >250 °C). IR (KBr, cm^{-1}) ν: 3121 (Ar-H), 3045 (=C-H), 2985, 2835 (CH_2, CH_3), 1735, 1716 (C=O), 1126 (C-O); ^{1}H NMR (600 MHz, $CDCl_3$, ppm) δ 8.50 (s, quinolone-2-*H*, 1H), 8.15 (s, quinolone-5-*H*, 1H), 7.54 (s, quinolone-8-*H*, 1H), 4.24 (d, *J* = 6.8 Hz, CH_2CH_3, 2H), 3.91 (m, morpholine-2,6-CH_2, 4H), 3.15 (m, morpholine-3,5-CH_2, 4H), 2.79 (s, $COCH_3$, 3H), 1.55 (t, *J* = 6.6 Hz, CH_2CH_3, 3H); ^{13}C NMR (150 MHz, $CDCl_3$, ppm): δ 197.5, 175.0, 147.2, 146.9, 134.8, 134.8, 129.3, 118.4, 118.1, 118.0, 67.0, 51.9, 49.0, 31.5, 14.5; MS (ESI): m/z 319 $[M+H]^+$; HRMS (ESI) calcd. for $C_{17}H_{19}FN_2O_3$ $[M+H]^+$, 319.1458; found, 319.1456.

Tert-butyl 4-(3-acetyl-1-ethyl-6-fluoro-4-oxo-1,4-dihydroquinolin-7-yl)piperazine-1-carboxylate (7d). Compound **7d** was prepared according to the procedure depicted for compound **7a**, starting from compound **4e** (0.267 g, 1 mmol), triethylamine (0.505g, 5 mmol) and tert-butyl piperazine-1-carboxylate (0.372 g, 2 mmol). Product **7d** (0.204 g) was obtained as yellow solid (Yield 49.1%, mp >250 °C). IR (KBr, cm^{-1}) ν: 3121 (Ar-H), 3045 (=C-H), 2985, 2835 (CH_2, CH_3), 1754, 1735, 1716 (C=O); ^{1}H NMR (600 MHz, $CDCl_3$, ppm) δ 8.52 (s, quinolone-2-*H*, 1H),

8.16 (m, quinolone-5-*H*, 1H), 7.55 (s, quinolone-8-*H*, 1H), 3.48 (dd, *J* = 36.6, 25.3 Hz, quinolone-7-N-(C*H*$_2$)$_2$, 4H), 3.17 (d, *J* = 10.6 Hz, Boc-N-(C*H*$_2$)$_2$, 4H), 4.24 (d, *J* = 6.8 Hz, C*H*$_2$CH$_3$, 2H), 2.79 (s, COC*H*$_3$, 3H), 1.55 (t, *J* = 6.6 Hz, CH$_2$C*H*$_3$, 3H), 1.51 (s, C(C*H*$_3$)$_3$, 9H); ^{13}C NMR (150 MHz, $CDCl_3$, ppm): δ 199.8, 176.1, 156.6, 150.7, 146.1, 143.0, 138.8, 115.2, 112.6, 110.5, 103.2, 79.2, 51.9, 48.9, 43.5, 31.5, 28.6, 14.5; MS (ESI): m/z 418 $[M+H]^+$; HRMS (ESI) calcd. for $C_{22}H_{28}FN_3O_4$ $[M+H]^+$, 418.2142; found, 418.2140.

3-(2-Aminothiazol-4-yl)-1-ethyl-6-fluoro-7-(piperidin-1-yl)quinolin-4(1H)-one (9a). Compound **9a** was prepared according to the procedure depicted for compound **6a**, starting from compound **8a** (0.394 g, 1 mmol) and thiourea (0.076 g, 1 mmol). Product **9a** (0.137 g) was obtained as yellow solid (Yield 36.8%, mp 242−243 °C). IR (KBr, cm^{-1}) ν: 3460, 3420 (*N*-H), 3112 (Ar-H), 3051 (=C-H), 2989, 2935 (CH_2, CH_3), 1738 (C=O); ^{1}H NMR (300 MHz, $CDCl_3$, ppm) δ 8.43 (s, quinolone-2-*H*, 1H), 7.68 (s, quinolone-5-*H*, 1H), 7.46 (s, thiazole-5-H, 1H), 6.79 (s, quinolone-8-*H*, 1H), 4.51 (t, *J* = 5.2 Hz, C*H*$_2$CH$_3$, 1H), 4.21 (q, *J* = 7.2 Hz, C*H*$_2$CH$_3$, 2H), 3.72 (q, *J* = 7.0 Hz, piperidine-*N*-C*H*$_2$, 4H), 2.12–1.95 (m, piperidine-C*H*$_2$, 4H), 1.88 (s, 2H), 1.54 (t, *J* = 7.2 Hz, CH$_2$C*H*$_3$, 3H), 1.25 (t, *J* = 7.0 Hz, piperidine-2*H*, 2H); ^{13}C NMR (150 MHz, $CDCl_3$): δ 174.4, 167.5, 153.2, 142.9, 137.3, 128.0, 123.5, 113.6, 113.7, 108.8, 106.5, 102.0, 54.6, 50.5, 26.8, 24.5, 14.7; MS (ESI): m/z 373 $[M+H]^+$; HRMS (ESI) calcd. for $C_{19}H_{21}FN_4OS$ $[M+H]^+$, 373.1498; found, 373.1500.

3-(2-Aminothiazol-4-yl)-1-ethyl-6-fluoro-7-(pyrrolidin-1-yl)quinolin-4(1H)-one (9b). Compound **9b** was prepared according to the procedure depicted for compound **6a**, starting from compound **8b** (0.380 g, 1 mmol) and thiourea (0.076 g, 1 mmol). Product **9b** (0.149 g) was obtained as yellow solid (Yield 41.5%, mp 217−219 °C). IR (KBr, cm^{-1}) ν: 3460, 3420 (*N*-H), 3112 (Ar-H), 3051 (=C-H), 2989, 2935 (CH_2, CH_3), 1738 (C=O); ^{1}H NMR (600 MHz, $CDCl_3$, ppm): δ 8.59 (s, quinolone-2-*H*, 1H), 7.97 (d, *J* = 1.9 Hz, quinolone-2-*H*, 1H), 7.95 (s, thiazole-5-

H, 1H), 7.48 (s, quinolone-8-*H*, 1H), 5.24 (s, thiazole-2-NH_2, 2H), 4.23 (q, *J* = 7.3 Hz, CH_2CH$_3$, 2H), 3.50–3.43 (m, pyrrolidine-2,5-CH_2, 4H), 2.03–1.95 (m, pyrrolidine-3,4-CH_2, 4H), 1.53 (t, *J* = 7.3 Hz, CH$_2$CH_3, 3H); ^{13}C NMR (150 MHz, CDCl$_3$, ppm): δ 174.3, 166.8, 144.2, 141.4, 132.3, 129.8, 126.6, 117.8, 116.9, 113.2, 105.9, 100.0, 51.3, 48.4, 25.2, 14.7; MS (ESI): m/z 359 $[M+H]^+$; HRMS (ESI) calcd. for $C_{18}H_{19}FN_4OS$ $[M+H]^+$, 359.1342; found, 359.1341.

3-(2-Aminothiazol-4-yl)-1-ethyl-6-fluoro-7-morpholinoquinolin-4(1H)-one (9c). Compound **9c** was prepared according to the procedure depicted for compound **6a**, starting from compound **8c** (0.396 g, 1 mmol) and thiourea (0.076 g, 1 mmol). Product **9c** (0.172 g) was obtained as yellow solid (Yield 46.1%, mp 221−223 °C). IR (KBr, cm^{-1}) ν: 3460, 3420 (*N*-H), 3112 (Ar-H), 3051 (=C-H), 2989, 2935 (CH$_2$, CH$_3$), 1738 (C=O), 1226 (C-O); ^{1}H NMR (600 MHz, CDCl$_3$, ppm): δ 8.65 (s, quinolone-2-*H*, 1H), 8.14 (d, *J* = 13.5 Hz, quinolone-5-*H*, 1H), 7.95 (s, thiazole-5-*H*, 1H), 6.76 (d, *J* = 6.8 Hz, quinolone-8-*H*, 1H), 5.50 (s, thiazole-2-NH_2, 2H), 4.27 (d, *J* = 7.3 Hz, CH_2CH$_3$, 2H), 3.98–3.86 (m, morpholine-2,6-CH_2, 4H), 3.29–3.19 (m, morpholine-3,5-CH_2, 4H), 1.55 (t, *J* = 7.2 Hz, CH$_2$CH_3, 3H); ^{13}C NMR (150 MHz, CDCl$_3$, ppm): δ 174.3, 167.4, 153.6, 142.0, 136.0, 126.0, 121.9, 113.1, 113.0, 109.7, 106.8, 102.8, 66.7, 50.5, 48.5, 14.7; MS (ESI): m/z 375 $[M+H]^+$; HRMS (ESI) calcd. for $C_{18}H_{19}FN_4O_2S$ $[M+H]^+$, 375.1291; found, 375.1290.

Tert-butyl 4-(3-(2-aminothiazol-4-yl)-1-ethyl-6-fluoro-4-oxo-1,4-dihydroquinolin-7-yl)piperazine-1-carboxylate (9d). Compound **9d** was prepared according to the procedure depicted for compound **6a**, starting from compound **8d** (0.496 g, 1 mmol) and thiourea (0.076 g, 1 mmol). Product **9d** (0.241 g) was obtained as yellow solid (Yield 51.1%, mp 232−235 °C). IR (KBr, cm^{-1}) ν: 3460, 3420 (*N*-H), 3112 (Ar-H), 3051 (=C-H), 2989, 2935 (CH$_2$, CH$_3$), 1753, 1738 (C=O); ^{1}H NMR (600 MHz, CDCl$_3$, ppm): δ 8.65 (s, quinolone-2-*H*, 1H), 8.14 (d, *J* = 13.5 Hz, quinolone-5-*H*, 1H), 7.95 (s, thiazole-5-*H*, 1H), 6.76 (d, *J* = 6.8 Hz, quinolone-8-*H*, 1H),

5.50 (s, thiazole-2-NH_2, 2H), 4.27 (d, J = 7.3 Hz, CH_2CH$_3$, 2H), 3.48 (dd, J = 36.6, 25.3 Hz, quinolone-7-N-(CH_2)$_2$, 4H), 3.17 (d, J = 10.6 Hz, Boc-N-(CH_2)$_2$, 4H), 1.55 (t, J = 7.2 Hz, CH$_2$CH_3, 3H), 1.51 (s, C(CH_3)$_3$, 9H); ^{13}C NMR (150 MHz, CDCl$_3$, ppm): δ 172.3, 167.4, 153.6, 142.0, 136.0, 126.0, 115.1, 113.0, 110.3, 109.8, 103.8, 79.2, 51.9, 48.9, 43.5, 31.5, 28.6, 14.5; MS (ESI): m/z 474 [M+H]$^+$; HRMS (ESI) calcd. for $C_{18}H_{20}FN_5OS$ [M+H]$^+$, 474.1975; found, 474.1972.

3-(2-Aminothiazol-4-yl)-1-ethyl-6-fluoro-7-(piperazin-1-yl)quinolin-4(1H)-one (9e). A mixture of compound **9e** (0.473 g, 1 mmol) was stirred at room temperature in TFA-CH_2Cl_2 solution (V/V = 1/1, 20 mL) for 3 h. When the reaction was completed (monitored by TLC, eluent, chloroform/methanol 30/1, V/V), the solvent was evaporated under reduced pressure. After ethyl acetate was added, the resulting mixture was washed with saturated sodium bicarbonate solution (3 × 20 mL). The organic phase was dried over anhydrous sodium sulfate and concentrated under reduced pressure. The residue was purified via silica gel column chromatography (eluent, chloroform/ methanol 30/1, V/V) to give compound **9e** (0.280 g) as light yellow solid (Yield 75.0%, mp 235−239 °C). IR (KBr, cm^{-1}) ν: 3460, 3420 (*N*-H), 3112 (Ar-H), 3051 (=C-H), 2989, 2935 (CH$_2$, CH$_3$), 1753, 1738 (C=O); ^{1}H NMR (600 MHz, CDCl$_3$, ppm): δ 8.57 (s, quinolone-2-*H*, 1H), 8.11 (d, J = 13.5 Hz, quinolone-5-*H*, 1H), 7.95 (s, thiazole-5-*H*, 1H), 6.72 (d, J = 6.8 Hz, quinolone-8-*H*, 1H), 5.78 (s, thiazole-2-NH_2, 2H), 4.25 (d, J = 7.3 Hz, CH_2CH$_3$, 2H), 3.32 (dd, J = 36.6, 25.3 Hz, quinolone-7-N-(CH_2)$_2$, 4H), 3.01 (d, J = 10.6 Hz, NH-(CH_2)$_2$, 4H), 1.55 (t, J = 7.2 Hz, CH$_2$CH_3, 3H); ^{13}C NMR (150 MHz, CDCl$_3$, ppm): δ 175.3, 166.3, 152.6, 142.1, 136.0, 126.0, 121.9, 113.1, 113.0, 109.7, 106.8, 102.8, 80.1, 51.3, 48.9, 43.5, 31.5, 28.6, 14.5; MS (ESI): m/z 374 [M+H]$^+$; HRMS (ESI) calcd. for $C_{23}H_{28}FN_5O_3S$ [M+H]$^+$, 374.1451; found, 374.1450.

3-Acetyl-7-chloro-1-ethyl-6-(piperidin-1-yl)quinolin-4(1H)-one (10a). Compound **10a** was prepared according to the procedure depicted for compound **7a**, starting from compound **4e** (0.267 g, 1 mmol), triethylamine (0.505g, 5 mmol) and piperidine (0.255 g, 3 mmol). Product **10a** (0.108 g) was obtained as yellow solid (Yield 32.5%, mp 231−234 °C). IR (KBr, cm^{-1}) ν: 3121 (Ar-H), 3035 (=C-H), 2985, 2945 (CH_2, CH_3), 1735, 1716 (C=O); ^{1}H NMR (300 MHz, $CDCl_3$, ppm): δ 8.44 (s, quinolone-2-*H*, 1H), 8.06 (d, *J* = 13.4 Hz, quinolone-5-*H*, 1H), 6.75 (d, *J* = 6.9 Hz, quinolone-8-*H*, 1H), 4.22 (dd, *J* = 7.0, 2.5 Hz, C*H*$_2$CH$_3$, 2H), 3.29–3.12 (m, piperidine-2,6-C*H*$_2$, 4H), 2.78 (s, COC*H*$_3$, 3H), 1.78 (d, *J* = 4.6 Hz, piperidine-3,5-C*H*$_2$, 4H), 1.66 (d, *J* = 4.7 Hz, piperidine-4-C*H*$_2$, 2H), 1.54 (t, *J* = 7.3 Hz, CH$_2$C*H*$_3$, 3H); ^{13}C NMR (150 MHz, $CDCl_3$, ppm): δ 197.9, 155.0, 147.1, 129.7, 123.1, 118.8, 113.5, 113.2, 103.8, 103.8, 51.4, 49.1, 31.6, 29.7, 25.8, 14.4; MS (ESI): m/z 333 $[M+H]^+$; HRMS (ESI) calcd. for $C_{18}H_{21}ClN_2O_2$ $[M+H]^+$, 333.1370; found, 333.1371.

3-Acetyl-7-chloro-1-ethyl-6-(pyrrolidin-1-yl)quinolin-4(1H)-one (10b). Compound **10b** was prepared according to the procedure depicted for compound **7a**, starting from compound **4e** (0.267 g, 1 mmol), triethylamine (0.505g, 5 mmol) and piperidine (0.255 g, 3 mmol). Product **10b** (0.113 g) was obtained as yellow solid (Yield 35.4%, mp >250 °C). IR (KBr, cm^{-1}) ν: 3121 (Ar-H), 3035 (=C-H), 2985, 2945 (CH_2, CH_3), 1735, 1716 (C=O); ^{1}H NMR (300 MHz, $CDCl_3$, ppm): δ 8.38 (s, quinolone-2-*H*, 1H), 7.99 (d, *J* = 14.6 Hz, quinolone-5-*H*, 1H), 6.30 (d, *J* = 7.2 Hz, quinolone-8-*H*, 1H), 4.16 (q, *J* = 7.2 Hz, C*H*$_2$CH$_3$, 2H), 3.56 (d, *J* = 2.5 Hz, pyrrolidine-2,5-C*H*$_2$, 4H), 2.80 (s, COC*H*$_3$, 3H), 2.03 (t, *J* = 6.3 Hz, pyrrolidine-3,4-C*H*$_2$, 4H), 1.52 (t, *J* = 7.2 Hz, CH$_2$C*H*$_3$, 3H); ^{13}C NMR (150 MHz, $CDCl_3$, ppm): δ 198.0, 174.6, 146.8, 141.3, 136.9, 118.5, 117.6, 113.2, 112.9, 98.2, 50.0, 48.9, 31.5, 25.4, 14.6; MS (ESI): m/z 319 $[M+H]^+$; HRMS (ESI) calcd. for $C_{17}H_{19}ClN_2O_2$ $[M+H]^+$, 319.1213; found, 319.1212.

3-Acetyl-7-chloro-1-ethyl-6-morpholinoquinolin-4(1H)-one (10c). Compound **10c** was prepared according to the procedure depicted for compound **7a**, starting from compound **4e** (0.267 g, 1 mmol), triethylamine (0.505g, 5 mmol) and piperidine (0.255 g, 3 mmol). Product **10c** (0.105 g) was obtained as yellow solid (Yield 31.6%, mp >250 °C). IR (KBr, cm^{-1}) ν: 3120 (Ar-H), 3055 (=C-H), 2985, 2935 (CH_2, CH_3), 1735, 1716 (C=O), 1270 (C-O); ^{1}H NMR (600 MHz, $CDCl_3$, ppm): δ 8.42 (s, quinolone-2-*H*, 1H), 7.85 (s, quinolone-5-*H*, 1H), 7.74 (s, quinolone-8-*H*, 1H), 4.24 (d, *J* = 6.8 Hz, C*H*$_2$CH$_3$, 2H), 3.95 (s, morpholine-2,6-C*H*$_2$, 4H), 3.25 (s, morpholine-3,5-C*H*$_2$, 4H), 2.79 (s, COC*H*$_3$, 3H), 1.55 (t, *J* = 6.6 Hz, CH$_2$C*H*$_3$, 3H); ^{13}C NMR (150 MHz, $CDCl_3$, ppm): δ 197.4, 174.6, 147.2, 139.8, 134.8, 131.6, 129.3, 117.5, 117.1, 116.8, 67.2, 51.9, 51.4, 31.5, 14.5; MS (ESI): m/z 335 $[M+H]^+$; HRMS (ESI) calcd. for $C_{17}H_{19}ClN_2O_3$ $[M+H]^+$, 335.1162; found, 335.1160.

Tert-butyl 4-(3-acetyl-7-chloro-1-ethyl-4-oxo-1,4-dihydroquinolin-6-yl)piperazine-1-carboxylate (10d). Compound **10d** was prepared according to the procedure depicted for compound **7a**, starting from compound **4e** (0.267 g, 1 mmol), triethylamine (0.505g, 5 mmol) and tert-butyl piperazine-1-carboxylate (0.372 g, 2 mmol). Product **10d** (0.145 g) was obtained as yellow solid (Yield 33.4%, mp >250 °C). IR (KBr, cm^{-1}) ν: 3121 (Ar-H), 3045 (=C-H), 2985, 2835 (CH_2, CH_3), 1754, 1735, 1716 (C=O); ^{1}H NMR (600 MHz, $CDCl_3$, ppm) δ 8.52 (s, quinolone-2-*H*, 1H), 7.78 (m, quinolone-5-*H*, 1H), 7.63 (s, quinolone-8-*H*, 1H), 3.48 (m, quinolone-7-N-(C*H*$_2$)$_2$, 4H), 3.17 (d, *J* = 10.6 Hz, Boc-N-(C*H*$_2$)$_2$, 4H), 4.24 (d, *J* = 6.8 Hz, C*H*$_2$CH$_3$, 2H), 2.79 (s, COC*H*$_3$, 3H), 1.55 (t, *J* = 6.6 Hz, CH$_2$C*H*$_3$, 3H), 1.51 (s, C(C*H*$_3$)$_3$, 9H); ^{13}C NMR (150 MHz, $CDCl_3$, ppm): δ 198.7, 176.1, 154.6, 152.5, 143.1, 143.3, 138.8, 115.2, 112.6, 110.5, 103.2, 79.2, 51.9, 48.9, 43.5, 31.5, 28.6, 14.7; MS (ESI): m/z 434 $[M+H]^+$; HRMS (ESI) calcd. for $C_{22}H_{28}ClN_3O_4$ $[M+H]^+$, 434.1847; found, 434.1845.

3-(2-Aminothiazol-4-yl)-7-chloro-1-ethyl-6-(piperidin-1-yl)quinolin-4(1H)-one (12a). Compound **12a** was prepared according to the procedure depicted for compound **6a**, starting from compound **8b** (0.380 g, 1 mmol) and thiourea (0.076 g, 1 mmol). Product **12a** (0.149 g) was obtained as yellow solid (Yield 41.5%, mp 240−242 °C). IR (KBr, cm^{-1}) ν: 3472, 3423 (*N*-H), 3170 (Ar-H), 3041 (=C-H), 2989, 2943 (CH_2, CH_3), 1746 (C=O); ^{1}H NMR (600 MHz, $CDCl_3$, ppm): δ 8.59 (s, quinolone-2-*H*, 1H), 7.97 (d, *J* = 1.9 Hz, quinolone-2-*H*, 1H), 7.95 (s, thiazole-5-*H*, 1H), 7.48 (s, quinolone-8-*H*, 1H), 5.24 (s, thiazole-2-NH_2, 2H), 4.23 (q, *J* = 7.3 Hz, CH_2CH$_3$, 2H), 3.50–3.43 (m, pyrrolidine-2,5-CH_2, 4H), 2.03–1.95 (m, pyrrolidine-3,4-CH_2, 4H), 1.53 (t, *J* = 7.3 Hz, CH$_2$CH_3, 3H); ^{13}C NMR (150 MHz, $CDCl_3$, ppm): δ 174.3, 166.8, 144.2, 141.4, 132.3, 129.8, 126.6, 117.8, 116.9, 113.2, 105.9, 100.0, 51.3, 48.4, 25.2, 14.7; MS (ESI): m/z 359 $[M+H]^+$; HRMS (ESI) calcd. for $C_{18}H_{19}FN_4OS$ $[M+H]^+$, 359.1342; found, 359.1341.

3-(2-Aminothiazol-4-yl)-7-chloro-1-ethyl-6-(pyrrolidin-1-yl)quinolin-4(1H)-one (12b). Compound **12b** was prepared according to the procedure depicted for compound **6a**, starting from compound **11b** (0.396 g, 1 mmol) and thiourea (0.076 g, 1 mmol). Product **12b** (0.301 g) was obtained as yellow solid (Yield 80.5%, mp 212−213 °C). IR (KBr, cm^{-1}) ν: 3472, 3423 (*N*-H), 3170 (Ar-H), 3041 (=C-H), 2989, 2943 (CH_2, CH_3), 1746 (C=O); ^{1}H NMR (600 MHz, $CDCl_3$, ppm): δ 8.51 (s, quinolone-2-*H*, 1H), 8.02 (d, *J* = 14.8 Hz, quinolone-5-*H*, 1H), 7.91 (s, thiazole-5-*H*, 1H), 5.39 (s, thiazole-NH_2, 2H), 6.30 (d, *J* = 7.6 Hz, quinolone-8-*H*, 1H), 4.30 (d, *J* = 7.2 Hz, CH_2CH$_3$, 2H), 3.52 (d, *J* = 2.6 Hz, pyrrolidine-2,5-CH_2, 4H), 2.50 (dt, *J* = 3.6, 1.8 Hz, pyrrolidine-3,4-CH_2, 4H), 1.37 (t, *J* = 7.1 Hz, CH$_2$CH_3, 3H); ^{13}C NMR (600 MHz, $CDCl_3$, ppm): δ 174.2, 165.7, 144.1, 140.8, 138.2, 129.2, 125.8, 117.6, 116.9, 113.1, 105.9, 101.9. 51.4, 48.4, 25.2, 14.6; MS (ESI): m/z 375 $[M+H]^+$; HRMS (ESI) calcd. for $C_{18}H_{19}ClN_4OS$ $[M+H]^+$, 375.1046; found, 375.1045.

3-(2-Aminothiazol-4-yl)-7-chloro-1-ethyl-6-morpholinoquinolin-4(1H)-one (12c). Compound **12c** was prepared according to the procedure depicted for compound **6a**, starting from compound **11c** (0.412 g, 1 mmol) and thiourea (0.076 g, 1 mmol). Product **12c** (0.341 g) was obtained as yellow solid (Yield 87.5%, mp >250 °C). IR (KBr, cm^{-1}) ν: 3472, 3423 (*N*-H), 3170 (Ar-H), 3041 (=C-H), 2989, 2943 (CH_2, CH_3), 1746 (C=O), 1250 (C-O); ^{1}H NMR (600 MHz, $CDCl_3$, ppm): δ 8.68 (s, quinolone-2-*H*, 1H), 8.15 (s, quinolone-5-*H*, 1H), 7.92 (s, thiazole-5-*H*, 1H), 7.55 (s, quinolone-8-*H*, 1H), 6.39 (s, thiazole-2-NH_2, 2H), 4.28 (d, *J* = 7.2 Hz, CH_2CH$_3$, 2H), 3.96–3.86 (m, morpholine-2,6-CH_2, 4H), 3.19–3.11 (m, morpholine-3,5-CH_2, 4H), 1.55 (dd, *J* = 9.6, 4.8 Hz, CH$_2$CH_3, 3H); ^{13}C NMR (150 MHz, $CDCl_3$, ppm): δ 174.0, 167.3, 153.3, 141.9, 137.4, 132.0, 121.9, 113.1, 112.7, 109.3, 106.5, 102.3, 66.2, 50.2, 48.5, 14.7; MS (ESI): m/z 391 $[M+H]^+$; HRMS (ESI) calcd. for $C_{18}H_{19}ClN_4O_2S$ $[M+H]^+$, 391.0995; found, 391.0993.

Tert-butyl 4-(3-(2-aminothiazol-4-yl)-7-chloro-1-ethyl-4-oxo-1,4-dihydroquinolin-6-yl)piperazine-1-carboxylate (12d). Compound **12d** was prepared according to the procedure depicted for compound **6a**, starting from compound **11d** (0.511 g, 1 mmol) and thiourea (0.076 g, 1 mmol). Product **12d** (0.390 g) was obtained as yellow solid (Yield 79.5%, mp >250 °C). IR (KBr, cm^{-1}) ν: 3460, 3420 (*N*-H), 3112 (Ar-H), 3051 (=C-H), 2989, 2935 (CH_2, CH_3), 1753, 1738 (C=O); ^{1}H NMR (600 MHz, $CDCl_3$, ppm): δ 8.65 (s, quinolone-2-*H*, 1H), 8.02 (s, quinolone-5-*H*, 1H), 7.95 (s, thiazole-5-*H*, 1H), 6.85 (s, quinolone-8-*H*, 1H), 5.50 (s, thiazole-2-NH_2, 2H), 4.27 (d, *J* = 7.3 Hz, CH_2CH$_3$, 2H), 3.48 (dd, *J* = 36.6, 25.3 Hz, quinolone-7-N-(CH_2)$_2$, 4H), 3.17 (d, *J* = 10.6 Hz, Boc-N-(CH_2)$_2$, 4H), 1.55 (t, *J* = 7.2 Hz, CH$_2$CH_3, 3H), 1.51 (s, C(CH_3)$_3$, 9H); ^{13}C NMR (150 MHz, $CDCl_3$, ppm): δ 169.9, 167.4, 153.6, 142.0, 136.0, 126.0, 115.1, 113.0, 110.3, 109.8, 103.8, 79.2, 51.9, 48.9, 43.5, 31.5, 28.6, 14.5; MS (ESI): m/z 490 $[M+H]^+$; HRMS (ESI) calcd. for $C_{18}H_{20}ClN_5OS$ $[M+H]^+$, 490.1680; found, 490.1677.

3-(2-Aminothiazol-4-yl)-7-chloro-1-ethyl-6-(piperazin-1-yl)quinolin-4(1H)-one (12e). Compound **12e** was prepared according to the procedure depicted for compound **9e**, starting from compound **12d** (0.489 g, 1 mmol). Product **12d** (0.315 g) was obtained as yellow solid (Yield 81.0%, mp 241−243 °C). IR (KBr, cm^{-1}) ν: 3454, 3420 (*N*-H), 3112 (Ar-H), 3051 (=C-H), 2989, 2935 (CH_2, CH_3), 1753, 1738 (C=O); ^{1}H NMR (600 MHz, $CDCl_3$, ppm): δ 8.56 (s, quinolone-2-*H*, 1H), 7.95 (s, thiazole-5-*H*, 1H), 7.61 (d, *J* = 13.5 Hz, quinolone-5-*H*, 1H),v6.81 (d, *J* = 6.8 Hz, quinolone-8-*H*, 1H), 5.78 (s, thiazole-2-NH_2, 2H), 4.25 (d, *J* = 7.3 Hz, CH_2CH$_3$, 2H), 3.43 (dd, *J* = 36.6, 25.3 Hz, quinolone-7-N-(CH_2)$_2$, 4H), 3.34 (d, *J* = 10.6 Hz, NH-(CH_2)$_2$, 4H), 1.55 (t, *J* = 7.2 Hz, CH$_2$CH_3, 3H); ^{13}C NMR (150 MHz, $CDCl_3$, ppm): δ 175.3, 163.3, 152.1, 142.1, 136.0, 126.0, 121.9, 113.1, 113.0, 109.7, 106.8, 102.8, 80.1, 51.3, 49.2, 43.5, 31.5, 28.6, 14.5; MS (ESI): m/z 390 $[M+H]^+$; HRMS (ESI) calcd. for $C_{23}H_{28}ClN_5O_3S$ $[M+H]^+$, 390.1155; found, 390.1153.

ASSOCIATED CONTENT

Supporting Information

(i) Emission spectra of HSA with compound **12b** at 303 K and 310 K. (ii) Isolating genomic DNA from MRSA bacteria. (iii) HRMS, ^{1}H NMR and ^{13}C NMR spectra for some important compounds. This material is available free of charge via the Internet at http://pubs.acs.org.

PDB ID Codes

http://www.rcsb.org/pdb/explore/explore.do?structureId=2XCT (DNA gyrase).

http://www.rcsb.org/pdb/explore/explore.do?structureId=3RAD (IV topoisomerase).

AUTHOR INFORMATION

Corresponding Author

* Tel.: +86-23-68254967; Fax: +86-23-68254967; E-mail: zhouch@swu.edu.cn (Cheng-He Zhou);

ACKNOWLEDGMENTS

This research was partially funded by National Natural Science Foundation of China (NSFC, No. 21172181 and 21372186), the Research Fund for International Young Scientists from International (Regional) Cooperation and Exchange Program of NSFC (No. 81450110451), the Key Program of Chongqing Natural Science Foundation (CSTC2012jjB10026), and the Specialized Research Fund for the Doctoral Program of Higher Education of China (SRFDP 20110182110007).

ABBREVIATIONS USED

MRSA, methicillin resistant *staphylococcus aureus*; SARs, structure-activity relationships; HSA, human serum albumin; ClogP, theoretically calculated values of log P; MEP, molecular electrostatic potential. ssDNA, single-stranded DNA; dsDNA, double-stranded DNA.

REFERENCES

(1) Srinivasan, S.; Shafreen R. M. B.; Nithyanand, P.; Manisankar, P.; Pandian S. K. Synthesis and in vitro antimicrobial evaluation of novel fluoroquinolone derivatives. *Eur. J. Med. Chem.* **2010**, *45*, 6101–6105.

(2) Cui, S.-F.; Peng, L.-P.; Zhang, H.-Z.; Rasheed, S.; Kumar, K. V. Zhou, C.-H. Novel hybrids of metronidazole and quinolones: Synthesis, bioactive evaluation, cytotoxicity, preliminary antimicrobial mechanism and effect of metal ions on their transportation by human serum albumin. *Eur. J. Med. Chem.* **2014**, *86*, 318–334.

(3) Cui, S.-F.; Ren, Y.; Zhang, S.-L.; Peng, X.-M.; Damu. G. L. V.; Geng, R.-X.; Zhou, C.-H. Synthesis and biological evaluation of a class of quinolone triazoles as potential antimicrobial

agents and their interactions with calf thymus DNA. *Bioorg. Med. Chem. Lett.* **2013**, *23*, 3267–3272.

(4) Higgins, P. G.; Fluit, A. C.; Schmitz, F. J. Fluoroquinolones: structure and target sites. *Curr. Drug Targets*. **2003**, *4*, 181–190.

(5) Hooper, D. C. Fluoroquinolone resistance among Gram-positive cocci. *Lancet Infect. Dis.* **2002**, *2*, 530–538.

(6) Aldred, K. J.; Kerns, R. J.; Osheroff, N. Mechanism of quinolone action and resistance. *Biochemistry*. **2014**, *53*, 1565−1574.

(7) Laponogov, I.; Sohi, M. K.; Veselkov. D. A.; Pan, X. S.; Sawhney, R.; Thompson, A. W.; McAuley, K. E.; Fisher, L. M.; Sanderson, M. R. Structural insight into the quinolone–DNA cleavage complex of type IIA topoisomerases. *Nat. Struct. Mol. Boil.* **2009**, *6*, 667–669.

(8) Drlica, K.; Malik, M.; Kerns, R. J.; Zhao, X. Quinolone-mediated bacterial death. *Antimicrob. Agents Chemother.* **2008**, *52*, 385–392.

(9) Leo, E.; Gould, K. A.; Pan, X. S.; Capranico, G.; Sanderson, M. R.; Palumbo, M.; Fishe, L. M. Novel symmetric and asymmetric DNA scission determinants for streptococcus pneumoniae Topoisomerase IV and gyrase are clustered at the DNA breakage site. *J. Biol. Chem.* **2005**, *280*, 14252–14263.

(10) Cui, S. F.; Zhou, C. H.; Geng, R. X.; Ji, Q. G. Recent advances in the researches on thiazole compounds as enzyme and acceptor inhibitors. *Chin*. *J*. *Biochem*. *Pharm*. **2012**, *33*, 311–315 (in Chinese).

(11) Cui, S. F.; Wang, Y.; Lv, J. S.; Damu, G. L. V.; Zhou, C. H. Recent advances in application of thiazole compounds. *Sci. Sin.: Chim.* **2012**, *42*, 1105−1131 (in Chinese).

(12) Kitagawa, H.; Ozawa, T.; Takahata, S.; Iida, M.; Saito, J.; Yamada, M. Phenylimidazole derivatives of 4-pyridone as dual inhibitors of bacterial enoyl-Acyl carrier protein reductases fabI and fabK. *J. Med. Chem.* **2007**, *50*, 4710−4720.

(13) Oka, Y.; Yabuuchi, T.; Oi, T.; Kuroda, S.; Fujii, Y.; Ohtake, H. Inoue, T.; Wakahara, S.; Kimura, K.; Fujita, K.; Endo, M.; Taguchi, K.; Sekiguchi, Y. Discovery of *N*-{5-[3-(3-hydroxypiperidin-1-yl)-1,2,4-oxadiazol-5-yl]-4-methyl-1,3-thiazol-2-yl}acetamide (TASP04159 14) as an orally potent phosphoinositide 3-kinase γ inhibitor for the treatment of inflammatory diseases. *Bioorg. Med. Chem.* **2013**, *21*, 7578–7583.

(14) Geronikaki, A. A.; Pitta, E. P.; Liaras, K. S.; Thiazoles and thiazolidinones as antioxidants. *Curr. Med. Chem.* **2013**, *36*, 4460–4480.

(15) Basarab, G. S.; Hill, P. J.; Garner, C. E.; Hull, K.; Green, O.; Sherer, B. A.; Dangel, P. B.; Manchester, J. I.; Bist, S.; Hauck, S.; Zhou, F.; Uria-Nickelsen, M.; Illingworth, R.; Alm, R.; Rooney, M.; Eakin, A. E. Optimization of pyrrolamide topoisomerase II inhibitors toward identification of an antibacterial clinical candidate (AZD5099). *J. Med. Chem*. **2014**, *57*, 6060–6082.

(16) Brvar, M.; Perdih, A.; Renko, M.; Anderluh, G.; Turk, D.; Solmajer, T.; Structure-based discovery of substituted 4,5'-bithiazoles as novel DNA gyrase inhibitors. *J. Med. Chem*. **2012**, *55*, 6413–6426.

(17) Zhang, L.; Kumar, K. V.; Rasheed, S.; Geng, R. X.; Zhou, C. H. Design, synthesis, and antimicrobial evaluation of novel quinolone imidazoles and interactions with MRSA DNA, *Chem. Biol. Drug Des.* **2015**, *86*, 648-655.

(18) Wang, Y.; Damu, G. L. V.; Lv, J. S.; Geng, R. X.; Yang, D. C.; Zhou, C. H. Design, synthesis and evaluation of clinafloxacin triazole hybrids as a new type of antibacterial and antifungal agents. *Bioorg. Med. Chem. Lett.* **2012**, *22*, 5363–5366.

(19) Zhang, L.; Kumar, K. V.; Rasheed, S.; Zhang, S. L.; Geng, R. X.; Zhou, C. H. Design, synthesis, and antibacterial evaluation of novel azolylthioether quinolones as MRSA DNA intercalators. *Med. Chem. Commun.* **2015**, *6*, 1303–1310.

(20) Peng, X. M.; Cai, G. X.; Zhou, C. H. Recent developments in azole compounds as antibacterial and antifungal agents. *Curr. Top. Med. Chem*. **2013**, *13*, 1963–2010;

(21) Zhang, H. Z.; Cui, S. F.; Nagarajan, S.; Rasheed, S.; Cai, G. X.; Zhou, C. H. A unique one-pot reaction via CAC cleavage from aminomethylene benzimidazoles to access benzimidazolones with wide potentiality. *Tetrahedron Lett.* **2014**, *55*, 4105–4109.

(22) Zhang, L.; Peng, X. M.; Damu, G. L. V.; Geng, R. X.; Zhou, C. H. Comprehensive review in current developments of imidazole-based medicinal chemistry. *Med. Res. Rev.* **2014**, *34*, 340−437.

(23) Zhou, C. H.; Wang, Y. Recent researches in triazole compounds as medicinal drugs. *Curr. Med. Chem.* **2012**, *19*, 239–280.

(24) Dai, L. L.; Zhang, H. Z.; Nagarajan, S.; Rasheed, S.; Zhou, C. H. Synthesis of tetrazole compounds as a novel type of potential antimicrobial agents and their synergistic effects with clinical drugs and interactions with calf thymus DNA. *Med. Chem. Commun*. **2015**, *6*, 147–154;

(25) Wang, X. L; Wan, K; Zhou, C. H. Synthesis of novel sulfanilamide-derived 1,2,3-triazoles and their evaluation for antibacterial and antifungal activities. *Eur. J. Med. Chem.* **2010**, *45*, 4631–4639.

(26) Kim, H. Y.; Wiles, J. A.; Wang, Q.; Pais, G. C. G.; Lucien, E.; Hashimoto, A.; Nelson, D. M. Thanassi, J. A.; Podos, S. D.; Deshpande, M.; Pucci, M. J.; Bradbury, B. J. Exploration of the activity of 7-pyrrolidino-8-methoxyisothiazoloquinolones against methicillin-resistant staphylococcus aureus (MRSA). *J. Med. Chem.* **2011**, *54*, 3268–3282.

(27) Zhao, Y.; Tian, Y.; Cui, Y; Liu, W.; Ma, W.; Jiang, X. Small molecule-capped gold nanoparticles as potent antibacterial agents that target Gram-negative bacteria. *J. Am. Chem. Soc*. **2010**, *132*, 12349–12356.

(28) Zhang, L.; Chang, J. J.; Zhang, S. L.; Damu, G. L. V.; Geng, R. X.; Zhou, C. H. Synthesis and bioactive evaluation of novel hybrids of metronidazole and berberine as new type of antimicrobial agents and their transportation behavior by human serum albumin. *Bioorg. Med. Chem*. **2013**, *21*, 4158–4169.

(29) Salas, P. F.; Herrmann, C.; Cawthray, J. F.; Nimphius, Corinna.; Kenkel, A.; Chen, J.; Kock, C.; Smith, P. J.; Patrick, B. O.; Adam, M. J.; Orvig, C. Structural characteristics of chloroquine-bridged ferrocenophane analogues of ferroquine may obviate malaria drug-resistance mechanisms. *J. Med. Chem.* **2013**, *56*, 1596−1613.

(30) Sharma, P.; Chhabra, S.; Rai, N.; Ghoshal, N. Exploration of rate-limiting conformational state for 5-[(7-chloro-4-quinolinyl)-amino]-3-[(alkylamino)methyl][1,1-biphenyl]-2-ols and N-oxides (tebuquine analogues) for antimalarial activity using molecular shape analysis and molecular field analysis studies. *J. Chem. Inf. Model*. **2007**, *47*, 1087−1096.

(31) Zhang, S. L.; Chang, J. J.; Damu, G. L. V.; Geng, R. X.; Zhou, C. H. Berberine azoles as antimicrobial agents: synthesis, biological evaluation and their interactions with human serum albumin. *Med. Chem. Commun.* **2013**, *4*, 839–846.

(32) Zhang, S. L.; Damu, G. L. V.; Zhang, L.; Geng, R. X.; Zhou, C. H. Synthesis and biological evaluation of novel benzimidazole derivatives and their binding behavior with bovine serum albumin. *Eur. J. Med. Chem.* **2012**, *55*, 164–175;

(33) Yin, B. T.; Yan, C. Y.; Peng, X. M.; Zhang, S. L.; Rasheed, S.; Geng, R. X.; Zhou, C. H. Synthesis and biological evaluation of a-triazolyl chalcones as a new type of potential antimicrobial agents and their interaction with calf thymus DNA and human serum albumin. *Eur. J. Med. Chem.* **2014**, *71*, 148–159.

(34) Sen, T.; Mandal, S.; Haldar, S.; Chattopadhyay, K.; Patra, A. Interaction of gold nanoparticle with human serum albumin (HSA) protein using surface energy transfer. *J. Phys. Chem. C*. **2011**, *115*, 24037–24044.

(35) Hua, Y. J.; Wang, Y.; Ou-Yang, Y.; Zhou, J.; Liu, Y. Characterize the interaction between naringenin and bovine serum albumin using spectroscopic approach. *J. Lumin*. **2010**, *130*, 1394–1399.

(36) Shen, L. L., Mitscher, L. A.; Sharma, P. N.; O'Donnel, T. J.; Chu, D. W. T.; Cooper, C. **S.;** Rosen, T.; Pernet, A. G. Mechanism of inhibition of DNA gyrase by quinolone antibacterials: a cooperative drug-DNA binding model. *Biochemistry*. **1989**, *28*, 3886–3894.

(37) Palù, G.; Valisena, S.; Ciarrocchit, G. Gattot, B.; Palumbot, M. Quinolone binding to DNA is mediated by magnesium ions. *Proc. Natl. Acad. Sci. USA*. **1992**, *89*, 9671–9675.

(38) Bax, B. D.; Chan, P. F.; Eggleston, D. S.; Fosberry, A.; Gentry, D. R.; Gorrec, F.; Giordano, I.; Hann, M. M.; Hennessy, A.; Hibbs, M.; Huang, J.; Jones, E.; Jones, J.; Brown, K. K.; Lewis, C. J.; May, E. W.; Saunders, M. R.; Singh, O.; Spitzfaden, C.; Shen, C.; Shillings, A.; Theobald, A. F., Wohlkonig, A.; Pearson, N. D.; Gwynn, M. N. Type IIA topoisomerase inhibition by a new class of antibacterial agents. *Nature*. **2010**, *466*, 935–940.

(39) Leo, E.; Gould, K. A.; Pan, X.-S.; Capranico, G.; Sanderson, M. R.; Palumbo, M.; Fisher, L. M. Novel symmetric and asymmetric DNA scission determinants for streptococcus pneumoniae topoisomerase IV and gyrase are clustered at the DNA breakage site. *J. Biolog. Chem*. **2005**, *14*, 14252–14263.

(40) Laponogov, I.; Pan, X. S.; Veselkov, D. A.; McAuley, K. E.; Fisher, L. M.; Sanderson, M. R. Structural basis of gate-DNA breakage and resealing by type II topoisomerases. *PLoS On*e. **2010**, *5*, e11338.

(41) Zhang, G.; Fu, P.; Wang, L.; Hu, M. Molecular spectroscopic studies of farrerol interaction with calf thymus DNA. *J. Agric. Food Chem*. **2011**, *59*, 8944–8952.

(42) Kanakis, C. D.; Nafisi, S.; Rajabi, M.; Shadaloi, A.; Tarantilis, P. A.; Polissiou, M. G.; Bariyanga, J.; Tajmir-Riahi, H. A. Structural analysis of DNA and RNA interactions with antioxidant flavonoids. *Spectroscopy.* **2009**, *23*, 29–43.

(43) Son, G. S.; Yeo, J.-A.; Kim, M.-S.; Kim, S. K.; Holmén, A.; Åkerman, B.; Nordén, B. Binding mode of Norfloxacin to calf thymus DNA. *J. Am. Chem. Soc.* **1998**, *120,* 6451–6457

(44) Akbay, N.; Seferoğlu, Z.; Gők, E. Fluorescence interaction and determination of calf thymus DNA with two ethidium derivatives. *J. Fluoresc*. **2009**, *19*, 1045–1051.

(45) Cai, C. Q.; Chen, X. M.; Ge, F. Analysis of interaction between tamoxifen and ctDNA in vitro by multi-spectroscopic methods. *Spectrochim. Acta A*. **2010**, *76*, 202–206.

(46) Shen, L. L.; Baranowski, J.; Pernet, A. G. Mechanism of inhibition of DNA gyrase by quinolone antibacterials: Specificity and cooperativity of drug binding to DNA. *Biochemistry*. **1989**, *28,* 3879–3885.

(47) Vandurm, P.; Guiguen, A.; Cauvin, C.; Georges, B.; Van, K. L.; Michaux, C.; Cardona, C.; Mbembac, G.; Mouscadet, J. F.; Hevesi, L.; Lint, C. V.; Wouters, J. Synthesis, biological evaluation and molecular modeling studies of quinolonyl diketo acid derivatives: New structural insight into the HIV-1 integrase inhibition. *Eur. J. Med. Chem*. **2011**, *46*, 1749–1756.

(48) Santo, R. D.; Costi, R.; Roux, A.; Miele, G.; Crucitti, G. C.; Iacovo, A.; Rosi, F.; Lavecchia, A.; Marinelli, L.; Giovanni, C. D.; Novellino, E.; Palmisano, L.; Andreotti, M.; Amici, R.; Galluzzo, C. M.; Nencioni, L.; Palamara, A. T.; Pommier, Y.; Marchand, C. Novel quinolinonyl diketo acid derivatives as HIV-1 Integrase Inhibitors: Design, Synthesis, and Biological Activities. *J. Med. Chem*. **2008**, *51*, 4744–4750.

Table of Contents graphic